DISSERTATION

γ-H2AX FOCI AND THE MEASUREMENT OF VARIATION IN RADIOSENSITIVITIES OF HUMAN AND RODENT CELLS

Submitted by
Takamitsu Kato
Department of Environmental & Radiological Health Sciences

In partial fulfillment of the requirements
For the Degree of Doctor of Philosophy
Colorado State University
Fort Collins, Colorado
Spring 2006

COLORADO STATE UNIVERSITY

MARCH 2, 2006

WE HEREBY RECOMMENDED THAT THE DISSERTATION PREPARED UNDER OUR SUPERVISION BY TAKAMITSU KATO

ENTITLED γ-H2AX FOCI AND THE MEASUREMENT OF VARIATION IN RADIOSENSITIVITIES OF HUMAN AND RODENT CELLS

BE ACCEPTED AS FULFILLING IN PART THE REQUIREMENTS FOR THE DEGREE OF DOCTOR OF PHILOSOPHY.

Committee on Graduate Work

Jonathan O. Carlson

Hatsumi Nagasawa

Ryuichi Okayasu

Robert L. Ullrich

Michael M. Weil

Adviser Joel S.Bedford

Department Head John D. Zimbrick

ABSTRACT OF DISSERTATION

γ-H2AX FOCI AND THE MEASUREMENT OF VARIATIONS IN RADIOSENSITIVITIES OF HUMAN AND RODENT CELLS

DNA double strand breaks produced by radiation or other agents results in massive phosphorylation of the H2AX histone variant in chromatin around the site of each break. Immunocytochemical detection of this phosphorylated form (γ-H2AX) reveals fluorescent foci in irradiated cells and was used in a low dose rate irradiation assay to resolve even relatively small differences in cellular radiosensitivity. This assay revealed highly significant differences in the radiation response for cells derived from humans and mice that were heterozygous or normal with respect to the *ATM* gene. The assay also revealed differences for cells from unaffected parents of children with retinoblastoma and for cells from about 30% of clinically normal individuals.

Variation in γ-H2AX induction and disappearance after irradiation were also measured in mutant and wild type CHO cells and in normal human fibroblasts. Disappearance of γ-H2AX foci after irradiation was much slower for mitotic than for G_1 cells although no differences were seen for another assay measuring DNA breakage by gel electrophoresis. The expressed γ-H2AX foci in G_0/G_1 or G_2 cells can persist into metaphase but the levels expressed in mitosis is dependent on the repair capacity for the different DNA damages. γ-H2AX foci can disappear with either rejoined or misrejoined DSBs. G_0 premature chromosome condensation analysis showed γ-H2AX foci disappeared after rejoining of DSBs and even after misrejoining. I also observed that high expression of γ-H2AX in S phase cells is related to DNA replication. After the process of

premature chromosome condensation, S-phase PCC showed huge expression of γ-H2AX foci related to replication.

Takamitsu Kato
Department of Environmental & Radiological Health Sciences
Colorado State University
Fort Collins, Colorado 80523
Spring 2006

Table of Contents

Chapter 1: Introduction

List of Abbreviations

53BP1	tumor protein p53 binding protein 1
A-T	Ataxia Telangiectasia disease
ATM	Ataxia Telangiectasia mutated gene
ATM	Ataxia Telangiectasia mutated protein
Atm	Ataxia Telangiectasia mutated gene for mouse
Atm	Ataxia Telangiectasia mutated protein for mouse
BER	Base Excision Repair
BLM	Bloom syndrome
BRCA1/2	Breast Cancer 1 gene/ 2 gene
BrdU	Bromodeoxyuridine
CFGE	Constant Field Gel Electrophoresis
CHK1/2	Cell cycle checkpoint kinase
CPT	Camptothecin
DAPI	Diaminophenylindol
DSBs	Double Strand Breaks
DNA-PKcs	DNA dependent protein kinase catalytic subinit
DNA-PK	DNA dependent protein kinase
ERCC1	Excision-repair, complementing defective, in Chinese hamster, 1
FANCD2	Fanconi anemia, complementation group D2
FISH	Fluorescence *in situ* hybridization
H2AX	variant of histone H2A
γ-H2AX	Phosphorylated form of histone H2AX
H_2O_2	Hydrogen Peroxide
HAU	hemagglutinating units
HDAC4	histone deacetylase 4
HR	Homologous Recombination
HDR	Homology dependent repair
Holiday junction	X-shaped structure observed in DNA undergoing recombination
IrdU/IUdR	Iododeoxyuridine
IR	Ionizing Radiation
Ku70	Thyroid autoantigen, 70-kD, G22P1
Ku80	X-ray repair, complementing defective, in Chinese hamster, 5
LDR	Low dose-rate
Ligase4	ligase IV, DNA, ATP-dependent
MDC1	Mediator of DNA damage checkpoint protein 1
MPF	Maturation Promoting Factor, Mitosis Promoting Factor
MRE11	Meiotic recombination 11
MRN	Mre11-Rad50-NBS1 complex
NBS	Nijmegen breakage syndrome
NHEJ	Non Homologous End Joining
PCC	Premature Chromosome Condensation
PCR	Polymerase Chain Reaction
PFGE	Pulsed Field Gel Electrophoresis
PI	Propidium iodide

PIKK	phosphatidylinositol 3-kinase-related kinase
RB	Retinoblastoma
RPA	Replication Protein A
SSA	Single Strand Annealing
SSBs	Single Strand Breaks
ssDNA	single strand DNA
TopBP1	Topoisomerase Binding Protein 1
UV	Ultraviolet
XP	Xeroderma Pigmentosum
XPF	Xeroderma Pigmentosum, complementation group F
XRCC4	X-ray repair, complementing defective, in Chinese hamster, 4
WRN	Werner syndrome

Figures and Tables

ACKNOWLEDGEMENT

The road for my Ph.D. was challenging and fulfilling, and without help from many people, it would have been impossible to complete. My advisor, Dr. Joel Bedford, was a great inspiration to my work and I truly appreciated his assistance throughout my entire graduate student life. My committee members Drs. Jonathan Carlson, Hatsumi Nagasawa, Ryuichi Okayasu, Robert Ullrich and Michael Weil were always providing assistance when I was in need. I want to say 'thank you' to the former graduate students, Drs. Paul Wilson and Yuanlin Peng, of the Bedford Lab. They provided great discussion and excellent advice, and were critical in the completion of my dissertation. I would also like to say thank you to all the workers who have helped me from the Bedford Lab (Zane & Christy).

Finally I appreciate my family members for their great help and their understanding. I dedicate this to the memory of my parents.

Chapter 1

INTRODUCTION

The research described in this dissertation utilized a relatively new and highly sensitive assay to study cell cycle related changes in radiation induced DNA breaks and their repair in normal and in radiosensitive mutant cells and to determine whether it can be used for distinguishing even mildly hypersensitive cells. This assay involves measurement of the phosphorylated form of the H2AX* histone variant that occurs in the form of amplified foci in chromatin around the site of DNA breaks. The following section reviews the background information pertinent to the study.

1-1: DNA Double Strand Breaks (DSBs*)

What is important about DNA DSBs?

There is strong circumstantial evidence to indicate that DNA is a principle target for many of the important biologic effects of ionizing radiation (IR*). DNA double strand breaks (DSBs) are considered the critical primary lesions that can lead to the formation of chromosome aberrations, and in turn, certain of these can lead to various biological responses including cell killing, mutation and oncogenic transformation (1-3).

Some lines of evidence supporting the importance of DNA DSBs include studies involving the energy deposition from decay of incorporated ^{125}IUdR*. The auger electrons have a very short range confined to the local neighborhood of the DNA and

each decay produces one DSB. Such decays can result in chromosomal aberrations and cell killing (4-8). Treatment of cells with restriction endonucleases gave direct evidence that chromosome aberrations can be produced when DSB is the only lesion induced (9-11). Revel and co-workers showed that after irradiation of G_1 cells are unable to form colonies but cells without micronuclei form colonies (12). Cornforth and Bedford reported a one-to-one relationship between the average number of lethal aberrations per cell and the log of the surviving fraction in AG1522 normal human fibroblasts exposed to x-rays (13). So in these studies DSBs directly correlated with chromosome aberrations that produce acentric fragments which, in turn resulted in cell death. In addition to these studies many have shown there are elevated levels of chromosomal aberrations after irradiation in DNA repair deficient cell lines. These cells are also more radiosensitive for cell killing, mutation induction and so called *in vitro* malignant transformation (14-17).

Source of DSB formation

DNA DSB can be formed if single strand breaks (SSBs*) in the two strands of DNA are directly opposite one another, or separated by only a few base pairs. Agents like H_2O_2* produce many SSBs, but few of these are close enough together on opposite strands to cause a DSB. Ionizing radiation is one of very few agents that directly and promptly produces DSBs because the SSBs are not produced randomly, but sometimes in close proximity along tracks of the charged particles delivering the dose. Restriction enzyme treatment forms only DSBs as blunt or cohesive ends. UV* or alkylating agents can result in lots of SSBs when repair processes try to excise the damaged bases and in some cases DSBs may be caused indirectly during DNA repair and replication (18,19).

DSB are not only induced by exogenous factors like IR but also can result from a variety of endogenous processes during the normal cellular metabolism, mediated by free radicals and can result from DNA replication, e.g. topoisomerases (20,21). An estimated ten DSBs arise spontaneously in each S-phase cell because of endogenously produced SSBs in a parental strand being passed by the replication fork (22). Normal cells generally repair such damage but repair deficient cells may fail to do so and thus may die from chromosome fragment loss.

The yield of DSB induction from irradiation depends on DNA association with protein and its state of condensation (23). There is an eightfold protection against radiation induced DSBs produced in DNA packed into a basic nucleosome repeat structure compared with naked DNA embedded in agarose (24), and a further fivefold protection of DNA when the nucleosomes are condensed into chromatin fibers .

Mechanism of DSB repair

Mechanisms of DSB repair have been reviewed recently by Thompson and Schild (25-27). DSBs can be repaired by three basic processes. One process is known as homologous recombination repair (HRR*), which is an error free pathway requiring an undamaged DNA strand such as a sister chromatid as a template in the repair. Another process is single strand annealing (SSA*) which is an error prone mechanism requiring nearby homologous sequence around DSB sites as template for repair. The third process is an end-to-end rejoining by a process known as nonhomologous end joining (NHEJ*) which is a more error prone mechanism. These pathways are outlined in Figure 1-1.

Figure 1-1.
Diagrams of DNA DSB repair

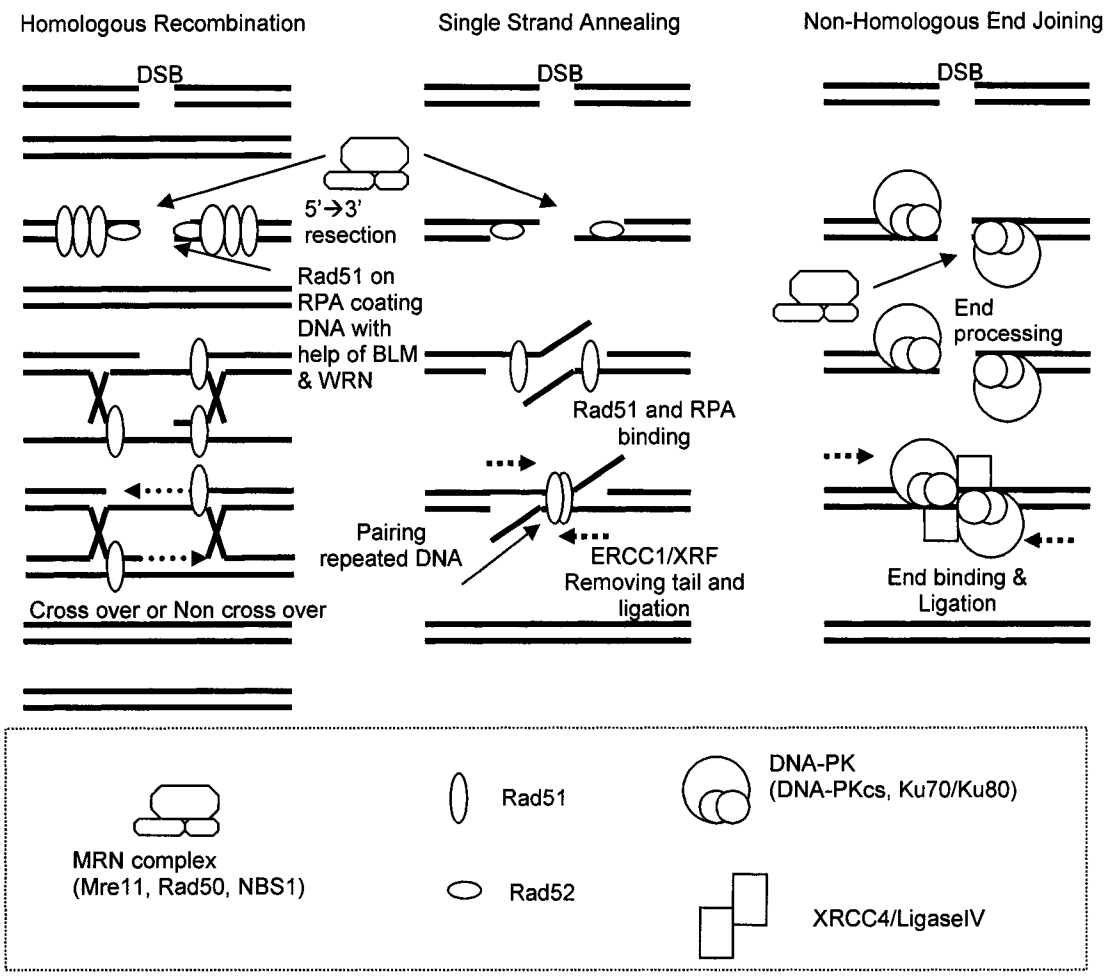

HRR is highly conserved process helping to maintain genome integrity from bacteria to mammals. For some situations involving the need to resolve DNA DSBs the error free process of HR plays an important role. In the early stages of the cellular response to the induction of DSBs, ATM* senses the DSB, and ATM and other PIKK* (phosphatidylinositol 3-kinase-related kinases) phosphorylate H2AX, which can then interact with BRCA1* and NBS1*. BRCA1 is reported to serve as an anchor and coordinator of the repair complex. The Mre11*-Rad50-NBS1 (MRN* complex) resects the DNA to provide single stranded DNA (ssDNA*) overhangs for DNA pairing and strand exchange. Rad51 binds to ssDNA tail coated by RPA* to initiate strand exchange. Rad52 helps Rad51 to form DNA exchange intermediates. BLM* interacts with the Holiday junctions* and forms foci with Rad51. WRN* interacts with Rad52 in Holiday juction. Following sister-chromatid pairing and strand invasion of DNA overhangs, HRR has two possibilities to finish the process either by non-crossing over or crossing over. Finally the gaps are filled in by DNA polymerase and fresh DNA ends joined together by ligase (This process is also reviewed in (28-33)).

In contrast to HR which is most active through late S- and G_2-phases of the cell cycle because HR requires homologous DNA, the NHEJ pathway is active during all cell cycle phases and appears to be reasonable for virtually all the repair of spontaneous and IR-induced DSB during G_0/G_1-phases in mammalian cells because homologous DNA sequence is not available in those phases. Following initial binding of the DNA end by Ku* heterodimer, Ku protein recruits DNA-PKcs* to the site. DNA-PKcs, after being activated by forming DNA-PK* complex (DNA-PKcs, Ku70/80), results in the release of DNA-PKcs from the extreme end of DNA. A complex of Ku, XRCC4*, DNA ligase IV*

and a DNA polymerase then forms at the end-to-end junction and catalyzes alignment-based gap filling and ligation (also review in (2,34-36)).

In addition to NHEJ and HRR pathways, Single Strand Annealing (SSA) can occur when, the broken ends of DSB are resected by a nuclease (reviewed in (37)). In the case of long homology sequences between direct repeats on the overhangs, RPA* and Rad52 are necessary for facilitating DNA pairing followed by removal of the tails by ERCC1/XPF* nuclease and gap filling by DNA polymerase.

Methods for the measurement of DSB

Historically four major approaches have been used for measuring DNA DSBs, all of which detect changes in DNA in size (reviewed in (38,39)). These methods include sedimentation (40-42), viscoelastometry (43), pulsed field gel electrophoresis (44), and neutral elution (45). All the methods have very high detection limits for DSB. The doses used in these methods are typically in the superlethal range for cells and for the most part not in the range of measurement of cell survival, mutation and chromosome aberrations.

An indirect method that has proved to be much more sensitive for detection of DSB was discovered in 1998, by Bonner and co-worker (46). They showed that a numerous H2AX molecules are phosphorylated around the site of a single DSB after IR exposure. This is defined as a focus. The yield of foci in the cell showing phosphorylation of H2AX was equivalent to the number of decays of incorporated ^{125}IrdU, each of which is known to produces one DSB (47). Currently phosphorylation of H2AX (γ-H2AX*) is the most sensitive assay to detect DNA DSB (Figure 1-2).

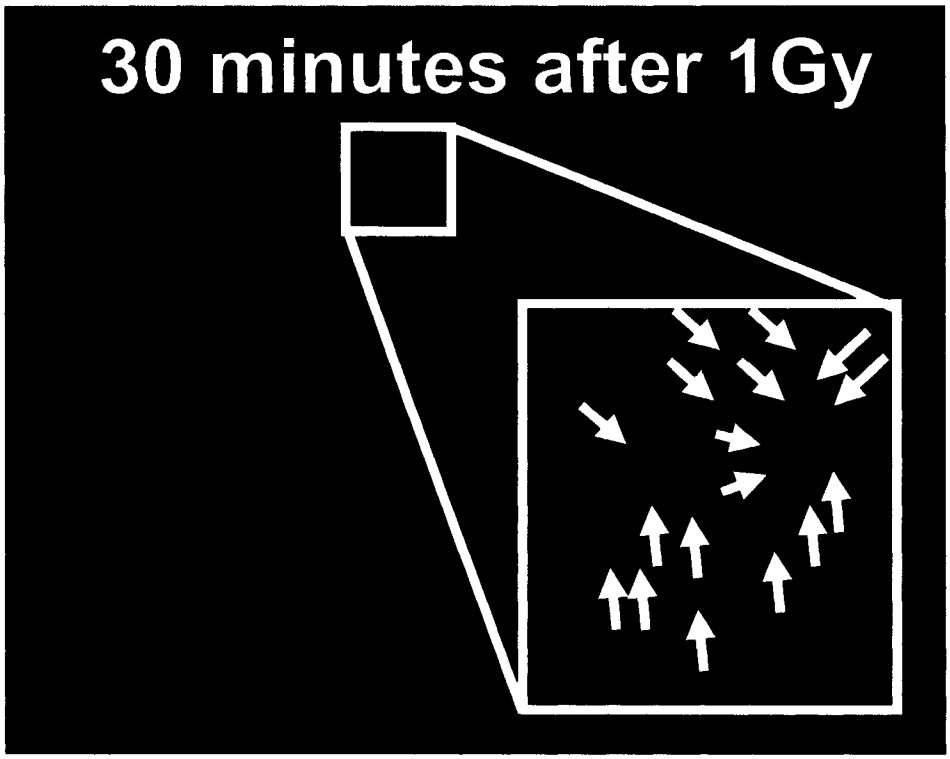

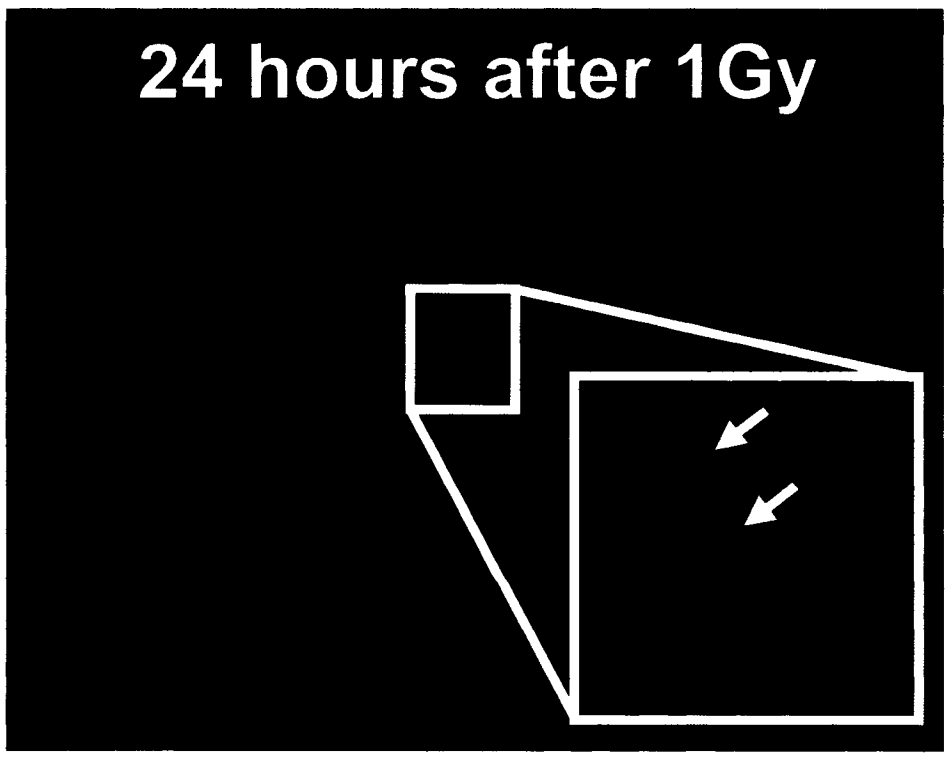

1-2: γ-H2AX

γ-H2AX

The proteins binding to DNA to form chromosomes are divided into histone or nonhistone chromosomal proteins. Histones are responsible for the nucleosome which is the most basic level of chromosome organization. Each individual nucleosome core particle consists of a complex of eight histone proteins (two of each H2A, H2B, H3, H4) and 146bp double-stranded DNA wrapped around inside. Each nucleosome core particle is separated from the next by linker DNA. The average nucleosome structure repeats itself at intervals of about 200bp, thus making liner DNA, on average, about 51 bp (48,49).

H2AX is one of the histone variants of H2A. It comprises about 10% of the total H2A in mammalian cells (49,50). H2AX is phosphorylated when a DNA double strand break (DSB) is produced either by an endogenous process or an exogenous process such as by IR. At the maximum time point, approximately 1% of the total H2AX becomes γ-phosphorylated per Gy of IR. It is known that about 30 to 40 DNA DSBs are introduced by each Gy of IR into 6×10^9 bp (about 4×10^{12} Dalton) contained in the mammalian diploid genome in the G_0/G_1-phase (4). About 0.03% of the chromatin appears to be involved per DNA DSBs in γ-H2AX foci formation (46). Thus, 2 Mbp of DNA or 10,000 nucleosomes per DSBs are involved with each DNA DSB.

γ-H2AX phosphorylation and dephosphorylation is unlikely to result from diffusion or replacement of free histones (51). H2AX phosphorylation appears to depend on ATM and other PIKK (52-54). Under most normal growth conditions, IR-induced

H2AX phosphorylation can be carried out by ATM and DNA-PK in a redundant, overlapping manner. After DNA DSBs are rejoined γ-H2AX dephosphorylation occurs and this may involve the protein phosphatase 1α because Calyculin A, a phosphatase inhibitor, inhibites early elimination of γ-H2AX and DSB rejoining (55).

H2AX gene

The histone H2AX gene, located 11Mb telomeric to ATM at 11q23.3, is in a region commonly deleted or translocated in several human hematological malignancies and solid tumors (56,57). H2AX +/– and H2AX–/– mice are viable, so H2AX is not necessary for their development. But H2AX –/– have a phenotype of hypersensitivity to radiation, growth retardation, immune deficiency, and mutant males are infertile (58,59). Cells from such H2AX–/– mice exhibit elevated levels of spontaneous and IR-induced genomic instability. They have an altered ability to recruit certain components of radiation-induced foci. NBS1, RAD51, and MRE11 foci stay longer, but BRCA1 and 53BP1 did not form foci after IR exposure (59). H2AX–/– cells show increased use of SSA, an error prone deletional mechanism of DSB repair. This leads to the genomic instability for the phenotype of H2AX –/– mice and explain common deletion of H2AX gene in hematological malignancies and solid tumors in human patients (58-60).

H2AX phosphorylation as a Biodosimeter

There is a direct correlation between the number of ^{125}I decays and the number of γ-H2AX foci per cell, consistent with the assumption that each ^{125}I decay yields a DNA DSB which yields a visible γ-H2AX focus. γ-H2AX antibody forms the basis of a

sensitive quantitative method for the detection of even a single DNA DSB in eukaryotic cells (61,62).

Cell line-dependent differences in the kinetics of γ-H2AX appearance after irradiation are related to radiosensitivity (63,64). It is reported that various radiosensitive DNA repair deficient mutants show higher residual levels of γ-H2AX foci after repair has occurred or altered kinetics of phosphorylation and dephosphorylation of H2AX after IR exposure (65).

γ-H2AX colocalization with other DNA repair proteins

γ-H2AX has been reported to colocalize within a few minutes with other DNA repair proteins such as MDC1*, 53BP1*, HDAC4*, ATM, Chk2p*, MRN complex (Mre11, Rad50 and NBS1) and much later with BRCA1, phosphorylated-DNA-PKcs, TopBP1, RPA, Rad 51, FANCD2*, BLM and WRN (27,66-68).

Although it is known that phosphorylation of H2AX occurs around DSBs about 2Mb (69), very little γ-H2AX can be detected in chromatin at shorter distance of 1-2kb of the break (70). In contrast, this region contains almost all the Mre11 and other repair proteins that bind as a result of the break (71).

Conditions Altering γ-H2AX foci formation

It is known that high salt solution condenses chromatin structure. Postirradiation incubation in hypertonic 0.5M Na^+ increases γ-H2AX expression about 4-fold, and results in the formation of larger foci. Further disappearance of γ-H2AX is inhibited after irradiation in high salt condition (72). This may indicate a reduced ability to repair DNA

damage or possible a reduced capacity to dephosphorylate γ-H2AX in the hypertonic environment (73).

Phosphorylation of H2AX occurs in hyperthermia without irradiation (74). Induction of γ-H2AX foci is correlated with the temperature dependence of cell killing. During periods when cells are exposed to heat, the cell cycle dependent pattern of cell killing is the same as the cell cycle pattern of γ-H2AX foci formation, i.e., γ-H2AX levels are high in heat sensitive S-phase, high in heat sensitive G_2/M and lower in the G_1 heat resistant phase (74).

Iron depletion induces DNA DSBs in treated cells, and activates a DNA damage response including γ-H2AX foci, RPA, and CHK1* kinase. Iron chelating may result in the higher free radical accumulation to cause DNA DSBs (75).

Phosphorylation of H2AX occurs without external stimulus. γ-H2AX foci accumulate in senescing human cell cultures and in aging mice (76). This may result from internal DSBs accumulation. It is also known that some tumor cells have high spontaneous or background levels of γ-H2AX foci (77).

Phosphorylation of H2AX is dose rate dependent. High dose-rate radiation exposure induces a significant number of foci in a dose-dependent manner, but at least for very low dose-rate radiation only a few γ-H2AX foci were observed (78). Clearly DNA DSBs induced by low dose-rate radiation are efficiently repaired during chronic irradiation.

Cell Cycle Effect for γ-H2AX foci

The levels of induction of γ-H2AX foci by radiation are cell cycle dependent. The total number of induced γ-H2AX foci in G_2/M phase is reported to be almost twice the number as seen in G_0/G_1-phase because the DNA content in G_2 cells is twice that for G_1. γ-H2AX levels have been reported to be approximately 3 times lower in unirradiated G_1-phase cells than S- and G_2-phase cells (79).

DNA DSBs can be formed not only directly by ionizing radiation but also as a result of secondary effects after UV exposure (19). Photolysis of BrdU-labeled DNA by UV light also induces DSBs and leads to H2AX phosphorylation (80). Xeroderma Pigmentosum (XP*) is known as UV sensitive syndrome involving a defect of Base Excision Repair (BER). XPV cells develop DNA DSBs during UV-induced replication arrest (81). These UV-induced foci occur in cells that are unable to carry out efficient bypass replication of UV damage. As a result, DNA DSBs can be produced along with γ-H2AX foci formation.

The highest degree of H2AX phosphorylation induced by UV was seen in S-phase cells, particularly during the early portion of S-phase. H2AX phosphorylation observed throughout S-phase reflects formation of DSBs due to the collision of replication forks with the UV-induced primary DNA lesions (80).

1-3: Ataxia-Telangiectasia

Ataxia-Telangiectasia

Ataxia-telangiectasia (A-T*) is an autosomal recessive disease syndrome. A-T patients are homozygous recessive for *ATM** mutant alleles that produce either defective or no protein product. Among numerous other clinical manifestations, these patients are

highly predisposed to cancer, extremely radiosensitive and have increased chromosomal radiosensitivities. The frequency of *ATM* −/− homozygotes is estimated to be about 1 in 40,000 while *ATM* +/− heterozygotes are thought to comprise about 1% of the general population (82-85).

There is a clear increased risk of lymphoid leukemia in A-T patients. Approximately 10% of A-T patients will develop lymphoid leukemia as children (86). Cancer of one form or another occurs in roughly one-third of A-T patients. For *ATM* heterozygotes younger than age 45, the risk of death from a malignant neoplasm was estimated to be greater than 5 times the risk for the general population. *ATM* heterozygotes may make up more than 5% of all persons dying from a cancer before age 45 (84).

When compared with non-carriers the estimated increased relative risk of cancer of all types among *ATM* heterozygotes was reported to be 3.8 in men and 3.5 in women. Breast cancers in heterozygous women have an increased relative risk of 5.1. *ATM* heterozygotes might account for between 1 and 13% of all breast cancer cases, with 3.8 % being proposed as the best estimate (82).

ATM (Ataxia Telangiectasia mutated) gene and ATM protein

ATM is mutated in patients with the autosomal recessive disorder ataxia telangiectasia. The *ATM* gene was mapped and identified by positional cloning on chromosome 11q22-23 (87). The gene is approximately 150kbp in length, and extends over 66 exons (88). The *ATM* transcript is 12 kbp and it's large 9168bp cDNA (cording region) encodes a 350kDa protein. The protein structure is similar to

phosphatidylinositol-3'kinase gene family (87). ATM protein is almost exclusively nuclear and is expressed in all cell lines and tissues that have been analyzed. While total ATM protein levels are not regulated in response to UV or IR, the protein kinase activity of ATM, as determined by immunoprecipitation kinase assays, increased two- to three-fold following exposure to IR (89). ATM expression is reduced dramatically or is absent in all A-T patients analyzed, including those predicted to express proteins that should be detected by antibody. The majority (85%) of known *ATM* mutations are truncating mutations, that do not allow synthesis of full length ATM protein (89).

A-T and DNA damages

A-T cells are unusually sensitive to IR and certain chemicals that produce prompt DNA DSBs like Bleomycin (90). IR produces a large number of lesions in DNA, including various kinds of base damage, single strand breaks (SSBs) and double-strand breaks (DSBs). Bleomycin produces SSBs and DSBs in DNA. In addition to an increased sensitivity of A-T cells to the production of chromosome type aberrations after irradiation of G_0 or G_1 cells, chromatid type aberrations are also produced (13,91).

Peripheral lymphocytes from A-T patients are about twice as sensitive as normal lymphocytes to the induction of chromatid-type aberrations by ionizing radiation after exposure during the G_2-phase of the cell cycle (92). Nagasawa and Little (93) reported that the capacity for repair of potentially lethal damage (PLD*) was almost absent in A-T cells, but normal in *ATM* heterozygotes and wild type individuals. The decline in chromosomal aberrations, seen in normal cells during confluent holding after IR, was absent in A-T cells consistent with the lack of PLD repair. Cornforth and Bedford

showed that the reduced PLD repair capacity in contact inhibited A-T cells was due to a defective repair of chromosome breaks entirely during the G_0 or G_1 phase of the cell cycle and had nothing to do with events that may have developed later in the cell cycle before cells reached mitosis (94).

However, the most studies on the induction and repair of DSB have established no clear relationship between DSB and the hypersensitivity of A-T cells (95,96), the study of Cornforth and Bedford showed an lower rejoining of PCC breaks during G_0 in A-T cells (94). Alkaline elution studies shown that there is no difference in repair of DNA SSBs in patients with A-T vs. normal cells (97).

The cause of increased radiosensitivity in A-T cell may be a defect in their ability to correctly repair to DNA damage rather than a defect in their ability to rejoin breaks at all (98,99). The reason that chromatid type aberrations are produced after irradiation of A-T cells in G_0 may in some way be related to an additional, but as yet unknown defect in their ability to repair base damages during S-phase.

*Mouse Atm**

The mouse homolog, *Atm*, has been identified and mapped to mouse chromosome 9C, which is syntenic to human 11q22-23 (100). Mouse Atm* shows 84% amino acid identity and 91% similarity with human ATM (100). Mice with a disruption of *Atm* are viable, as is the case in human A-T. *Atm* homozygous mice show significantly reduced body weight compared to their wild type littermates, while heterozygous mice have similar weight of wild type mice (101). *Atm* is essential for germ cell development and fertility (101). *Atm* mutant mice develop malignant thymic lymphomas between two to

four months of age (101). The analysis of metaphase spreads from primary cultures of the thymomas arising in A-T mice revealed multiple, recurrent rearrangements in their chromosomes (101).

Atm mice are also extremely radiosensitive to the acute lethal effects of radiation (101). All *Atm* homozygous mice irradiated at 8 Gy died 3-5 days post-irradiation and two thirds of the homozygous mice died within 7 days after 4 Gy of irradiation. On the other hand, all heterozygotes and wild type mice survived the same 4 weeks duration after 4 Gy of irradiation, and two thirds of them died within 18 days after 8 Gy of irradiation. The cause of death in these experiments was severe damage from radiation to the gastrointestinal tracts (101).

Not only acute effects, but late effects of radiation are also dependent on *Atm* status (102). If one eye of *Atm* wild-type, heterozygous and homozygous knockout mice were exposed to various doses of radiation, a large difference was reported for a given dose for cataract development in the animals of all three groups (102). The lenses of *Atm* −/− mice were the first to opacify for doses above 0.5Gy (102). Cataracts generally appeared earlier in the heterozygote versus wild-type animals (102). Radiation carcinogenesis studies with *Atm* mice were also reported Weil and his colleagues who reported that radiation induced genomic instability and mammary ductal dysplasia is *Atm* heterozygous mice (103). Smilenov and his co-workers (104) and Spring and co-workers (105) also showed *Atm* heterozygous cells were more sensitive to radiation oncogenesis than normal cells.

Role of ATM protein in the DSB repair pathway

The role of ATM and other proteins in DSB repair has been reviewed recently by Kurz and Lees-Miller and by Lavin and his co-workers (106,107).

ATM is a serine-threonine protein kinase that undergoes autophosphorylation after DNA damage. This subsequently initiates a signaling cascade that involves the phosphorylation of several substrates. ATM normally exists on a dimeric protein and IR-induced activation occurs through intermolecular autophosphorylation of Ser-1981, which causes dissociation of the ATM dimers and enhancement of kinase activity. Although ATM binds preferentially to DNA ends in vitro (108), the *in vivo* activation is thought to result from changes in chromatin structure instead of DNA binding (109). Active ATM or other PIKK (ATR or DNA-PKcs) rapidly phosphorylates histone H2AX Ser139 extending over a region of 2Mbp from the site for each DNA DSBs. The MRE11-RAD50-NBS1 complex (MRN complex) is also recruited to the DNA lesion site together with BRCA1. MRN nuclease/helicase complex is believed to process the DNA ends to obtain ssDNA overhangs in order to facilitate binding to proteins. This multiprotein complex apparently coordinates co-localization of active ATM together with other factors including MDC1/NFBD1 and 53BP1. This cascade of phosphorylations may aid the recruitment of DNA repair proteins such as Ku70/80, DNA-PKcs, XRCC4 and Ligase IV for NHEJ or the Rad 51 complex for HRR.

Although the key sensor proteins that first recognize DSBs are still not identified unequivocally, ATM is a major candidate. It could act alone or in combination with other proteins such as 53BP1 and MDC1/NFBD1 that localize within minutes to sites of DSBs.

ATM heterozygotes

As mentioned above, A-T patients who are homozygous recessive for the *ATM* gene are extremely radiosensitive and have a high risk of cancer. Even though the parents of A-T patients (obligate heterozygotes) do not have the A-T disorder, numerous studies have indicated they are mildly radiosensitive and also have a higher risk for development of cancer. The relation ship between *Atm* heterozygosity and radiation induced cancer risk is also reported (103-105). Determination of *ATM* heterozygosity is therefore of medical interest (84,104,110-114). Unfortunately, it is very difficult and expensive to diagnose A-T heterozygosity in clinical situation by PCR* based methods because the mutation is not known except where it may have been identified in A-T families. Recently cells from many apparently normal individuals have been shown to be mildly hypersensitive to radiation. The number of those radiosensitive people reported by Nagasawa and Little (115) is so high that the frequency cannot be explained even from contribution of inherited mutation of *ATM* and *BRCA*. Therefore, diagnosis of *ATM* heterozygosity by detection of a mild increase in radiosensitivity is not likely to be specific for ATM.

Detection of ATM heterozygotes by radiation hypersensitivity

There is no doubt that A-T patients and their cells are radiosensitive, and that A-T patients have a higher cancer risk than normal populations (84,104,110-114). Therefore, it is of interest to distinguish *ATM* heterozygotes and other sensitive subpopulations from the general public and to estimate their radiosensitivity and risk for carcinogenesis.

Chen and his co-workers reported identification of a series of A-T obligate heterozygotes based on the sensitivity of lymphoblastoid cell lines to IR (116). Detection

of increased radiosensitivity in heterozygous carriers of the *ATM* gene have been reported by G_2-phase chromosomal radiosensitivity of peripheral blood lymphocytes (117,118). Both A-T patients and obligate heterozygotes showed significantly increased levels of radiation-induced chromatid damage relative to that of normal controls.

Cell cycle analysis of postirradiation samples is another useful method that can detect increased radiosensitivity in *ATM* heterozygotes (119). Relative to normal cells much larger fractions of cells from A-T heterozygous were irreversibly blocked in G_1-phase when density-inhibited confluent cell cultures are irradiated and immediately subcultured to release them into the cell cycle. This blocking was determined by following cumulative labeling indices during incubation with ^{3}H-thymidine. Little or no such block occurred in cells from normal individuals or A-T patients.

1-4. Radiosensitivity of cells derived from apparently normal individuals

The human population is now more than 6 billion. Human beings have spread on almost the entire earth and adapted to many environmental conditions. Obviously our genetic diversity is huge compared to inbred mice strains and there are many phenotypic differences among individuals. Accordingly it is not surprising that there are differences of radiosensitivity among people.

As mentioned above, genetic disorders such as those involving DNA repair associated genes like *ATM* contribute radiosensitivity. While some people may be mildly radiosensitive as a result of heterozygosity for a gene like *ATM* or perhaps *BRCA,* it seems unlikely that the limited number of currently known genes of this kind could account for more than 5% to 10% of the population. Nevertheless, Nagasawa and Little

reported 3 out of 10 apparently normal human fibroblast cell lines (GM2987, GM3348, and GM3377) showed moderate degree of radiosensitivity (115). They examined cell survival, cell cycle delay, and chromosomal aberrations. The radiosensitivities in those cells were not as severe as in A-T cells but falling within the range of normal population. Also Deschavanne and co-workers have reported a range of sensitivities of cells from apparently normal individuals (120).

Fitzek and his co-workers reported unexpected hypersensitivity to radiation of fibroblasts from unaffected parents of children with hereditary retinoblastoma (121). Unexpected sensitivity to cell killing and cell cycle delay were observed in at least one parental fibroblast strain. Parental strains were equally, or even more hypersensitive than the probands. They suggested increased parental cell sensitivity to radiation may come from the presence of an as yet unrecognized genetic event occurring in one or both parents of children with retinoblastoma. Although it is not known, the radiosensitive population may have elevated risk of hereditary mutation.

1-5. Useful techniques to determine radiosensitivity

In this dissertation, the very sensitive γ-H2AX assay that detects the presence of DNA DSBs was used in combination with low dose rate irradiations with the idea that this might amplify small differences in radiosensitivity seen for acute high dose-rate irradiation. The G_2 irradiated γ-H2AX foci in metaphase was also used.

Low dose-rate irradiation

A single low LET electron track from a γ ray exposure can deposit anything from 0.001cGy up to about 2.5cGy, rarely, and the average track will deposit about 0.1cGy when it traverses a cell nucleus. It is known that a 1 Gy dose of γ-rays produces about 30-40 DSBs in a nucleus, so 0.25cGy irradiation would, on average, induce 1 DSB per cell nucleus (122). Such a single low LET electron track also produces other kinds of damage to the DNA such as a base change, and SSBs, in addition to DSBs, or possible complex damage from an ionization cluster (122).

Dose rate is one of the principle factors that determine the biological response for a given absorbed dose. As the dose rate is lowered and exposure time extended, the biological effect of a given dose generally is reduced. Cells have more opportunity for DNA repair to reduce a biological effect from radiation during the prolonged exposure time (123-125). The magnitude of the dose rate effect from the repair of sublethal damage varies enormously among different types of cells. A cell which has high repair capacity, exemplified by a broad shoulder of their acute survival curve shows a correspondingly large dose rate effect. The dose rate effect caused by repair of sublethal damage is most dramatic between 0.01 and 1 Gy/min. A pronounced dose rate effect was observed over the range between 55.6 and 0.29 Gy/h, but a limit to the repair dependent dose rate effect was reached at 0.29 Gy/h since no further reduction in effect per unit dose was observed when the dose rate was lowered to 0.17 or 0.06 Gy/h (126).

Low dose rate effect for radiosensitive cells

A significant reduction in the radiation sensitivity of cell with the normal DNA repair capacity was observed for continuous low dose rate radiation exposure compared

to the results from acute exposure, but for DNA repair deficient cell lines there seem to be small or no difference in the survival curves when low dose rate and acute exposure were compared. This occurs not because the radiosensitive cells become more sensitive at low dose rates, but rather because there is a large dose rate effect for normal cells which become more radioresistant at low dose rate (17,127).

In yeast, a certain radiosensitive mutant strain can't rejoin DSB at all. In such mutants approximately one DSB per cell corresponds to a lethal event, suggesting a DSB is a potentially lethal lesion. The dose rate effect is based on DSB repair during irradiation; it is absent in DSB repair deficient mutants (128).

Because low dose rate irradiation has increased the differences in response for repair proficient vs. deficient cells, chronic exposure should better differentiate the smaller differences in normal and intermediate sensitive cells related to acute high dose rate exposures. In one study low dose rate exposure demonstrated an enhanced degree of radiation hypersensitivity in fibroblast strains derived from obligate *ATM* heterozygote donors (124,129). In the study of Blocher and co-workers, the response of 10 *ATM* heterozygous strains was indistinguishable from that of 5 normal controls for acute exposure but chronic exposure *ATM* heterozygote responses were intermediate between normal and *ATM* homozygous strains (129).

G_2-chromosomal radiosensitivity assay

The G_2 chromosome radiosensitivity assay developed from the work of Sanford and co-workers (130,131). Briefly, cycling cells were irradiated with a dose of 0.5-2 Gy. Following a 0.5 hour incubation time to allow mitotic cells present during irradiation to

enter G_1-phase, Colcemid is added for 1-3 hours. The cells thus observed at metaphase would have been in the G_2-phase of the cell cycle at the time of irradiation.

Numerous studies have reported on a correlation between cancer susceptibility and an increased sensitivity to the induction of G_2 chromosomal aberration induction following exposure to ionizing radiation or other treatments that directly or indirectly produce DNA DSBs (130-135). One interesting example has involved approaches to the identification of A-T heterozygotes who are at increased risk for breast cancer (eg., (130,134-139)). Scott and his colleagues have reported that numerous factors associated with experimental protocols can influence the outcome of the assay itself (135). However, they have shown that by including appropriate matched controls within each assay protocol to reduce inter-experiment variation, then with the protocol they use, a statistically significant ($P = 0.048$) distinction in G_2 chromosomal radiosensitivity was observed for a group of 10 individuals who were A-T heterozygotes. Only two of these 10 had mean G_2 aberration scores outside the 95% confidence limits of the control group of 53 individuals (135). In the earlier report of Scott and co-workers it is of interest to note that some 9% of samples from the control population showed G_2 chromosomal radiosensitivities overlapping the range seen for A-T heterozygotes (140). The assay has generally been recognized as very useful even if some have reported it to be less than robust (eg., (141)).

Does the G_2 Assay reflect DNA repair defects measured by γ-H2AX?

In the G_2-assay, chromosome aberrations are scored. If chromatid exchanges are the result of misrepair of DSB, and chromatid gaps and breaks are the result of unrepaired

DSB, then γ-H2AX should be located at the points of the aberration. Further, if γ-H2AX dephosphorylation occurs after DSB rejoining completed, it may be possible to observe slow but completed DSB on correctly repaired breaks.

Premature Chromosome Condensation

The induction of Premature Chromosome Condensation (PCC*) is an approach that has been used to study the breakage and rejoining of chromosome during interphase (94,142-148). Fusion between mitotic and interphase cells result in rapid chromosome condensation, with dissolution of the nuclear envelope within 30 minutes after treatment with inactivated Sendai virus (142,143). The morphology of Prematurely Condensed Chromosomes (PCC) varies according to the stage of the interphase cells in the cell cycle at the time of fusion. Thus, the PCC of G_1 phase cells were very long, single chromatids, those of G_2 are elongated and slender double chromatids, and those of the S phase are characterized by their fragmented appearance (146).

In X-irradiated G_1 cells, Waldren and Johnson reported in early G_1 HeLa cells the net number of chromosome fragments per cell increases linearly with dose up to 1800 rad, with about 10 fragments produced per Gy (146). If fragmentation is equated with metaphase chromatid breakage, the degree of damage in PCC exceeds by a factor of about 10 the expected aberration frequency at the first mitosis.

Cornforth and Bedford reported x-ray induced PCC breakage and rejoining of contact inhibited G_0 normal human fibroblast AG1522 and other cell strains (94,147-149). They showed a dose response curve shortly after irradiation with a slope of 6.3 excess PCC fragments per Gy in a cell. The initial rate of decrease in breaks due to rejoining was

similar to the rate of increase in survival after incubation because of the repair of potentially lethal damage. The rate of rejoining is also in close agreement with the rejoining of DNA DSB obtained from measurements with pulse field gel electrophoresis.

The numbers of chromosome breaks per cell produced by 1 Gy of irradiation from PCC method by Waldren and Johnson (146) and Cornforth and Bedford (147) are significantly lower than the number of DNA DSBs measured by other method like pulsed field gel electrophoresis and γ-H2AX foci assay (23,47). One reason for this is that with the PCC method a cell fusion and incubation time of 10-20 minutes is required for chromatin condensation. Since the fast component of DSB repair occurs with a half time less than 30 minutes, many DSBs would be expected to repair during the process of PCC induction. Another possibility is that not all the DSBs are revealed as PCC breaks since chromatin may be hold together by more than just the DNA.

1-6: Issues studied in this dissertation

The γ-H2AX assay provides means for studying the production and repair of DNA DSBs not previously possible for low doses of radiation in the biologically relevant range. The aim of this dissertation was, first, to determine the usefulness of the assay for resolving relatively small differences in radiosensitivity using low dose rate as opposed to high dose rate exposure conditions. The second aim was to more carefully characterize the γ-H2AX assay with respect to its applications for cells in different phases of the cell cycle where large differences in chromatin condensation occur and to change in cellular radiosensitivity.

REFERENCES

1. M. Frankenberg-Schwager, Induction, repair and biological relevance of radiation-induced DNA lesions in eukaryotic cells, *Radiat.Environ.Biophys.* **29**, 273-292 (1990).

2. A. J. Pierce and M. Jasin, NHEJ deficiency and disease, *Mol.Cell* **8**, 1160-1161 (2001).

3. D. Murray, R. Simpson, E. Rosenberg, A. Carraway and R. Britten, Correlation between gamma-ray-induced DNA double-strand breakage and cell killing after biologically relevant doses: analysis by pulsed-field gel electrophoresis, *Int.J.Radiat.Biol* **65**, 419-426 (1994).

4. G. Iliakis, G. E. Pantelias, R. Okayasu and R. Seaner, I-125 Durd-Induced Chromosome Fragments, Assayed by Premature Chromosome Condensation, and Dna Double-Strand Breaks Have Similar Repair Kinetics in G1-Phase Cho-Cells, *Int.J.Radiat.Biol.* **52**, 705-722 (1987).

5. R. P. Virsik, C. Schafer, D. Harder, D. T. Goodhead, R. Cox and J. Thacker, Chromosome-Aberrations Induced in Human-Lymphocytes by Ultrasoft Alk and Ck X-Rays, *Int.J.Radiat.Biol.* **38**, 545-557 (1980).

6. N. C. Arslan, C. R. Geard and E. J. Hall, Low dose-rate effects of cesium-137 and iodine-125 on cell survival, cell progression, and chromsomal alterations, *Am.J.Clin.Oncol.* **9**, 521-526 (1986).

7. T. R. Munro, The relative radiosensitivity of the nucleus and cytoplasm of Chinese hamster fibroblasts, *Radiat.Res.* **42**, 451-470 (1970).

8. R. L. Warters and K. G. Hofer, Radionuclide toxicity in cultured mammalian cells. Elucidation of the primary site for radiation-induced division delay, *Radiat.Res.* **69**, 348-358 (1977).

9. A. T. Natarajan, G. Obe, A. A. van Zeeland, F. Palitti, M. Meijers and E. A. Verdegaal-Immerzeel, Molecular mechanisms involved in the production of chromosomal aberrations. II. Utilization of Neurospora endonuclease for the study of aberration production by X-rays in G1 and G2 stages of the cell cycle, *Mutat.Res.* **69**, 293-305 (1980).

10. P. E. Bryant, Enzymatic restriction of mammalian cell DNA using Pvu II and Bam H1: evidence for the double-strand break origin of chromosomal aberrations, *Int.J.Radiat.Biol Relat Stud.Phys.Chem.Med.* **46**, 57-65 (1984).

11. A. T. Natarajan and T. S. Zwanenburg, Mechanisms for chromosomal aberrations in mammalian cells, *Mutat.Res.* **95**, 1-6 (1982).

12. S. H. Revell, Relationship between chromosome damage and cell death, *in* "Radiation-Induced Chromosome Damage in Man" (T. Ishihara and M. S. Sasake, Eds.), Alan Liss, New York (1983).

13. M. N. Cornforth and J. S. Bedford, A quantitative comparison of potentially lethal damage repair and the rejoining of interphase chromosome breaks in low passage normal human fibroblasts., *Radiat.Res.* **111**, 385-405 (1987).

14. H. Nagasawa, J. B. Little, W. C. Inkret, S. Carpenter, M. R. Raju, D. J. Chen and G. F. Strniste, Response of X-ray-sensitive CHO mutant cells (xrs-6c) to radiation. II. Relationship between cell survival and the induction of chromosomal damage with low doses of alpha particles, *Radiat.Res.* **126**, 280-288 (1991).

15. G. C. Li, H. Ouyang, X. Li, H. Nagasawa, J. B. Little, D. J. Chen, C. C. Ling, Z. Fuks and C. Cordon-Cardo, Ku70: a candidate tumor suppressor gene for murine T cell lymphoma, *Mol.Cell* **2**, 1-8 (1998).

16. L. M. Fried, C. Koumenis, S. R. Peterson, S. L. Green, P. van Zijl, J. Allalunis-Turner, D. J. Chen, R. Fishel, A. J. Giaccia, J. M. Brown and C. U. Kirchgessner, The DNA damage response in DNA-dependent protein kinase-deficient SCID mouse cells: replication protein A hyperphosphorylation and p53 induction, *Proc.Natl.Acad.Sci.U.S.A* **93**, 13825-13830 (1996).

17. M. A. Stackhouse and J. S. Bedford, An ionizing radiation-sensitive mutant of CHO cells: irs-20. III. Chromosome aberrations, DNA breaks and mitotic delay, *Int.J.Radiat.Biol.* **65**, 571-582 (1994).

18. H. D. Halicka, X. Huang, F. Traganos, M. A. King, W. Dai and Z. Darzynkiewicz, Histone H2AX phosphorylation after cell irradiation with UV-B: relationship to cell cycle phase and induction of apoptosis, *Cell Cycle* **4**, 339-345 (2005).

19. C. L. Limoli, E. Giedzinski, W. M. Bonner and J. E. Cleaver, UV-induced replication arrest in the xeroderma pigmentosum variant leads to DNA double-strand breaks, gamma-H2AX formation, and Mre11 relocalization, *Proceedings of the National Academy of Sciences of the United States of America* **99**, 233-238 (2002).

20. J. B. Leppard and J. J. Champoux, Human DNA topoisomerase I: relaxation, roles, and damage control, *Chromosoma* **114**, 75-85 (2005).

21. A. C. Porter and C. J. Farr, Topoisomerase II: untangling its contribution at the centromere, *Chromosome Res.* **12**, 569-583 (2004).

22. J. E. Haber, DNA recombination: the replication connection, *Trends Biochem.Sci.* **24**, 271-275 (1999).

23. L. Metzger and G. Iliakis, Kinetics of DNA double-strand break repair throughout the cell cycle as assayed by pulsed field gel electrophoresis in CHO cells, *Int.J.Radiat.Biol.* **59**, 1325-1339 (1991).

24. U. Hagen, Mechanisms of induction and repair of DNA double-strand breaks by ionizing radiation: some contradictions, *Radiat.Environ.Biophys.* **33**, 45-61 (1994).

25. L. H. Thompson and D. Schild, Homologous recombinatorial repair of DNA ensures mammalian chromosome stability, *Mutation Res.* **477**, 131-153 (2001).

26. L. H. Thompson and D. Schild, Recombinational DNA repair and human disease, *Mutat.Res.* **509**, 49-78 (2002).

27. L. H. Thompson, Origin, recognition Repair, signaling, and repair of DNA double-strand breaks in mammalian cells., *in* "Eukaryotic DNA Damage Surveillance and Repair" (K. Caldecot, Ed.), Landes Press, Georgetown, TX (2003).

28. K. Rothkamm, I. Kruger, L. H. Thompson and M. Lobrich, Pathways of DNA double-strand break repair during the mammalian cell cycle, *Mol.Cell Biol.* **23**, 5706-5715 (2003).

29. E. A. Wong and M. R. Capecchi, Homologous recombination between coinjected DNA sequences peaks in early to mid-S phase, *Molec.Cell.Biol.* **7**, 2294-2295 (1987).

30. R. S. Nairn, G. M. Adair, C. B. Christmann and R. M. Humphrey, Ultraviolet stimulation of intermolecular homologous recombination in Chinese hamster ovary cells, *Mol.Carcinogen.* **4**, 519-526 (1991).

31. S. Subramani and B. L. Seaton, Homologous recombination in mitotically dividing mammalian cells, *in* "Genetic Recombination" (R. S. Kucherlapati and G. R. Smith, Eds.), American Society for Microbiology, Washington, D.C. (1992).

32. F. Liang, M. Han, P. J. Romanienko and M. Jasin, Homology-directed repair is a major double-strand break repair pathway in mammalian cells, *Proc.Natl.Acad.Sci.U.S.A* **95**, 5172-5177 (1998).

33. P. A. Jeggo, The fidelity of repair of radiation damage, *Radiation Protection Dosimetry* **99**, 117-122 (2002).

34. E. A. Hendrickson, Cell-cycle regulation of mammalian DNA double-strand-break repair, *Am.J.Hum.Genet.* **61**, 795-800 (1997).

35. G. Iliakis, H. Wang, A. R. Perrault, W. Boecker, B. Rosidi, F. Windhofer, W. Wu, J. Guan, G. Terzoudi and G. Pantelias, Mechanisms of DNA double strand break repair and chromosome aberration formation, *Cytogenet.Genome Res.* **104**, 14-20 (2004).

36. S. P. Lees-Miller and K. Meek, Repair of DNA double strand breaks by non-homologous end joining, *Biochimie* **85**, 1161-1173 (2003).

37. G. Petukhova, S. A. Stratton and P. Sung, Single strand DNA binding and annealing activities in the yeast recombination factor Rad59, *J.Biol Chem.* **274**, 33839-33842 (1999).

38. I. R. Radford, The dose-response for low-LET radiation-induced DNA double-strand breakage: methods of measurement and implications for radiation action models, *Int.J.Radiat.Biol* **54**, 1-11 (1988).

39. M. I. Nunez, T. J. McMillan, M. T. Valenzuela, J. M. Ruiz de Almodovar and V. Pedraza, Relationship between DNA damage, rejoining and cell killing by radiation in mammalian cells, *Radiother.Oncol.* **39**, 155-165 (1996).

40. R. A. McGrath and R. W. Williams, Reconstruction in vivo of irradiated Escherichia coli deoxyribonucleic acid; the rejoining of broken pieces, *Nature* **212**, 534-535 (1966).

41. A. R. Lehmann and M. G. Ormerod, Double-strand breaks in the DNA of a mammalian cell after x-irradiation, *Biochim.Biophys.Acta* **217**, 268-277 (1970).

42. R. W. Clark and C. S. Lange, The sucrose gradient and native DNA S20,W, an examination of measurement problems, *Biochim.Biophys.Acta* **454**, 567-577 (1976).

43. R. Kavenoff and B. H. Zimm, Chromosome-sized DNA molecules from Drosophila, *Chromosoma* **41**, 1-27 (1973).

44. D. Blocher, M. Einspenner and J. Zajaclowski, CHEF electrophoresis, a sensitive technique for the determination of DNA double-strand breaks, *Int.J.Radiat.Biol.* **56**, 437-448 (1989).

45. M. O. Bradley and K. W. Kohn, X-ray induced double strand break production and repair in mammalian cells as measured by neutral filter elution, *Nucl.Acids Res.* 7, 793-804 (1979).

46. E. P. Rogakou, D. R. Pilch, A. H. Orr, V. S. Ivanova and W. M. Bonner, DNA double-stranded breaks induce histone H2AX phosphorylation on serine 139, *J Biol.Chem.* **273**, 5858-5868 (1998).

47. O. A. Sedelnikova, E. P. Rogakou, I. G. Panyutin and W. M. Bonner, Quantitative detection of (125) IdU-induced DNA double-strand breaks with gamma-H2AX antibody, *Radiat.Res.* **158**, 486-492 (2002).

48. J. O. Thomas and R. D. Kornberg, An octamer of histones in chromatin and free in solution, *Proc.Natl.Acad.Sci.U.S.A* **72**, 2626-2630 (1975).

49. M. H. West and W. M. Bonner, Histone 2A, a heteromorphous family of eight protein species, *Biochemistry* **19**, 3238-3245 (1980).

50. V. S. Ivanova, C. L. Hatch and W. M. Bonner, Characterization of the Human Histone H2A.X Gene - Comparison of Its Promoter with Other H2A Gene Promoters, *Journal of Biological Chemistry* **269**, 24189-24194 (1994).

51. J. S. Siino, I. B. Nazarov, M. P. Svetlova, L. V. Solovjeva, R. H. Adamson, I. A. Zalenskaya, P. M. Yau, E. M. Bradbury and N. V. Tomilin, Photobleaching of GFP-labeled H2AX in chromatin: H2AX has low diffusional mobility in the nucleus, *Biochem.Biophys.Res.Commun.* **297**, 1318-1323 (2002).

52. S. Burma, B. P. Chen, M. Murphy, A. Kurimasa and D. J. Chen, ATM phosphorylates histone H2AX in response to DNA double-strand breaks, *J.Biol.Chem.* **276**, 42462-42467 (2001).

53. T. Stiff, M. O'Driscoll, N. Rief, K. Iwabuchi, M. Lobrich and P. A. Jeggo, ATM and DNA-PK function redundantly to phosphorylate H2AX after exposure to ionizing radiation, *Cancer Res.* **64**, 2390-2396 (2004).

54. E. Riballo, M. Kuhne, N. Rief, A. Doherty, G. C. Smith, M. J. Recio, C. Reis, K. Dahm, A. Fricke, A. Krempler, A. R. Parker, S. P. Jackson, A. Gennery, P. A. Jeggo and M. Lobrich, A pathway of double-strand break rejoining dependent upon ATM, Artemis, and proteins locating to gamma-H2AX foci, *Mol.Cell* **16**, 715-724 (2004).

55. I. B. Nazarov, A. N. Smirnova, R. I. Krutilina, M. P. Svetlova, L. V. Solovjeva, A. A. Nikiforov, S. L. Oei, I. A. Zalenskaya, P. M. Yau, E. M. Bradbury and N. V. Tomilin, Dephosphorylation of histone gamma-H2AX during repair of DNA double-strand breaks in mammalian cells and its inhibition by calyculin A, *Radiat.Res.* **160**, 309-317 (2003).

56. V. S. Ivanova, D. Zimonjic, N. Popescu and W. M. Bonner, Chromosomal Localization of the Human Histone H2A.X Gene to 11Q23.2-Q23.3 by Fluorescence In-Situ Hybridization, *Hum Genet* **94**, 303-306 (1994).

57. O. Monni and S. Knuutila, 11q deletions in hematological malignancies, *Leuk.Lymphoma* **40**, 259-266 (2001).

58. C. H. Bassing, K. F. Chua, J. Sekiguchi, H. Suh, S. R. Whitlow, J. C. Fleming, B. C. Monroe, D. N. Ciccone, C. Yan, K. Vlasakova, D. M. Livingston, D. O. Ferguson, R. Scully and F. W. Alt, Increased ionizing radiation sensitivity and genomic instability in the absence of histone H2AX, *Proc.Natl.Acad.Sci.U.S.A* **99**, 8173-8178 (2002).

59. A. Celeste, S. Petersen, P. J. Romanienko, O. Fernandez-Capetillo, H. T. Chen, O. A. Sedelnikova, B. Reina-San-Martin, V. Coppola, E. Meffre, M. J. Difilippantonio, C. Redon, D. R. Pilch, A. Olaru, M. Eckhaus, R. D. Camerini-

Otero, L. Tessarollo, F. Livak, K. Manova, W. M. Bonner, M. C. Nussenzweig and A. Nussenzweig, Genomic instability in mice lacking histone H2AX, *Science* **296**, 922-927 (2002).

60. A. Xie, N. Puget, I. Shim, S. Odate, I. Jarzyna, C. H. Bassing, F. W. Alt and R. Scully, Control of sister chromatid recombination by histone H2AX, *Mol.Cell* **16**, 1017-1025 (2004).

61. K. Rothkamm and M. Lobrich, Evidence for a lack of DNA double-strand break repair in human cells exposed to very low x-ray doses, *Proceedings of the National Academy of Sciences of the United States of America* **100**, 5057-5062 (2003).

62. E. P. Rogakou, C. Boon, C. Redon and W. M. Bonner, Megabase chromatin domains involved in DNA double-strand breaks in vivo, *J.Cell Biol.* **146**, 905-915 (1999).

63. S. H. MacPhail, J. P. Banath, T. Y. Yu, E. H. M. Chu, H. Lambur and P. L. Olive, Expression of phosphorylated histone H2AX in cultured cell lines following exposure to X-rays, *Int.J Radiat.Biol.* **79**, 351-358 (2003).

64. P. L. Olive and J. P. Banath, Phosphorylation of histone H2AX as a measure of radiosensitivity, *Int.J Radiat.Oncol.Biol.Phys.* **58**, 331-335 (2004).

65. E. Riballo, M. Kuhne, N. Rief, A. Doherty, G. C. M. Smith, M. J. Recio, C. Reis, K. Dahm, A. Fricke, A. Krempler, A. R. Parker, S. P. Jackson, A. Gennery, P. A. Jeggo and M. Lobrich, A pathway of double-strand break rejoining dependent upon ATM, artemis, and proteins locating to gamma-H2AX foci, *Molecular Cell* **16**, 715-724 (2004).

66. T. Furuta, H. Takemura, Z. Y. Liao, G. J. Aune, C. Redon, O. A. Sedelnikova, D. R. Pilch, E. P. Rogakou, A. Celeste, H. T. Chen, A. Nussenzweig, M. I. Aladjem, W. M. Bonner and Y. Pommier, Phosphorylation of histone H2AX and activation of Mre11, Rad50, and Nbs1 in response to replication-dependent DNA double-strand breaks induced by mammalian DNA topoisomerase I cleavage complexes, *J Biol.Chem.* **278**, 20303-20312 (2003).

67. W. H. Cheng, S. Sakamoto, J. T. Fox, K. Komatsu, J. Carney and V. A. Bohr, Werner syndrome protein associates with gamma H2AX in a manner that depends upon Nbs1, *FEBS Lett.* **579**, 1350-1356 (2005).

68. J. Kobayashi, Molecular mechanism of the recruitment of NBS1/hMRE11/hRAD50 complex to DNA double-strand breaks: NBS1 binds to gamma-H2AX through FHA/BRCT domain, *J.Radiat.Res.(Tokyo)* **45**, 473-478 (2004).

69. E. P. Rogakou, C. Boon, C. Redon and W. M. Bonner, Megabase chromatin domains involved in DNA double-strand breaks in vivo, *J Cell Biol.* **146**, 905-916 (1999).

70. R. Shroff, A. Arbel-Eden, D. Pilch, G. Ira, W. M. Bonner, J. H. Petrini, J. E. Haber and M. Lichten, Distribution and dynamics of chromatin modification induced by a defined DNA double-strand break, *Curr.Biol* **14**, 1703-1711 (2004).

71. E. Unal, A. Arbel-Eden, U. Sattler, R. Shroff, M. Lichten, J. E. Haber and D. Koshland, DNA damage response pathway uses histone modification to assemble a double-strand break-specific cohesin domain, *Mol.Cell* **16**, 991-1002 (2004).

72. T. J. Reitsema, J. P. Banath, S. H. MacPhail and P. L. Olive, Hypertonic saline enhances expression of phosphorylated histone H2AX after irradiation, *Radiat.Res.* **161**, 402-408 (2004).

73. N. I. Dmitrieva, Q. Cai and M. B. Burg, Cells adapted to high NaCl have many DNA breaks and impaired DNA repair both in cell culture and in vivo, *Proc.Natl.Acad.Sci.U.S.A* **101**, 2317-2322 (2004).

74. A. Takahashi, H. Matsumoto, K. Nagayama, M. Kitano, S. Hirose, H. Tanaka, E. Mori, N. Yamakawa, J. Yasumoto, K. Yuki, K. Ohnishi and T. Ohnishi, Evidence for the involvement of double-strand breaks in heat-induced cell killing, *Cancer Res.* **64**, 8839-8845 (2004).

75. D. Szuts and T. Krude, Cell cycle arrest at the initiation step of human chromosomal DNA replication causes DNA damage, *J.Cell Sci.* **117**, 4897-4908 (2004).

76. O. A. Sedelnikova, I. Horikawa, D. B. Zimonjic, N. C. Popescu, W. M. Bonner and J. C. Barrett, Senescing human cells and ageing mice accumulate DNA lesions with unrepairable double-strand breaks, *Nature Cell Biology* **6**, 168-+ (2004).

77. J. P. Banath, S. H. MacPhail and P. L. Olive, Radiation sensitivity, H2AX phosphorylation, and kinetics of repair of DNA strand breaks in irradiated cervical cancer cell lines, *Cancer Res.* **64**, 7144-7149 (2004).

78. K. Ishizaki, Y. Hayashi, H. Nakamura, Y. Yasui, K. Komatsu and A. Tachibana, No induction of p53 phosphorylation and few focus formation of phosphorylated H2AX suggest efficient repair of DNA damage during chronic low-dose-rate irradiation in human cells, *J.Radiat.Res.(Tokyo)* **45**, 521-525 (2004).

79. S. H. MacPhail, J. P. Banath, Y. Yu, E. Chu and P. L. Olive, Cell cycle-dependent expression of phosphorylated histone H2AX: reduced expression in unirradiated but not X-irradiated G1-phase cells, *Radiat.Res.* **159**, 759-767 (2003).

80. X. Huang, M. A. King, H. D. Halicka, F. Traganos, M. Okafuji and Z. Darzynkiewicz, Histone H2AX phosphorylation induced by selective photolysis of BrdU-labeled DNA with UV light: relation to cell cycle phase, *Cytometry A* **62**, 1-7 (2004).

81. C. L. Limoli, E. Giedzinski, W. M. Bonner and J. E. Cleaver, UV-induced replication arrest in the xeroderma pigmentosum variant leads to DNA double-strand breaks, gamma -H2AX formation, and Mre11 relocalization, *Proc.Natl.Acad.Sci.U.S.A* **99**, 233-238 (2002).

82. M. Swift, L. Sholman, M. Perry and C. Chase, Malignant neoplasms in the families of patients with ataxia-telangiectasia., *Cancer Res.* **36**, 209-215 (1976).

83. M. Swift, D. Morrell, E. Cromartie, A. R. Chamberlin, M. H. Skolnick and D. T. Bishop, The incidence and gene frequency of ataxia-telangiectasia in the United States, *Am.J Hum.Genet.* **39**, 573-583 (1986).

84. M. Swift, D. Morrell, R. B. Massey and C. L. Chase, Incidence of cancer in 161 families affected by ataxia-telangiectasia, *NEJM* **325**, 1831-1836 (1991).

85. D. F. Easton, Cancer risks in A-T heterozygotes, *Int.J Radiat.Biol.* **66**, S177-S182 (1994).

86. A. M. Taylor, What has the cloning of the ATM gene told us about ataxia telangiectasia?, *Int.J Radiat.Biol.* **73**, 365-371 (1998).

87. K. Savitsky, A. Bar-Shira, S. Gilad, G. Rotman, Y. Ziv, L. Vanagaite, D. A. Tagle, S. Smith, T. Uziel, S. Sfez, M. Askenazi, I. Pecker, M. Frydman, R. Harnik, S. R. Patanjali, A. Simmons, G. A. Clines, R. A. Sartiel, R. A. Gatti, L. Chessa, O. Sanal, M. F. Lavin, N. G. J. Jaspers, A. M. R. Taylor, C. F. Arlett, T. Miki, S. M. Weissman, M. Lovett, F. Collins and Y. Shiloh, A single ataxia telangiectasia gene with a product similar to PI-3 kinase, *Science* **268**, 1749-1753 (1995).

88. T. Uziel, K. Savitsky, M. Platzer, Y. Ziv, T. Helbitz, M. Nehls, T. Boehm, A. Rosenthal, Y. Shiloh and G. Rotman, Genomic Organization of the ATM gene, *Genomics* **33**, 317-320 (1996).

89. N. D. Lakin, P. Weber, T. Stankovic, S. T. Rottinghaus, A. M. Taylor and S. P. Jackson, Analysis of the ATM protein in wild-type and ataxia telangiectasia cells, *Oncogene* **13**, 2707-2716 (1996).

90. A. M. Taylor, C. M. Rosney and J. B. Campbell, Unusual sensitivity of ataxia telangiectasia cells to bleomycin, *Cancer Res.* **39**, 1046-1050 (1979).

91. A. M. R. Taylor, D. G. Harnden, C. F. Arlett, a. r. Harcourt, A. R. Lehmann, S. Stevens and B. A. Bridges, Ataxia-telangiectasia: a human mutation with abnormal radiation sensitivity, *Nature* **258**, 427-429 (1975).

92. M. A. Bender, J. M. Rary and R. P. Kale, G2 chromosomal radiosensitivity in ataxia telangiectasia lymphocytes, *Mutat.Res.* **152**, 39-47 (1985).

93. J. B. Little and H. Nagasawa, Effect of confluent holding on potentially lethal damage repair, cell cycle progression, and chromosomal aberrations in human normal and ataxia-telangiectasia fibroblasts, *Radiat.Res.* **101**, 81-93 (1985).

94. M. N. Cornforth and J. S. Bedford, On the nature of a defect in cells from individuals with ataxia telangiectasia., *Science* **227**, 1589-1591 (1985).

95. Y. Shiloh, E. Tabor and Y. Becker, Abnormal response of ataxia-telangiectasia cells to agents that break the deoxyribose moiety of DNA via a targeted free radical mechanism, *Carcinogenesis* **4**, 1317-1322 (1983).

96. M. S. Meyn, Ataxia-telangiectasia and cellular responses to DNA damage, *Cancer Res.* **55**, 5991-6001 (1995).

97. A. J. Fornace and J. B. Little, Normal repair of DNA single-strand breaks in patients with ataxia telangiectasia, *Biochim.Biophys.Acta* **607**, 432-437 (1980).

98. R. B. Painter and B. R. Young, Radiosensitivity in ataxia-telangiectasia: a new explanation, *Proc.Natl.Acad.Sci.U.S.A* **77**, 7315-7317 (1980).

99. J. P. Murnane and R. B. Painter, Complementation of the defects of DNA synthesis in irradiated and unirradiated ataxia-telangiectasia cells, *Proc.Natl Acad.Sci.U.S.A* **79**, 1960-1963 (1982).

100. I. Pecker, K. B. Avraham, D. J. Gilbert, K. Savitsky, G. Rotman, R. Harnik, T. Fukao, E. Schrock, S. Hirotsune, D. A. Tagle, F. S. Collins, A. Wynshaw-Boris, T. Ried, N. G. Copeland, N. A. Jenkins, Y. Shiloh and Y. Ziv, Identification and chromosomal localization of Atm, the mouse homolog of the ataxia-telangiectasia gene, *Genomics* **35**, 39-45 (1996).

101. C. Barlow, S. Hirotsune, R. Paylor, M. Liyanage, M. Eckhaus, F. Collins, Y. Shiloh, J. N. Crawley, T. Ried, D. Tagle and A. Wynshaw-Boris, Atm-deficient mice: a paradigm of ataxia telangiectasia, *Cell* **86**, 159-171 (1996).

102. B. V. Worgul, L. Smilenov, D. J. Brenner, A. Junk, W. Zhou and E. J. Hall, Atm heterozygous mice are more sensitive to radiation-induced cataracts than are their wild-type counterparts, *Proc.Natl.Acad.Sci.U.S.A* **99**, 9836-9839 (2002).

103. M. M. Weil, F. S. Kittrell, Y. Yu, M. McCarthy, R. C. Zabriskie and R. L. Ullrich, Radiation induces genomic instability and mammary ductal dysplasia in Atm heterozygous mice, *Oncogene* **20**, 4409-4411 (2001).

104. L. B. Smilenov, D. J. Brenner and E. J. Hall, Modest increased sensitivity to radiation oncogenesis in ATM heterozygous versus wild-type mammalian cells, *Cancer Res.* **61**, 5710-5713 (2001).

105. K. Spring, F. Ahangari, S. P. Scott, P. Waring, D. M. Purdie, P. C. Chen, K. Hourigan, J. Ramsay, P. J. McKinnon, M. Swift and M. F. Lavin, Mice heterozygous for mutation in Atm, the gene involved in ataxia-telangiectasia, have heightened susceptibility to cancer, *Nature Genet.* **32**, 185-190 (2002).

106. E. U. Kurz and S. P. Lees-Miller, DNA damage-induced activation of ATM and ATM-dependent signaling pathways, *DNA Repair (Amst)* **3**, 889-900 (2004).

107. M. F. Lavin, G. Birrell, P. Chen, S. Kozlov, S. Scott and N. Gueven, ATM signaling and genomic stability in response to DNA damage, *Mutat.Res.* **569**, 123-132 (2005).

108. G. C. Smith, R. B. Cary, N. D. Lakin, B. C. Hann, S. H. Teo, D. J. Chen and S. P. Jackson, Purification and DNA binding properties of the ataxia-telangiectasia gene product ATM, *Proc.Natl.Acad.Sci.U.S.A* **96**, 11134-11139 (1999).

109. C. J. Bakkenist and M. B. Kastan, DNA damage activates ATM through intermolecular autophosphorylation and dimer dissociation, *Nature* **421**, 499-506 (2003).

110. M. Swift, P. J. Reitnauer, D. Morrell and C. L. Chase, Breast and other cancers in families with ataxia-telangiectasia, *N.Engl.J Med.* **316**, 1289-1294 (1987).

111. E. C. Pippard, A. J. Hall, J. P. Barker and B. A. Bridges, Cancer in heterozygotes of ataxia-telangiectasia and xeroderma pigmentosum in Britian, *Cancer Res.* **48**, 2929-2932 (1988).

112. D. Thompson, S. Duedal, J. Kirner, L. McGuffog, J. Last, A. Reiman, P. Byrd, M. Taylor and D. F. Easton, Cancer Risks and Mortality in Heterozygous ATM Mutation Carriers, *J Natl Cancer Inst* **97**, 813-822 (2005).

113. M. C. Paterson, A. K. Anderson, B. P. Smith and P. J. Smith, Enhanced radiosensitivity of cultured fibroblasts from ataxia telangiectasia heterozygotes manifested by defective colony-forming ability and reduced DNA repair replication after hypoxic gamma-irradiation, *Cancer Res.* **39**, 3725-3734 (1979).

114. J. Cole, C. F. Arlett, M. H. Green, S. A. Harcourt, A. Priestley, L. Henderson, H. Cole, S. E. James and F. Richmond, Comparative human cellular radiosensitivity: II. The survival following gamma-irradiation of unstimulated (G0) T-lymphocytes, T-lymphocyte lines, lymphoblastoid cell lines and fibroblasts from normal donors, from ataxia-telangiectasia patients and from ataxia-telangiectasia heterozygotes, *Int.J.Radiat.Biol.* **54**, 929-943 (1988).

115. H. Nagasawa and J. B. Little, Radiosensitivities of ten apparently normal human diploid fibroblast strains to cell killing, G2-phase chromosomal aberrations, and cell cycle delay, *Cancer Res.* **48**, 4535-4538 (1988).

116. P. C. Chen, M. F. Lavin, C. Kidson and D. Moss, Identification of ataxia telangiectasia heterozygotes, a cancer prone population, *Nature* **274**, 484-486 (1978).

117. C. M. West, S. A. Elyan, P. Berry, R. Cowan and D. Scott, A comparison of the radiosensitivity of lymphocytes from normal donors, cancer patients, individuals with ataxia-telangiectasia (A-T) and A-T heterozygotes, *Int.J.Radiat.Biol.* **68**, 197-203 (1995).

118. A. Tchirkov, J. O. Bay, D. Pernin, Y. J. Bignon, P. Rio, M. Grancho, F. Kwiatkowski, M. Giollant, P. Malet and P. Verrelle, Detection of heterozygous carriers of the ataxia-telangiectasia (ATM) gene by G2 phase chromosomal radiosensitivity of peripheral blood lymphocytes, *Hum.Genet.* **101**, 312-316 (1997).

119. H. Nagasawa, K. H. Kraemer, Y. Shiloh and J. B. Little, Detection of ataxia telangiectasia heterozygous cell lines by postirradiation cumulative labeling index: measurements with coded samples, *Cancer Res.* **47**, 398-402 (1987).

120. P. J. Deschavanne, D. Debieu, D. Fertil and E. P. Malaise, Re-evaluation of *in vitro* radiosensitivity of human fibroblasts of different genetic origins, *Internation Journal of Radiation Biology* **50**, 279-293 (1986).

121. M. M. Fitzek, W. K. Dahlberg, H. Nagasawa, S. Mukai, J. E. Munzenrider and J. B. Little, Unexpected sensitivity to radiation of fibroblasts from unaffected parents of children with hereditary retinoblastoma, *Int.J.Cancer* **99**, 764-768 (2002).

122. D. T. Goodhead, Initial events in the cellular effects of ionizing radiations: clustered damage in DNA, *Int.J.Radiat.Biol.* **65**, 7-17 (1994).

123. J. S. Bedford and E. J. Hall, Survival of Hela cells cultured *in vitro* and exposed to protracted gamma radiation, *Int.J.Radiat.Biol.* 7, 377-383 (1963).

124. R. Cox, A cellular description of the repair defect in ataxia-telangiectasia, *in* "Ataxia. Telangiectasia : A Cellular and Molecular Link Between Cancer, Neuropathology and. Immune Deficiency" (B. A. Bridges and D. G. Harden, Eds.), John Wiley and Sons Ltd., Chichester, UK (1982).

125. K. Sax, The time factor in x-ray production of chromosomal aberrations, *Proc.Natl.Acad.Sci.USA* **25**, 225-233 (1939).

126. R. L. Wells and J. S. Bedford, Dose-rate effects in mammalian cells. IV. Repairable and nonrepairable damage in noncycling C3H 10T 1/2 cells, *Radiat.Res.* **94**, 105-134 (1983).

127. M. A. Stackhouse and J. S. Bedford, An ionizing radition-sensitive mutant of CHO cells: irs-20 Isolation and initial characterization, *Radiat.Res.* **136**, 241-249 (1993).

128. C. B. Bennett, A. L. Lewis, K. K. Baldwin and M. A. Resnick, Lethality induced by a single site-specific double-strand break in a dispensable yeast plasmid, *Proc.Natl.Acad.Sci.U.S.A* **90**, 5613-5617 (1993).

129. D. Blocher, D. Sigut and M. A. Hannan, Fibroblasts from ataxia telangiectasia (AT) and AT heterozygotes show an enhanced level of residual DNA double-strand breaks after low dose-rate gamma-irradiation as assayed by pulsed field gel electrophoresis, *Int.J Radiat.Biol.* **60**, 791-802 (1991).

130. R. Parshad, K. K. Sanford and G. M. Jones, Chromatid damage after G2 phase x-irradiation of cells from cancer-prone individuals implicates deficiency in DNA repair, *Proc.Natl.Acad.Sci.USA* **80**, 5612-5616 (1983).

131. R. Parshad, K. K. Sanford and G. M. Jones, Chromosmal radiosensitivity during the G2 cell-cycle period of skin fibroblasts from individuals with familal cancer, *Proc.Natl.Acad.Sci.USA* **82**, 5400-5403 (1983).

132. Y. Shiloh, R. Parshad, M. Frydman, K. K. Sanford, S. Portnoi, Y. Ziv and G. M. Jones, G2 chromosomal radiosensitivity in families with ataxia-telangiectasia, *Hum.Genet.* **84**, 15-18 (1989).

133. K. K. Sanford, R. Parshad, F. M. Price, R. E. Tarone and W. F. Benedict, Cytogenetic responses to G(2) phase x-irradiation of cells from retinoblastoma patients, *Cancer Genet.Cytogenet.* **88**, 43-48 (1996).

134. K. K. Sanford and R. Parshad, Detection of cancer-prone individuals using cytogenetic response to X-rays, *in* "Chromosome Aberrations, Basic and Applied Aspects" (G. Obe and A. T. Natarajan, Eds.), Springer-Verlag, Berlin (1990).

135. D. Scott, A. R. Spreadborough, L. A. Jones, S. A. Roberts and C. J. Moore, Chromosomal radiosensitivity in G_2-phase lymphocytes as an indicator of cancer predisposition, *Radiat.Res.* **145**, 3-16 (1996).

136. K. K. Sanford, R. Parshad, R. R. Gantt and R. E. Tarone, A deficiency in chromatin repair, genetic instability, and predisposition to cancer, *CRC Critical Reviews in Oncogenesis* **1**, 323-341 (1989).

137. S. A. Roberts, A. R. Spreadborough, B. Bulman, J. B. Barber, D. G. R. Evans and D. Scott, Heritability of cellular radiosensitivity: a marker of low-penetrance predisposition genes in breast cancer?, *American Journal of Human Genetics* **65**, 784-794 (1999).

138. D. Scott, L. A. Jones, S. A. G. Elyan, A. Spreadborough, R. Cowan and G. Ribiero, Identification of A-T heterozygotes, *in* "Atataxia-telangiectasia" (R. A. Gatti and R. B. Painter, Eds.), Springer-Verlag, Berlin (1992).

139. D. Scott, J. B. Barber, A. R. Spreadborough, W. Burrill and S. A. Roberts, Increased chromosomal radiosensitivity in breast cancer patients: a comparison of two assays, *Int.J.Radiat.Biol.* **75**, 1-10 (1999).

140. D. Scott, A. Spreadborough, E. Levine and S. A. Roberts, Genetic predisposition in breast cancer, *Lancet* **344**, 1444 (1994).

141. A. Vral, H. Thierens, A. Baeyens and R. L. De, The micronucleus and G2-phase assays for human blood lymphocytes as biomarkers of individual sensitivity to ionizing radiation: limitations imposed by intraindividual variability, *Radiat.Res.* **157**, 472-477 (2002).

142. P. N. Rao and R. T. Johnson, Mammalian cell fusion: I. Studies on the regulation of DNA synthesis and mitosis, *Nature* **225**, 159-164 (1970).

143. R. T. Johnson and P. N. Rao, Mammalian cell fusion: induction of premature chromosome condensation in interphase nuclei, *Nature* **226**, 717-722 (1970).

144. P. N. Rao and R. T. Johnson, Premature chromosome condensation: a mechanism for the elimination of chromosomes in virus-fused cells, *J.Cell Sci.* **10**, 495-513 (1972).

145. E. Gotoh, Y. Asakawa and H. Kosaka, Inhibition of Protein-Serine Threonine Phosphatases Directly Induces Premature Chromosome Condensation in Mammalian Somatic-Cells, *Biomedical Research-Tokyo* **16**, 63-68 (1995).

146. C. A. Waldren and R. T. Johnson, Analysis of interphase chromosome damage by means of premature chromosome condensation after X-ray and ultraviolet irradiation, *Proc.Natl.Acad.Sci.USA* **71**, 1137-1141 (1974).

147. M. N. Cornforth and J. S. Bedford, X-ray induced breakage and rejoining of human interphase chromosomes., *Science* **222**, 1141-1143 (1983).

148. M. N. Cornforth and J. S. Bedford, High-resolution measurement of breaks in prematurely condensed chromosomes by differential staining, *Chromosoma* **88**, 315-318 (1983).

149. M. N. Cornforth and J. S. Bedford, Measurement of Chromosome Breaks During Interphase - the Dose-Response and Rejoining Kinetics in Human-Cells Following Low-Doses of X-Rays, *Radiat.Res.* **94**, 570 (1983).

Chapter 2

γ-H2AX Foci after Low Dose-Rate Irradiation Reveal Mouse *Atm* Haploinsufficiency

ABSTRACT

I have investigated the use of the γ-H2AX assay, reflecting the presence of DNA double strand breaks (DSBs), as a possible means for identifying individuals who may be intermediate with respect to the extremes of hyper-radiosensitivity phenotypes. In this case, cells were studied from mice that were normal (*Atm*+/+), heterozygous (*Atm* +/–), or homozygous recessive (*Atm* –/–) for a truncating mutation in the *Atm* gene. After single acute (high dose-rate) exposures, differences in mean numbers of γ-H2AX foci per cell between samples from *Atm* +/+ and *Atm* –/– mice were clear at nearly all sampling times, but at no sampling time was there a clear distinction for cells from *Atm*+/+ vs. *Atm* +/– mice. In contrast, under conditions of low dose-rate irradiation at 10 cGy/hour, appreciable differences in the levels of γ-H2AX foci per cell were observed in synchronized G_1 cells derived from *Atm* +/– mice relative to cells from *Atm* +/+ mice. The levels were intermediate between those for cells from *Atm* +/+ and *Atm* –/– mice. After 24 hours exposure at this dose-rate, measurements in cells from four different mice for each genotype yielded mean frequencies of foci per cell of 1.77 ± 0.13 (SEM) for *Atm* +/+ cells, 4.75 ± 0.2 for the *Atm* +/– cells, and 11.10 ± 0.33 for the *Atm* –/– cells. The distributions of foci per G_1 cell were not significantly different from Poisson. To the

extent that variations in sensitivity with respect to γ-H2AX foci formation reflect variations in radiosensitivity for biological effects of concern, such as carcinogenesis, this assay may provide a relatively straightforward means for distinguishing individuals who are also mildly hypersensitive to radiation, such as I observed for *Atm* heterozygous mice.

INTRODUCTION

Numerous studies have reported on a correlation between cancer susceptibility and an increased sensitivity to the induction of G_2 chromosomal aberration induction following exposure to ionizing radiation or other treatments that directly or indirectly produce DNA DSBs. One interesting example has involved approaches to the identification of A-T heterozygotes who are at increased risk for breast cancer (eg., (1-7)). Scott and his colleagues have reported that numerous factors associated with experimental protocols can influence the outcome of assay itself (5). However, they have shown that by including appropriate matched controls within each assay a significant G_2 chromosomal hyper-radiosensitivity was observed for a group of A-T heterozygotes relative to controls. This assay has also been used to show an elevated G_2 chromosomal radiosensitivity in lymphocytes of randomly selected breast cancer patients of unknown *ATM* genotype, compared to cells from normal control individuals (4,8). The proportion of these breast cancer patients whose lymphocytes showed elevated sensitivity was some 40%; far greater than the expected population frequency of A-T heterozygotes (of the order of 0.5% to 1%), and even greater than the total expected frequency of this population together with populations of individuals with mutations of *BRCA1, BRCA2, and TP53*, which add less than another 5% (4,7,9). In the earlier report of Scott and co-workers it is of interest to note that some 9% of samples from the control population showed G_2 chromosomal radiosensitivities overlapping the range seen for A-T heterozygotes (8). The assay has generally been recognized as very useful even if some have reported it to be less that robust (eg., (10,11)).

Another potentially useful assay, involving chromosomal aberrations measured by whole chromosome painting by fluorescence *in situ* hybridization, was reported using human lymphocytes and lymphoblast lines from A-T and Nijmegen Breakage Syndrome (NBS) families (12). This report showed that both A-T and NBS heterozygotes could be distinguished from normal individuals by hypersensitivity to radiation. The mean number of chromosome breakpoints per cell were significantly higher for cells from individuals from these groups relative to controls, although some 15 to 20% of the mean values for heterozygotes fell in the range of means for the normal controls

A different G_2 chromosomal aberration assay was reported recently by Johnson and colleagues (13), based on their earlier observation that camptothecin (CPT*) causes DNA DSBs by promoting the collapse of replication forks during S phase, and that A-T fibroblasts are defective in the repair of these kinds of DSBs (14). This assay clearly distinguished A-T heterozygotes, largely due to a higher sensitivity for induction of chromatid exchanges in prematurely condensed chromosomes of G_2 cells (14) .

Predating most of the so-called "G_2 assays" showing hyper-radiosensitivity for *ATM* heterozygotes, Nagasawa and Little and their colleagues demonstrated a significant difference in radiation induced G_1 blocks and delayed entry into S phase following irradiation and subculture of different strains of contact inhibited fibroblasts derived from *ATM* heterozygotes relative to both normal individuals and *ATM* homozygotes (15-17). In most cases, the cells from *ATM* heterozygotes were also mildly hypersensitive to radiation induced cell killing (17).

To the extent that variations in DNA DSB processing pathways contribute to variations in susceptibilities among individuals to cancer, measurement of γ-H2AX foci

in cells promises to be a sensitive marker for tracking these variations indirectly (18-20). For acute high dose-rate exposures to sparsely ionizing radiations, the initial induction of DSBs per cell (per unit of DNA) is approximately the same for a given dose, regardless of genetic defects that may lead to altered radiation responses. Thus, differences in responses depend largely on differences in DNA DSB repair capacity and the balance of repair vs. misrepair and other processes that occur after irradiation.

Virtually all important biological effects of radiation, such as mutagenesis, carcinogenesis, and cell killing are influenced by dose-rate or the manner in which a dose is administered in time (eg, (21-29)). The dose-rate effect is due, in large part, to the capacity for cells to repair important molecular lesions, such as DSBs. A given dose is generally less effective if it is spread over a period of hours, days or weeks, as opposed to being administered acutely within a few minutes. Cells defective in such repair processes generally show much reduced sparing by low dose-rate irradiation compared to the relatively larger dose-rate effect for repair proficient cells. Consequently, a much larger difference in responses between defective and proficient cells is generally seen for low than for high dose-rate exposure conditions (30-33). This property was the basis for a strategy used in this laboratory to isolate radiosensitive mutant cell lines that proved to have defects in DNA DSB damage processing (31,32,34,35), so I reasoned that a γ-H2AX assay carried out at low dose-rate might also provide a more sensitive means for distinguishing even mildly hyper-radiosensitive individuals than would be possible for acute high dose-rate exposures. I tested this hypothesis by comparing numbers of γ-H2AX foci in cells from mice that were heterozygous for the *Atm* gene (*Atm +/–)* with

cells from *Atm* +/+ and *Atm* −/− mice after either 24 hours of continuous irradiation at a dose-rate of 10 cGy per hour, or at various times after a single acute γ-ray dose of 1 Gy.

I found that for the 1 Gy acute (high dose-rate) exposure there was a clear separation in the mean numbers of γ-H2AX foci per cell for *Atm*+/+ and *Atm* −/− mice at most sampling times after irradiation, but there was very little difference in the means between the *Atm*+/+ and *Atm* +/− mice. The same γ-H2AX assay carried out at low dose-rate, however, revealed a highly significant difference in foci per cell between cells from *Atm* +/− and *Atm* +/+ mice, allowing an unequivocal distinction between mice of these genotypes and, as expected, an even greater difference between cells from the *Atm*+/+ and the *Atm* −/− mice.

MATERIALS AND METHODS

Mice and Cell Strains

The cell strains were primary cultures derived from ear punch biopsies from mice that were being used to generate congenic strains for the Atm^{tm1Awb} knockout allele (36). The founder strain is 129S6/SvEvTac- Atm^{tm1Awb}. At the time tissues were collected, the knockout allele was fully introgressed onto the A/J background and partially introgressed onto the CBA/J background. The progeny of $Atm^{tm1Awb/+}$ × $Atm^{tm1Awb/+}$ matings were genotyped by PCR amplification of tail snip DNA using a protocol provided by Dr Carrolee Barlow. The amplification primers used were GACTTCTGTCAGATGTTGCTGCC (ATM-F), CGAATTTGCAGGAGTTGCTGAG (ATM-B), and GGGTGGGATTAGATAAATGCCTG (ATM-Neo). The strains, genotypes, and sex of mice used for establishing the cultures are summarized in Table 2-1.

Cell Culture

Cells were cultured in Minimum Essential Medium (MEM) supplemented with 10% Fetal Bovine Serum (FBS), 100units/ml of penicillin and 100μg/ml of streptomycin, and were maintained at 37°C in a humidified atmosphere of 5% CO_2 in air. Because cells in S-phase have much higher levels of spontaneous γ-H2AX foci, and also because the number of foci per cell depends on DNA content (19), I carried out these experiments with cells synchronized and maintained in G_1 during the irradiation exposures using the isoleucine deprivation method (37).

Table 2-1
Mouse cell strains characteristics.

Atm status	Mouse ID #	Mouse Strain	Genotype	Sex
+/+	362	129S6-CBA/J mixed	*Atm* $^{+/+}$	Male
	390	129S6		Male
	412	129S6		Male
	659	129S6		Female
+/–	370	129S6-CBA/J mixed	*Atm* $^{tm1Awb/+}$	Male
	407	129S6		Male
	416	129S6		Male
	420	129S6		Male
–/–	338	129S6	*Atm* $^{tm1Awb/tm1Awb}$	Male
	347	129S6		Male
	417	129S6		Male
	679	129S6		Male

Since polyploidy and aneuploidy can sometimes develop in cultures after several serial subcultures following their establishment from primary explants, and could therefore contribute to a non-uniform population of cells with respect to DNA content, I measured the distribution of DNA content per cell in cultures at the time the experiments were carried out. As an internal reference standard I utilized a mosquito cell line which has approximately 30% of the DNA content of mammalian cells, and these were mixed together and stained with the mouse cell samples during the flow cytometry measurements (38,39). After cells were grown in normal medium to approximately 80% confluence, this medium was removed and replaced with MEM made without the addition of isoleucine, and containing 5% dialyzed FBS. Between 20 and 40 hours after this medium change, 95% of cells had accumulated in the G_1-phase as confirmed by BrdU uptake analysis (by immunocytochemistry) and by DNA content analysis by flow cytometry as described above and on previous occasions (38-40).

The flow cytometry and BrdU uptake results indicated that the DNA content heterogeneity was not likely to be a serious problem, but to minimize contamination of the synchronized diploid G_1 sample populations with S or G_2, or any polyploid cells at the time of scoring γ-H2AX foci, I scored only the smaller cell nuclei, avoiding occasional larger cell nuclei. As will be shown and discussed below the distributions of foci per cell observed by scoring only these smaller nuclei did not show evidence of appreciable contamination with S-, G_2-, or polyploid cells or with cells of appreciably different radiosensitivity, that would have resulted in distortions of the expected Poisson distributions for uniform populations of G_1 cells. I therefore concluded that any such

contamination would not be sufficient to affect conclusions drawn from this study, and in any case I saw no evidence that any heterogeneities that were observed were any different for samples from the different groups of mice with different *Atm* genotypes.

Irradiations:

Irradiations were carried out using either a J.L. Shepherd Model Mark I-68 6000 Ci ^{137}Cs irradiator or in a 37°C low dose-rate irradiation facility in which (depending on the dose-rate desired) samples can be placed at various distances above a plane of from one to twelve 4Ci ^{137}Cs sources that are remotely positioned under the cell cultures or retracted into the shielded safe position. These irradiation facilities have been described previously (34,41,42). Dose-rates and field uniformities over the position of samples were measured using an ion chamber (Radcal 2025AC Radiation monitor with 20x5-180 Electrometer/Ion chamber). The dose-rate for the acute high dose-rate exposure was 250cGy/min. The dose-rate for the 24-hour protracted low-dose rate exposures was 9.9 to 10.2 cGy/hour.

Cells were grown on chamber slides or flaskettes to form a monolayer as described above, and when samples were ready for irradiation, flasks were sealed and placed in position in the appropriate irradiator. After the low dose-rate exposures, cells were immediately (within 5 minutes) processed for immunocytochemistry as described below. After the high dose rate exposures samples were returned to the incubator and processed at various times later to determine the time course of γ-H2AX development.

γ-H2AX: Immunocytochemistry

After irradiation, cells were washed with ice cold PBS and fixed in PBS containing 4% paraformaldehyde for 15min. After three further washes with PBS for 10min, cells were treated with 0.2% Triton X-100 solution in PBS for 5min. Before immunocytochemical detection of γ-H2AX, cells were blocked with 10% goat serum solution for 1 hour at room temperature or overnight at 4°C to reduce subsequent non-specific antibody binding.

Primary rabbit polyclonal antibody from Trevigen (Gaitherburg, MD) or mouse monoclonal antibody from Upstate (Chicago, IL), was diluted 1:100 or 1:500 respectively, and chamber slides or flaskettes with the cell monolayers were incubated in the diluted antiserum for 1 hour at 37°C. Cells were then washed with PBS 3 times for 10min. each, and secondary antibody (Alexa Fluor, Molecular Probes (Eugene, OR)) diluted 1:100 for anti-rabbit primary or 1:500 for anti-mouse primary was added and the slides were incubated for another 1 hour at 37°C. Slides were mounted in a solution of 1.5μg/ml DAPI containing slow-fade (Molecular Probes) after 4 washes with PBS for 10min each. There were some differences in levels of fluorescence signal strength from individual foci depending on whether the rabbit polyclonal or mouse monoclonal antibodies were used, but the number of foci was approximately the same.

γ-H2AX: Scoring Foci

Images of cells were obtained using an Olympus AX-70 fluorescence microscope equipped with a PSI image analysis system utilizing the MAC-Probe package. The thickness of the cell nuclei for these mouse cell strains when the cells are attached and flattened to the culture vessel surface is typically around 2 micrometers (43) and the foci

were sufficiently intense that focusing the microscope approximately midway through the nuclei revealed virtually all the γ-H2AX foci present, as judged by counting all the foci as the focal plane was moved from the top to the bottom of the nuclei compared to the numbers for counts taken with the focal plane midway through the nucleus. There was often some non-specific background signal over and between cells that was smaller and less intensely fluorescent than the γ-H2AX foci, so before counting foci the images were processed by a "background subtraction" applied uniformly across the microscope fields. The processed images were stored and cells from these were later scored. As mentioned above, only the smaller cell nuclei were scored, and the occasional larger nuclei were ignored. Samples were coded so the scorer did not know their origin.

RESULTS

Acute high dose-rate irradiation:

The time course for development and disappearance γ-H2AX foci after an acute high dose-rate γ-ray exposure of 1 Gy was measured for cells from the six of the twelve mouse cell strains, two from each *Atm* genotype (Mouse ID Numbers 390, 412, 407, 416, 347 and 417 shown in Table 2-1). After irradiation, the cultures were incubated for 5, 10, 15, 20, 30, 45, 60 minutes, and 3, 6, 12, and 24 hours and then processed for examination and enumeration of γ-H2AX foci per cell. The results are plotted in Figure 2-1.

The general patterns of change in the appearance and disappearance of γ-H2AX foci as a function of time after irradiation were dependent on the *Atm* genotype. In the cells from normal *Atm* +/+ mice, the number of γ-H2AX foci increased rapidly, reaching a maximum about 20 minutes after irradiation, then decreased to half its maximum value by about 40 minutes, and finally decreased more slowly with another halving of the number of foci per cell occurring some 2 hours later. By 12 or 24 hours after irradiation the number of foci per cell had decreased to only about 5% of the maximum value. These estimates allow for a zero-dose background

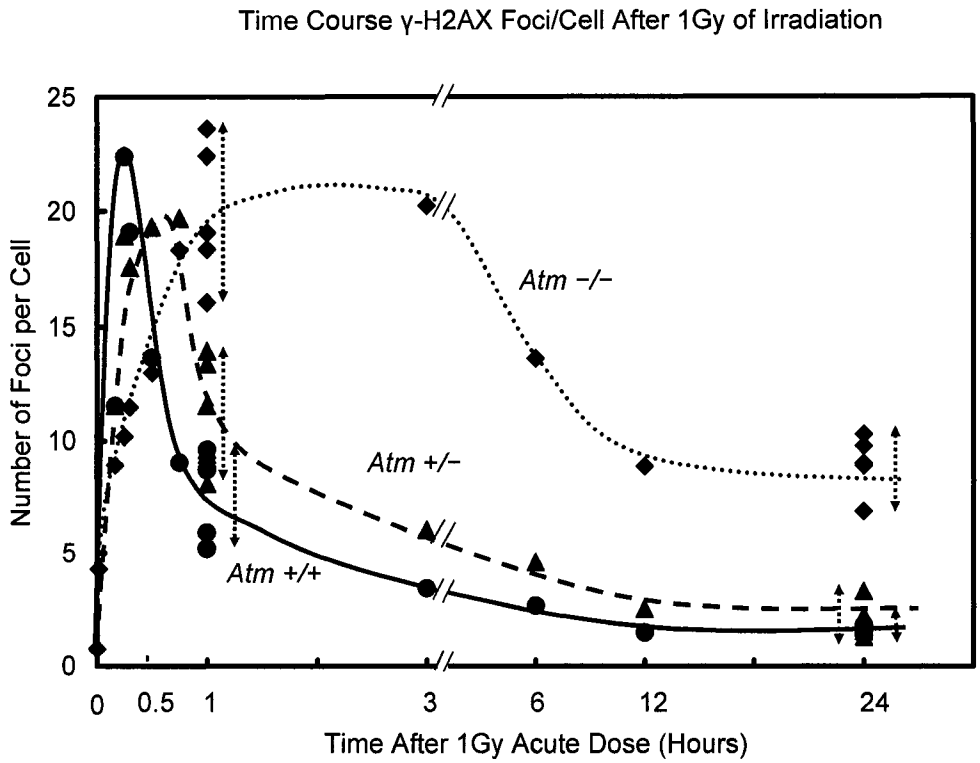

Figure 2-1

The time course of γ-H2AX foci formation and disappearance after an acute γ-ray dose of 1 Gy for cells from wild-type *Atm* +/+ mice (●); heterozygous *Atm* +/− mice (▲) and homozygous recessive *Atm* −/− mice (♦). Vertical dashed lines drawn at 1 hour on the abscissa show the range of values at the time where there was a maximum separation for cells from the mice of different *Atm* genotype. Vertical dashed lines also indicate the separation at 24 hours.

frequency of about 1 focus per cell. This pattern is not too different from the rejoining kinetics of G_1 chromosome breaks and for DNA DSBs reported for normal cells on numerous occasions following radiation doses less than 10 Gy (35,44-50).

At the other extreme, cells from *Atm* −/− mice showed a slower initial development of foci, reaching a maximum after about 1 hour. The number of foci then remained relatively constant for the next 2 hours and then began to decline. About 35% of the maximum number of foci remained up to 24 hours after irradiation. Again, the similar early maximum for normal vs. A-T cells and the difference in residual levels was also comparable to observed initial and residual levels measured previously for interphase chromosome breakage and rejoining in human normal and AT cells (45)

The time course for cells from *Atm* +/− mice showed an intermediate pattern of formation and disappearance of foci after irradiation. The number reached a maximum level similar to that for normal or *Atm* −/− cells at 30-45 minutes, but after this maximum, the rate of decrease was not remarkably different from that for normal cells. Neither were the residual levels after 12 or 24 hours significantly different between the *Atm* +/− and *Atm* +/+ cells.

Since the optimum time for distinguishing *Atm* +/− from normal cells appeared to be at about 1 hour after the 1 Gy acute high dose-rate exposure, I carried out additional experiments at this dose and sampling time for all 12 cell strains, and also included samples for measurement 24 hours after irradiation. The mean values and uncertainties derived from the data from these experiments for the 0 Gy controls and for the 1 hour and 24 hour sample times after 1 Gy, are summarized in Table 2-2. The data for the low dose rate experiments described below are also summarized in Table 2-2.

Continuous Low Dose-Rate Irradiation - (24h at 10cGy/h)

After a continuous exposure of cells for 24 hours at a low dose-rate of 10 cGy per hour, γ-H2AX foci were scored and the results are shown in Table 2-2 and summarized graphically in Figure 2-2. The mean values and uncertainties are summarized in the last column in Table 2-2. It is informative to present the data for the low dose rate irradiations more completely to include the distributions of γ-H2AX foci per cell as this allows a better appreciation of the variation among cells within a strain and between strains from different mice.

With the exception of the data for cells from the homozygous *Atm* −/− mouse #338, where the observed distribution was significantly underdispersed relative to a Poisson with the observed mean, no other significant deviations were observed from the expectation of a Poisson distribution of foci per cell among cells in the individual populations, and the pooled data also were well fit by Poisson distributions (Figure 2-2, lower panels). This would indicate relatively homogenous populations of similar sensitivities in each case. I cannot explain the underdispersion in the above sample, except to speculate that some unknown factor in the sample preparation or image processing may have been involved.

γ-H2AX foci formation after 10 cGy/h for 24 hours irradiation

Individual Mouse Cell Lines

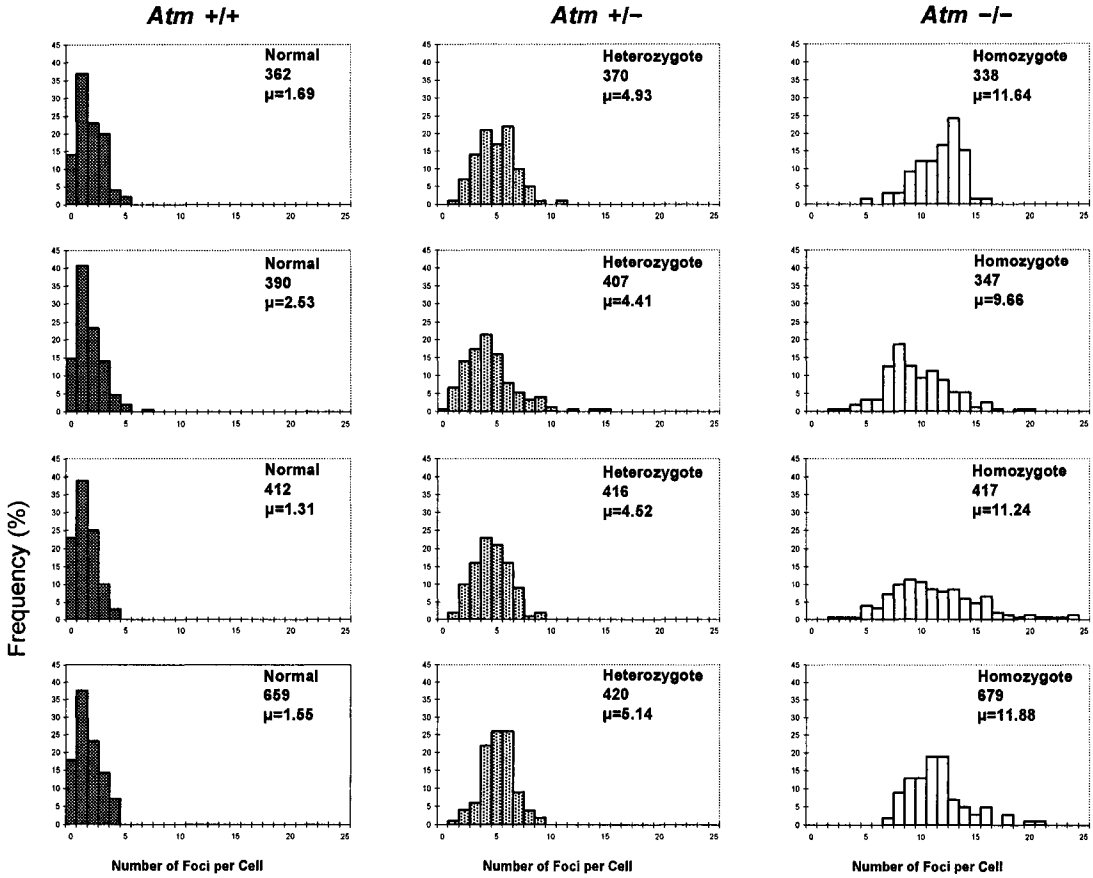

Pooled Data from 4 Individual Mice

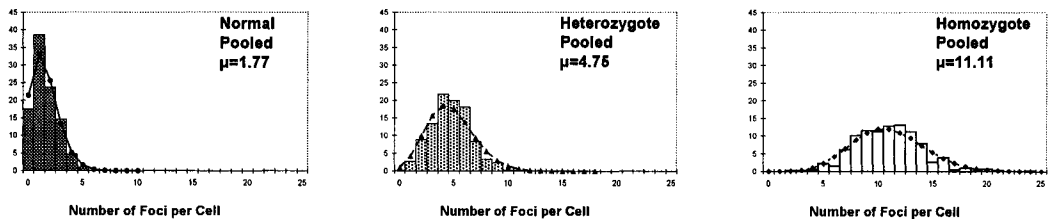

Atm genotype	Mouse ID#	Mean Number of Foci per Cell (±95% CI.)			
		0Gy	High dose rate 1Gy+1h	1Gy+24h	Low dose rate 10cGy/h × 24h
+/+	362	**0.76** (0.62-0.92)	**5.22** (4.27-6.37)	**1.68** (1.37-2.05)	**1.69** (1.38-2.06)
	390	**0.62** (0.51-0.76)	**5.18** (4.23-6.31)	**1.36** (1.11-1.66)	**2.53** (2.07-3.09)
	412	**0.85** (0.70-1.04)	**5.92** (4.84-7.2)	**1.84** (1.51-2.24)	**1.31** (1.07-1.60)
	659	**1.23** (1.01-1.50)	**9.62** (7.87-11.74)	**1.80** (1.47-2.20)	**1.55** (1.27-1.90)
	Mean of Means (±SEM)	**0.87 (±0.075)**	**6.49 (±0.25)**	**1.67 (±0.13)**	**1.77 (±0.13)**
+/−	370	**1.50** (1.23-1.83)	**9.62** (7.87-11.74)	**1.30** (1.06-1.59)	**4.93** (4.03-6.01)
	407	**1.13** (0.92-1.38)	**8.10** (6.63-9.88)	**2.20** (1.80-2.68)	**4.41** (3.61-5.38)
	416	**1.34** (1.10-1.63)	**9.22** (7.54-11.25)	**1.54** (1.26-1.88)	**4.52** (3.70-5.51)
	420	**1.35** (1.10-1.65)	**11.56** (9.46-14.10)	**1.86** (1.52-2.27)	**5.14** (4.20-6.27)
	Mean of Means (±SEM)	**1.33 (±0.12)**	**9.63 (±0.31)**	**1.73 (±0.13)**	**4.75 (±0.22)**
−/−	338	**0.96** (0.79-1.17)	**22.4** (18.32-27.33)	**10.28** (8.41-12.54)	**11.64** (9.52-14.20)
	347	**1.65** (1.35-2.01)	**16.06** (13.14-19.59)	**6.86** (5.61-8.37)	**9.66** (7.90-11.79)
	417	**1.84** (1.51-2.24)	**18.34** (15.00-22.37)	**9.00** (7.36-10.98)	**11.24** (9.19-13.71)
	679	**0.95** (0.78-1.16)	**19.06** (15.59-23.25)	**9.76** (7.98-11.91)	**11.88** (9.72-14.49)
	Mean of Means (±SEM)	**1.35 (±0.12)**	**18.97 (±0.44)**	**8.98 (±0.30)**	**11.11 (±0.33)**

The mean values of foci per cell and the uncertainties for the series involving low dose-rate irradiations, summarized in the last column of Table 2, show that not only is there a highly significant increase in mean values of γ-H2AX foci per cell for samples from *Atm* +/– mice relative to *Atm* +/+ mice, but the difference is large. The probability that any of the mean values of foci per cell for any of the samples from the four *Atm* +/– mice is actually *not* different from the mean observed for the control population is much smaller than 0.001, and therefore, the probability that none of the means from the four *Atm* +/– samples are different from the control mean is extremely small. The mean of the means for the samples from the four *Atm* +/+ mice was 1.77 ± 0.13 (SEM) foci per cell and the mean of means for the samples from the *Atm* +/– mice was 4.75 ± 0.22 (SEM). Thus, the mean foci per cell for the samples for *Atm* +/– mice was approximately 2.7-fold higher that that for the *Atm* +/+ samples. The numbers of foci per cell was even larger (11.10 ± 0.33 SEM or about 6.3-fold larger) for samples from *Atm* –/– mice.

These results are graphically summarized in Figure 2-3, where the means and estimated standard errors of the means for the zero dose controls and the corresponding values for the low dose-rate irradiated groups for each of the 3 sets (*Atm* +/+, *Atm* +/–, and *Atm* –/–) are plotted.

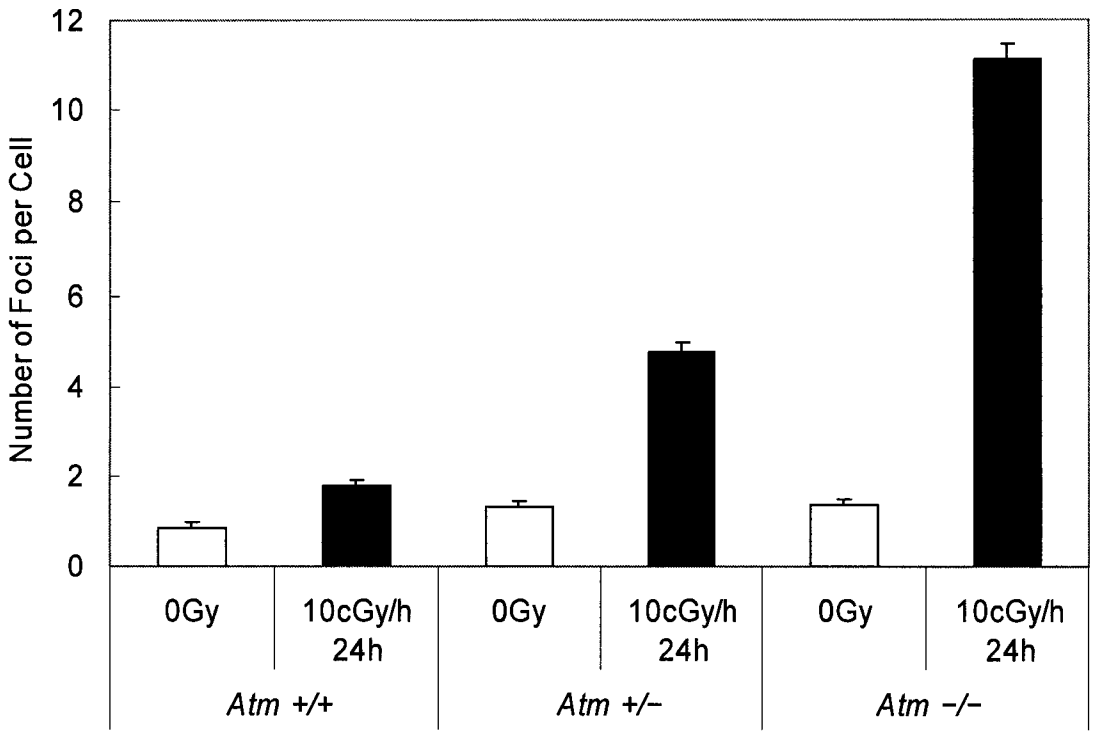

Figure 2-3

The means and standard errors of the number of γ-H2AX foci per cell for pooled data for unirradiated control mice or mice irradiated continuously at 10 cGy/h for 24 hours (from the data summarized in Table 2) are shown for *Atm* +/+, *Atm* +/–, *and Atm* –/– mice.

DISCUSSION

The γ-H2AX assay I describe involving a continuous low dose-rate irradiation protocol, enables a clear distinction to be made between cell samples derived from *Atm* +/– and *Atm* +/+ mice but of course the assay is indicative only of hypersensitivity to the radiation effect measured, i.e., the levels of these foci. While a high level of these foci for a sample of unknown origin might be expected to result from any of a number of other known or even unknown genetic factors, this should be considered an advantage if the assay is more generally applicable to assess radiation sensitivity.

To the extent that alterations in the processing of DSBs revealed by the γ-H2AX assay reflect the radiosensitivity status for biological effects of concern, such as carcinogenesis, the assay could have several useful applications. Preliminary experiments in our laboratory (data not shown) have indicated that cytocentrifuge preparations of lymphoblastoid cell lines yield perfectly acceptable material for quantitative measurements of γ-H2AX foci, so peripheral blood lymphocytes, the classical example of a non-cycling G_0 cell population that is free from high background foci S-phase cells, should provide material by a minimally invasive procedure for a rapid assay to help identify hypersensitive individuals. Then, if the individual so desires, further genetic testing might be carried out to identify the nature of the defect, or help identify unknown genes affecting this phenotype. Preliminary studies in our laboratory concerning the application of the approach described here to human cells indicate that such phenotypic screening may indeed be possible.

Beyond any potential practical applications, it is noteworthy that the γ-H2AX assay used here identifies a defect involving the processing of a particular kind of DNA damage produced by ionizing radiations, eg., DNA DSBs. While it may be reasonable to suggest that the chromosome-damage assays discussed earlier reflect differences in the repair or processing of DNA damage (eg, (1,2)), this is nevertheless an assumption. The present study does not identify the nature of the biochemical mechanisms involved in the damage processing defect, but it does identify DNA DSBs as the principal component of the initial damage being processed.

REFERENCES

1. R. Parshad, K. K. Sanford and G. M. Jones, Chromatid damage after G2 phase x-irradiation of cells from cancer-prone individuals implicates deficiency in DNA repair, *Proc.Natl.Acad.Sci.USA* **80**, 5612-5616 (1983).

2. K. K. Sanford, R. Parshad, R. R. Gantt and R. E. Tarone, A deficiency in chromatin repair, genetic instability, and predisposition to cancer, *CRC Critical Reviews in Oncogenesis* **1**, 323-341 (1989).

3. K. K. Sanford and R. Parshad, Detection of cancer-prone individuals using cytogenetic response to X-rays, *in* "Chromosome Aberrations, Basic and Applied Aspects" (G. Obe and A. T. Natarajan, Eds.), Springer-Verlag, Berlin (1990).

4. S. A. Roberts, A. R. Spreadborough, B. Bulman, J. B. Barber, D. G. R. Evans and D. Scott, Heritability of cellular radiosensitivity: a marker of low-penetrance predisposition genes in breast cancer?, *American Journal of Human Genetics* **65**, 784-794 (1999).

5. D. Scott, A. R. Spreadborough, L. A. Jones, S. A. Roberts and C. J. Moore, Chromosomal radiosensitivity in G_2-phase lymphocytes as an indicator of cancer predisposition, *Radiat.Res.* **145**, 3-16 (1996).

6. D. Scott, L. A. Jones, S. A. G. Elyan, A. Spreadborough, R. Cowan and G. Ribiero, Identification of A-T heterozygotes, *in* "Atataxia-telangiectasia" (R. A. Gatti and R. B. Painter, Eds.), Springer-Verlag, Berlin (1992).

7. D. Scott, J. B. Barber, A. R. Spreadborough, W. Burrill and S. A. Roberts, Increased chromosomal radiosensitivity in breast cancer patients: a comparison of two assays, *Int.J.Radiat.Biol.* **75**, 1-10 (1999).

8. D. Scott, A. Spreadborough, E. Levine and S. A. Roberts, Genetic predisposition in breast cancer, *Lancet* **344**, 1444 (1994).

9. J. M. Varley, D. G. Evans and J. M. Birch, Li-Fraumeni syndrome--a molecular and clinical review, *Br.J Cancer* **76**, 1-14 (1997).

10. A. Vral, H. Thierens, A. Baeyens and R. L. De, The micronucleus and G2-phase assays for human blood lymphocytes as biomarkers of individual sensitivity to ionizing radiation: limitations imposed by intraindividual variability, *Radiat.Res.* **157**, 472-477 (2002).

11. A. Vral, H. Thierens, A. Baeyens and R. L. De, Chromosomal aberrations and in vitro radiosensitivity: intra-individual versus inter-individual variability, *Toxicol.Lett.* **149**, 345-352 (2004).

12. S. Neubauer, R. Arutyunyan, M. Stumm, T. Dork, R. Bendix, M. Bremer, R. Varon, R. Sauer and E. Gebhart, Radiosensitivity of ataxia telangiectasia and Nijmegen

breakage syndrome homozygotes and heterozygotes as determined by three-color FISH chromosome painting, *Radiat.Res.* **157**, 312-321 (2002).

13. J. C. Leonard, A. M. Mullinger, J. Schmidt, H. J. Cordell and R. T. Johnson, Genome instability in ataxia telangiectasia (A-T) families: camptothecin-induced damage to replicating DNA discriminates between obligate A-T heterozygotes, A-T homozygotes and controls, *Biosci.Rep.* **24**, 617-629 (2004).

14. R. T. Johnson, E. Gotoh, A. M. Mullinger, A. J. Ryan, Y. Shiloh, Y. Ziv and S. Squires, Targeting double-strand breaks to replicating DNA identifies a subpathway of DSB repair that is defective in ataxia-telangiectasia cells., *Biochem Biophys Res Commun* **261**, 317-325 (1999).

15. H. Nagasawa, S. A. Latt, M. E. Lalande and J. B. Little, Effects of X-irradiation on cell cycle progression, induction of chromosomal aberrations and cell killing in ataxia telangiectasia, *Mutation Res.* **148**, 71-82 (1985).

16. J. B. Little and H. Nagasawa, Effect of confluent holding on potentially lethal damage repair, cell cycle progression, and chromosomal aberrations in human normal and ataxia-telangiectasia fibroblasts, *Radiat.Res.* **101**, 81-93 (1985).

17. H. Nagasawa, K. H. Kraemer, Y. Shiloh and J. B. Little, Detection of ataxia telangiectasia heterozygous cell lines by postirradiation cumulative labeling index: measurements with coded samples, *Cancer Res.* **47**, 398-402 (1987).

18. K. Rothkamm and M. Lobrich, Evidence for a lack of DNA double-strand break repair in human cells exposed to very low x-ray doses, *Proc.Natl.Acad.Sci.U.S.A* **100**, 5057-5062 (2003).

19. S. H. MacPhail, J. P. Banath, T. Y. Yu, E. H. Chu, H. Lambur and P. L. Olive, Expression of phosphorylated histone H2AX in cultured cell lines following exposure to X-rays, *Int.J Radiat.Biol.* **79**, 351-358 (2003).

20. E. P. Rogakou, D. R. Pilch, A. H. Orr, V. S. Ivanova and W. M. Bonner, DNA double-stranded breaks induce histone H2AX phosphorylation on serine 139, *J Biol.Chem.* **273**, 5858-5868 (1998).

21. D. E. Lea, Actions of Radiations on Living Cells, Cambridge Univ. Press, London (1955).

22. K. Sax, The time factor in x-ray production of chromosomal aberrations, *Proc.Natl.Acad.Sci.USA* **25**, 225-233 (1939).

23. W. L. Russell, L. B. Russell and Kelly.E.M., Radiation dose rate and mutation frequency, *Science* **128**, 1546-1550 (1958).

24. M. M. Elkind and H. Sutton, X-ray damage and recovery in mammalian cells in culture, *Nature* **184**, 1293-1295 (1959).

25. J. S. Bedford and E. J. Hall, Survival of Hela cells cultured *in vitro* and exposed to protracted gamma radiation, *Int.J.Radiat.Biol.* **7**, 377-383 (1963).

26. R. L. Ullrich, M. C. Jernigan, G. E. Cosgrove, L. C. Satterfield, N. D. Bowles and J. B. Storer, The influence of dose and dose rate on the incidence of neoplastic disease in RFM mice after neutron irradiation, *Radiat.Res.* **68**, 115-131 (1976).

27. R. L. Wells and J. S. Bedford, Dose-rate effects in mammalian cells. IV. Repairable and nonrepairable damage in noncycling C3H 10T 1/2 cells, *Radiat.Res.* **94**, 105-134 (1983).

28. R. L. Ullrich and J. B. Storer, Influence of gamma irradiation on the development of neoplastic disease in mice. III. Dose-rate effects, *Radiat.Res.* **80**, 325-342 (1979).

29. R. L. Ullrich, M. C. Jernigan, L. C. Satterfield and N. D. Bowles, Radiation carcinogenesis: time-dose relationships, *Radiat.Res.* **111**, 179-184 (1987).

30. Cox, R. A cellular description of the repair defect in ataxia-telangiectasia. Bridges, B. A. and Harnden, D. G. 141-153. 1982. Chichester, New York, Brisbane, Toronto, Singapore, John Wiley & Sons. Ataxia-Telangiectasia: A Cellular and Molecular Link Between Cancer, Neuropathology, and Immune Defeciency.

31. M. A. Stackhouse and J. S. Bedford, An ionizing radiation-sensitive mutant of CHO cells: irs-20 Dose-rate effects and cellular recovery processes, *Radiat.Res.* **136**, 250-254 (1993).

32. A. Priestley, H. J. Beamish, D. Gell, A. G. Amatucci, M. C. Muhlmann-Diaz, B. K. Singleton, Smith G.C., T. Blunt, L. C. Schalkwyk, J. S. Bedford, Jackson S.P., P. A. Jeggo and G. E. Taccioli, Molecular and biochemical characterization of DNA-dependent protein kinase-defective rodent mutant irs-20, *Nucl.Acids Res.* **26**, 1965-1973 (1998).

33. H. Nagasawa, D. J. Chen and G. F. Strniste, Response of X-ray-sensitive CHO mutant cells to gamma radiation. I. Effects of low dose rates and the process of repair of potentially lethal damage in G1 phase, *Radiat.Res.* **118**, 559-567 (1989).

34. M. A. Stackhouse and J. S. Bedford, An ionizing radition-sensitive mutant of CHO cells: irs-20 Isolation and initial characterization, *Radiat.Res.* **136**, 241-249 (1993).

35. M. A. Stackhouse and J. S. Bedford, An ionizing radiation-sensitive mutant of CHO cells: irs-20. III. Chromosome aberrations, DNA breaks and mitotic delay, *Int.J.Radiat.Biol.* **65**, 571-582 (1994).

36. C. Barlow, S. Hirotsune, R. Paylor, M. Liyanage, M. Eckhaus, F. Collins, Y. Shiloh, J. N. Crawley, T. Ried, D. Tagle and A. Wynshaw-Boris, Atm-deficient mice: a paradigm of ataxia telangiectasia, *Cell* **86**, 159-171 (1996).

37. R. A. Tobey and K. D. Ley, Isoleucine-mediated regulation of genome repliction in various mammalian cell lines, *Cancer Res.* **31**, 46-51 (1971).

38. J. S. Bedford and M. C. Muhlmann-Diaz, Damage selectivity in chromosomes, (W. C. Dewey, M. Edington, R. J. M. Fry, E. J. Hall and G. F. Whitmore, Eds.), Academic Press, San Diego (1992).

39. T. J. Monroe, M. C. Mühlmann-Díaz, M. J. Kovach, J. O. Carlson, J. S. Bedford and B. J. Beaty, Stable transformation of a mosquito cell line results in extraordinarily high copy numbers of plasmids, *Proc.Natl.Acad.Sci.USA* **89**, 5725-5729 (1992).

40. M. C. Muhlmann-Diaz, R. G. Dullea and J. S. Bedford, Application of 5-bromo-2'deoxyuridine as a label for in situ hybridization in chromosome microdissection and painting, and 3'OH DNA end labeling for apoptosis, *BioTechniques* **21**, 82-86 (1996).

41. M. C. Mühlmann-Díaz and J. S. Bedford, Breakage of human chromosomes 4,19, and Y in G_0 cells immediately after exposure to gamma-rays., *Int.J.Radiat.Biol.* **65**, 165-173 (1994).

42. R. J. Amdur and J. S. Bedford, Dose-rate effects between 0.3 and 30 Gy/h in a normal and a malignant human cell line, *Int.J.Radiat.Oncol.Biol.Phys.* **30**, 83-90 (1994).

43. M. R. Raju, Y. Eisen, S. Carpenter and W. C. Inkret, Radiobiology of alpha particles. III. Cell inactivation by alpha-particle traversals of the cell nucleus, *Radiat.Res.* **128**, 204-209 (1991).

44. M. N. Cornforth and J. S. Bedford, X-ray induced breakage and rejoining of human interphase chromosomes., *Science* **222**, 1141-1143 (1983).

45. M. N. Cornforth and J. S. Bedford, On the nature of a defect in cells from individuals with ataxia telangiectasia., *Science* **227**, 1589-1591 (1985).

46. L. Metzger and G. Iliakis, Kinetics of DNA double-strand break repair throughout the cell cycle as assayed by pulsed field gel electrophoresis in CHO cells, *Int.J.Radiat.Biol.* **59**, 1325-1339 (1991).

47. C. Badie, G. Iliakis, N. Foray, G. Alsbeih, B. Cedervall, N. Chavaudra, G. Pantelias, C. Arlett and E. P. Malaise, Induction and rejoining of DNA double-strand breaks and interphase chromosome breaks after exposure to X rays in one normal and two hypersensitive human fibroblast cell lines, *Radiat.Res.* **144**, 26-35 (1995).

48. G. Iliakis, H. Wang, A. R. Perrault, W. Boecker, B. Rosidi, F. Windhofer, W. Wu, J. Guan, G. Terzoudi and G. Pantelias, Mechanisms of DNA double strand break

repair and chromosome aberration formation, *Cytogenet.Genome Res.* **104**, 14-20 (2004).

49. M. Lobrich and P. A. Jeggo, The two edges of the ATM sword: co-operation between repair and checkpoint functions, *Radiother.Oncol.* **76**, 112-118 (2005).

50. P. L. Olive, Detection of DNA damage in individual cells by analysis of histone H2AX phosphorylation, *Methods Cell Biol.* **75**, 355-373 (2004).

Chapter 3

Levels of γ-H2AX Foci after Low Dose-Rate Irradiation Distinguish Human *ATM* Heterozygotes and other Mildly Radiosensitive Individuals

ABSTRACT

I have investigated the use of the γ-H2AX assay, reflecting the presence of DNA double strand breaks, as a possible means for identifying individuals such as ATM heterozygotes who may be intermediate between the extremes of normal radiosensitivity and hypersensitive phenotypes. I compared levels of γ-H2AX foci after irradiation in cells from six apparently normal individuals as well as from individuals from two separate A-T families including the proband, mother, father, and three unaffected siblings in each family. After a 1 Gy single acute (high dose-rate) γ-ray dose delivered to non-cycling contact inhibited monolayers of cells, clear differences were seen between samples from normal individuals (*ATM* +/+) and probands (*ATM* −/−) at nearly all sampling times after irradiation, but no clear distinctions were seen for cells from normal vs. obligate heterozygotes (*ATM* +/–). In contrast, after 24 hours of continuous irradiation at a dose rate of 10 cGy/hour, appreciable differences in foci per cell were observed for cells from individuals for all the known *ATM* genotypes as compared with controls. Four unaffected siblings had mean numbers of foci per cell similar to that for the obligate heterozygotes, whereas the other two had mean values similar to that for normal controls. I determined independently that those siblings with mean foci per cell

in the range of *ATM* heterozygotes bore the mutant allele, while both siblings with a normal number of foci per cell after irradiation had normal alleles. A more limited set of experiments using lymphoblastoid cell strains in the low dose-rate assay also revealed distinct differences for normal vs. *ATM* heterozygotes, and opens the possibility of utilizing peripheral blood lymphocytes as a more suitable material for an assay in humans.

INTRODUCTION

Many cellular phenotypic tests readily reveal extreme differences in radiosensitivity between individuals, but unequivocal detection of mild or less extreme hypersensitivity has proven more difficult (1-18). Differences in biological responses to a given dose of a particular radiation depend largely on differences in DNA DSB repair capacity and the balance of repair vs. misrepair and other processes that occur after irradiation. In general, biological effects of radiation, such as mutation, carcinogenesis and cell killing, are reduced for low LET radiation exposures that are protracted or spread over a period of hours or days compared to the same total dose delivered acutely in a few seconds or minutes (eg (19-27)). Cells defective in DNA damage processing show much reduced dose-rate effects compared to the relatively larger dose-rate effect for the proficient system, so there is generally a much larger difference in responses for doses delivered as protracted low dose rate exposures than for the same doses delivered as acute high dose-rate exposures (28,29). This property was the basis for a strategy used in this laboratory to isolate radiosensitive mutant cell lines that proved to have defects in DNA DSB damage processing (28-31), and also to test a γ-H2AX focus assay carried out at low dose rate to provide a more sensitive means for distinguishing even mildly hyper-radiosensitive individuals than would be possible for acute, high dose-rate exposures. Others have also used the same rationale to enhance discrimination of mild hypersensitivity in the G_2 assay (32).

In a recent previous report I found that for low dose-rate irradiation (10 cGy/h for 24 hours) a clear distinction was observed between cells from normal *Atm* +/+ vs. *Atm* +/− mice using the γ-H2AX assay (33) and even larger differences were seen for cells from *Atm* −/− mice. In this case cells from mice with altered *Atm* genotypes were all obtained from mice with the same knockout alleles, so the same specific mutation was involved for all heterozygotes and other differences in genetic background were minimized. Thus, differences observed in the radiosensitivity phenotype were almost certainly due to differences in the *Atm* genotype rather that some other more complex differences in genetic background.

The present report extends this study to cells derived from different human individuals and different families of individuals, where the diversity of genetic background would be greater. While differences in *ATM* genotypes would certainly be expected to contribute to differences in γ-H2AX foci phenotypes after irradiation, it is doubtful that this would be the only source of such differences. In the present study I compared numbers of γ-H2AX foci in contact inhibited low passage cultured fibroblasts from two A-T families where a proband, both parents, and three unaffected siblings from each family were available. I generally refer to these contact inhibited low passage cultures of normal or untransformed human fibroblasts as being composed of G_0 cells, for reasons outlined below in the Methods section. For the normal controls, low passage cells from six apparently normal individuals were used. The comparisons in the present study were made after either 24 hours of continuous irradiation at a dose-rate of 10 cGy per hour as used in the previous study, or at various times after a single acute γ-ray dose of 1 Gy. Because an assay such as the one I have studied here would be of much greater

practical use if it could be applied to cells, such as peripheral blood lymphocytes that are more easily sampled from individuals, I carried out a limited number of experiments using the low dose-rate assay with lymphoblastoid cell strains derived from individuals who were either apparently normal, *ATM* +/− heterozygotes or affected A-T probands (*ATM* −/−).

MATERIALS AND METHODS

Cells

Nearly all cell strains used in this study were from the Coriell Institute Cell Repository. The apparently normal fibroblast strains were GM08680 (46, XY, foreskin), GM08429 (46,XY, skin, ear tag), GM08402 (46,XY, skin), GM08400 (46,XX skin), GM05400 (46,XY inguinal skin biopsy), and GM02149 (46, XX, skin, clinically normal wife of patient with Huntington Chorea). The fibroblast strains derived from individuals belonging to A-T family 605 (Coriell designation number) were GM03395 (proband), GM 03396 (mother), GM03397 (father), GM03398 (unaffected sister of proband), GM03399 (unaffected sister of proband), and GM03490 (unaffected brother of proband). The cells from individuals belonging to A-T family 516 (Coriell designation number) were GM03487 (proband), GM03489 (mother), GM03488 (father), GM03490 (unaffected brother of proband), GM03491 (unaffected sister of proband), and GM03492 (unaffected sister of proband).

Five lymphoblastoid cell strains were also used. From the NIGMS Coriell Institute lymphoblastoid cells derived from A-T family 516 (also used in the fibroblast study) were GM03187 (father), GM03188 (mother), and GM03189 (proband). Another lymphoblastoid strain designated L3 from an A-T patient (*ATM−/−*) bearing a homozygous truncation mutation, and a normal strain designated C3 (C3ABR) was kindly supplied by Dr. Martin Lavin of the Queensland Institute of Medical Research, Herston Queensland, Australia (34). The growth and maintenance of these cells in our laboratory have been described previously (35).

Cell Culture

Cells were cultured in Minimum Essential Medium (MEM) supplemented with 15% Fetal Bovine Serum (FBS), 100units/ml of penicillin and 100μg/ml of streptomycin, and were maintained at 37°C in a humidified atmosphere of 5% CO_2 in air. Cells were grown on chamber slides or flaskettes to form a monolayer as described above, and when samples were ready for irradiation, flasks were sealed and placed in position in the appropriate irradiator. Because unirradiated cells in S-phase have much higher levels of γ-H2AX foci, and also because the number of foci per cell depends on DNA content (17), I carried out these experiments with non-cycling contact inhibited G_0 cells as reported on other occasions (36-38). It may also be worth noting that I generally refer to these contact inhibited low passage cultures of normal or untransformed human fibroblasts as being composed of "G_0" cells since earlier observations in our laboratory had shown that 1) virtually all the cells under these conditions were completely negative in immunocytochemical tests for DNA polymerase α, 2) virtually all had a G_1 DNA content, 3) cycling G_1 cells, whether the G_1 transit time is long or short, stain intensely with anti-DNA polymerase α antibody, and 4) only a very low proportion of cells in such cultures incorporate tritiated thymidine even after 24 hours of continuous labeling (39,40). As will be shown and discussed below the observed distributions of foci per cell were generally well fitted to the expected Poisson distributions for uniform populations.

Before experiments were carried out, the cell cultures were coded so the person performing the experiments and scoring the slides did not know the origin of the cells. Only after the samples were scored and the data were compiled and summarized, were

the samples decoded. At least three independent experiments were carried out for each fibroblast strain and irradiation condition.

For the limited studies with the lymphoblastoid strains, cells were cultured in suspension in medium RPMI containing 15% fetal bovine serum. These cells do not undergo contact inhibition and enter a non-cycling G_0 state. As previous work has shown that even unirradiated S phase cells have a very high background of γ-H2AX foci, and because rapidly proliferating cell cultures are not suitable for the low dose-rate assay, I synchronized the cells in G_1 before irradiation using the isoleucine deprivation method (41). G_1 phase synchronization after isoleucine deprivation was confirmed by flow cytometry (DNA content), and after labeling with BrdU, by immunocytochemistry using an anti-BrdU antibody.

Irradiations:

Irradiations were carried out using either a J.L. Shepherd Model Mark I-68 6000 Ci ^{137}Cs irradiator or in a 37°C low dose rate irradiation facility in which, depending on the dose-rate desired, samples can be placed at various distances above a plane of from one to twelve 4Ci ^{137}Cs sources that are remotely placed under the cell cultures or retracted into the shielded safe position. These irradiation facilities have been described on numerous occasions (30,38,42). Dose-rates and field uniformities over the position of samples were measured using an ion chamber (Radcal 2025AC Radiation monitor with 20x5-180 Electrometer/Ion chamber). The dose rate for the acute high dose rate exposure was 250cGy/min. The dose rate for the 24 hour chronic low dose rate exposures was 9.9 to 10.2 cGy/hour.

When fibroblasts were ready for irradiations the monolayer cultures on the chamber slides or flaskettes were sealed and placed in position in the appropriate irradiator. After the low dose-rate exposures, cells were immediately (within 5 minutes) processed for immunocytochemistry as described below. After the high dose rate exposures samples were returned to the incubator and processed at various times later to determine the time course of γ-H2AX development.

For the lymphoblast cells, synchronized G_1 phase cultures were irradiated in T25 flasks in suspension, and only the low dose-rate protocol was used.

γ-H2AX: Immunocytochemistry

After irradiation, cells were washed with ice cold PBS and fixed in PBS containing 4% paraformaldehyde for 15 minutes. After three further washes with PBS for 10 minutes, cells were treated with 0.2% Triton X-100 solution in PBS for 5 minutes. Before immunocytochemical detection of γ-H2AX, cells were blocked with 10% goat serum solution for 1 hour at room temperature or overnight at 4°C to reduce subsequent non-specific antibody binding.

Mouse monoclonal antibody from Upstate (Chicago, IL), was diluted 1:500, and chamber slides or flaskettes with the cell monolayers were incubated in the diluted antiserum for 1 hour at 37°C. Cells were then washed with PBS 3 times for 10 minutes each, and secondary antibody (Alexa Fluor 488 conjugated goat anti mouse, Molecular Probes (Eugene, OR) diluted 1:500 was added and the slides were incubated for another 1 hour at 37°C. Slides were mounted in a solution of 1.5μg/ml DAPI containing slow-fade (Molecular Probes, Eugene, OR) after 4 washes with PBS for 10 minutes each

For the lymphoblastoid lines, cells were centrifuged onto slides using a cytocentrifuge. The slides were then rinsed with PBS, and fixed using paraformaldehyde. Further processing was the same as for the fibroblast cultures as described above.

γ-H2AX: Scoring Foci

Images of cells were obtained using an Olympus AX-70 fluorescence microscope equipped with a PSI image analysis system utilizing the MAC-Probe package. The thickness of the cell nuclei for these cell strains when the cells are attached and flattened to the culture vessel surface is typically around 2 micrometers and the foci were sufficiently intense that focusing the microscope approximately midway through the nuclei revealed virtually all the γ-H2AX foci present, as judged by counting all the foci as the focal plane was moved from the top to the bottom of the nuclei compared to the numbers for counts taken with the focal plane midway through the nucleus. There was often some non-specific background signal over and between cells that was generally somewhat smaller and less intensely fluorescent than the γ-H2AX foci, so before counting foci the images were processed by a "background subtraction" applied uniformly across the microscope fields. The processed images were stored and cells from these were later scored

In cases where there is a very low average number of foci per cell and the number of cells with a Poisson expectation of 1 or 2 foci per cell is appreciable, this subtraction can lead to a spurious increase in the 0 or 1 focus per cell class, but the distortion in the picture is generally obvious. In these cases bimodal distributions, were fitted to make a minor adjustment to the mean values used for comparisons among cell strains.

Otherwise, comparing means for slightly more sensitive vs. less sensitive cells in the assay could lead to a bias toward concluding a significant difference occurred when there was actually no difference. The correction applied would actually increase the means for less sensitive cells with virtually no change for more sensitive cells, thus reducing the differences for cell samples with lower (eg. normal) compared to the higher (eg. *ATM* heterozygotes) mean numbers of foci per cell. In no case in the present study, whether or not this correction was applied, our conclusions would not be altered.

ATM Genotyping by PCR and Sequencing

The *ATM* genotypes of the unaffected siblings in A-T families 516 and 605 were unknown to us at the time the γ-H2AX focus assays were carried out, but the mutations in the probands of these families are know, so I genotyped coded samples of DNA from the sibs' fibroblasts for the relevant mutations. Genotyping was accomplished by amplifying the relevant regions of the gene and sequencing the amplification products. The proband in family 516 is a compound heterozygote with an 8266A>T base substitution on the maternal allele and a 4 basepair insertion at nucleotide 1141 on the paternal allele (Coriell Institute for Medical Research, NIGMS Catalogue). The proband in family 605 is homozygous for a 7913G>A mutation. The primers used to PCR amplify the 8266A>T region were AGATGCTGTCATGCAACAGG and GCCTCCCAAAGCATTATGAA, and the primers for the 1141ins4 region were GCAACAACAGCGAAACTCTG and CCAAGGCACAAGATCAAAATC. The 7913G>A region was amplified with a primer set consisting of ATCGAACAGAGGCTGCAAAT and TGAAAAAGTAACCAGGGAATGC. Following 31 cycles of amplification (94°C, 30

sec denaturation, 57°C, 30 sec annealing and 72°C, 60 sec extension) the PCR products were purified by agarose gel electrophoresis and sequenced by a commercial sequencing service (Davis Sequencing, Inc.,Davis, CA)

RESULTS

Acute high dose-rate irradiation:

The time course for development and disappearance γ-H2AX foci after an acute high dose-rate γ-ray exposure of 1 Gy was measured by fixing and processing cultures that had been incubated for 15, 20, 30, 45, 60 minutes, and 2, 3, 6, 12, and 24 hours after irradiation, and these were then examined by fluorescence microscopy for enumeration of γ-H2AX foci per cell. The results are plotted in Figure 3-1.

The general patterns of change in the appearance and disappearance of γ-H2AX foci as a function of time after irradiation were dependent on the *ATM* genotype. In the cells from apparently normal individuals, the number of γ-H2AX foci increased rapidly, reaching a maximum about 20 minutes after irradiation, then decreased to half its maximum value by about 40 minutes, and finally decreased more slowly with another halving of the number of foci per cell occurring some 2 hours later. By 12 or 24 hours after irradiation the number of foci per cell had decreased to only about 5% of the maximum value. This pattern is not too different from the rejoining kinetics of interphase G_0 chromosome breaks measured by premature chromosome condensation and for DNA DSBs, as well as for the disappearance of γ-H2AX foci reported for normal cells on numerous occasions following such relatively low radiation doses (31,37,39,43-47).

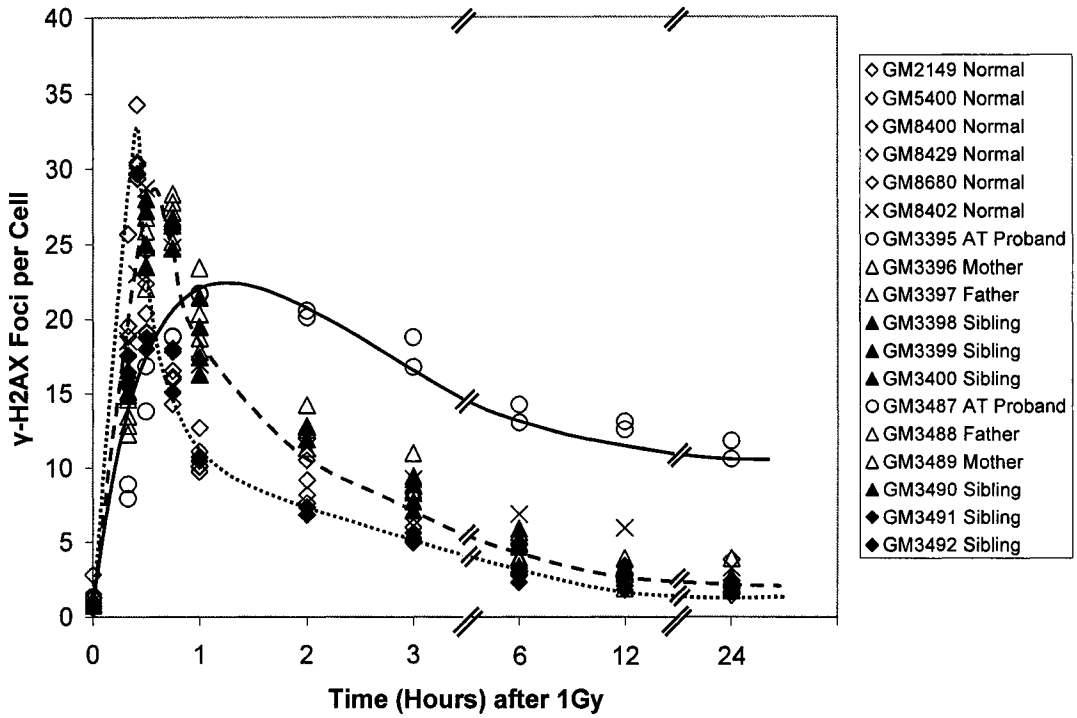

Figure 3-1

The development and disappearance of γ-H2AX foci in contact inhibited monolayer cultures is shown for various human fibroblast strains as a function of time after a acute (high dose-rate) gamma radiation dose of 1 Gy. The dotted line traces the pattern for cells from apparently normal human cell strains, the dashed line for *ATM* heterozygotes, and the solid line, for affected A-T individuals. The symbols and corresponding cell strain designations are shown in the insert.

At the other extreme, cells from *ATM* −/− homozygotes showed a slower initial development of foci, reaching a maximum after about 1 hour. The maximum foci per cell at this time was only about 22; lower than the maximum of about 34 observed for cells derived from normal individuals. The number of foci then remained relatively constant for the next 2 hours until after 3 hours the number began to decline. About half of the maximum number remained up to 24 hours after irradiation. The lower early maximum value for cells from A-T patients relative to that for normal individuals may reflect a slower initial phosphorylation of H2AX in the *ATM* −/− cells required for the development of foci but of course other explanations are also possible.

The time course for cells from *ATM* +/− heterozygotes showed an intermediate pattern of formation and disappearance of foci after irradiation. The number reached a maximum level that was also somewhat lower (~27 foci per cell) as well as later (around 45 minutes) relative to that for normal cells, but after this maximum, the rate of decrease was not remarkably different from that for normal cells. Neither were the residual levels after 12 or 24 hours significantly different for the *Atm* +/− and *Atm* +/+ cells. The delayed maximum for cells from *ATM* +/− heterozygotes, however, did result in a significant distinction between the cells from heterozygotes and apparently normal individuals with this for sampling times between 45 and 60 minutes, but there was no difference at 60 minutes between samples from probands and heterozygotes.

Continuous Low Dose-Rate Irradiation - (24h at 10cGy/h)

The results for 24 h protracted or continuous irradiation at a low dose-rate of 10 cGy per hour are shown in figure 3-2. It is informative to present the data for the low dose rate irradiations more completely to include the distributions of γ-H2AX foci per cell as this allows a better appreciation of the variation in numbers of foci among cells in a sample and between samples from different individuals. The mean numbers of foci per cell and the estimated standard deviations for the cells from the various individuals are summarized in Table 3-1. Also summarized are the pooled means for particular sets (e.g., normal, *ATM* hets, probands) and estimated standard errors of the means for the sets. These standard errors are worth noting because it is the dispersion of mean values among a set of similar genotypes or putative radiosensitivity phenotypes that allows distinctions or inferences to be drawn about the significance of differences that may exist between samples. I also note, as mentioned in the Methods section, that the image analysis approach I used for scoring foci per cell involves a small background subtraction and even though the nuclei scored are relatively flattened (~2 microns thick) occasional foci that are at the extreme ranges of the optical focal plane result in flaring and dimming of the image and may also be subtracted. The resulting distortion of the distributions is most apparent at the very lowest numbers of foci per cell resulting in a spurious increase noticeable in the numbers of cells with zero or one γ-H2AX focus. This is apparent as a bimodal distribution. Therefore, rather than taking a mean value of a distribution that is clearly bimodal, spuriously biasing the mean to lower values, I fitted data to bimodal distributions and utilized the means (μ_2) and estimated errors of the higher distributions. The light dashed lines in figure 3-2 show the fitted Poisson distributions, and bimodal

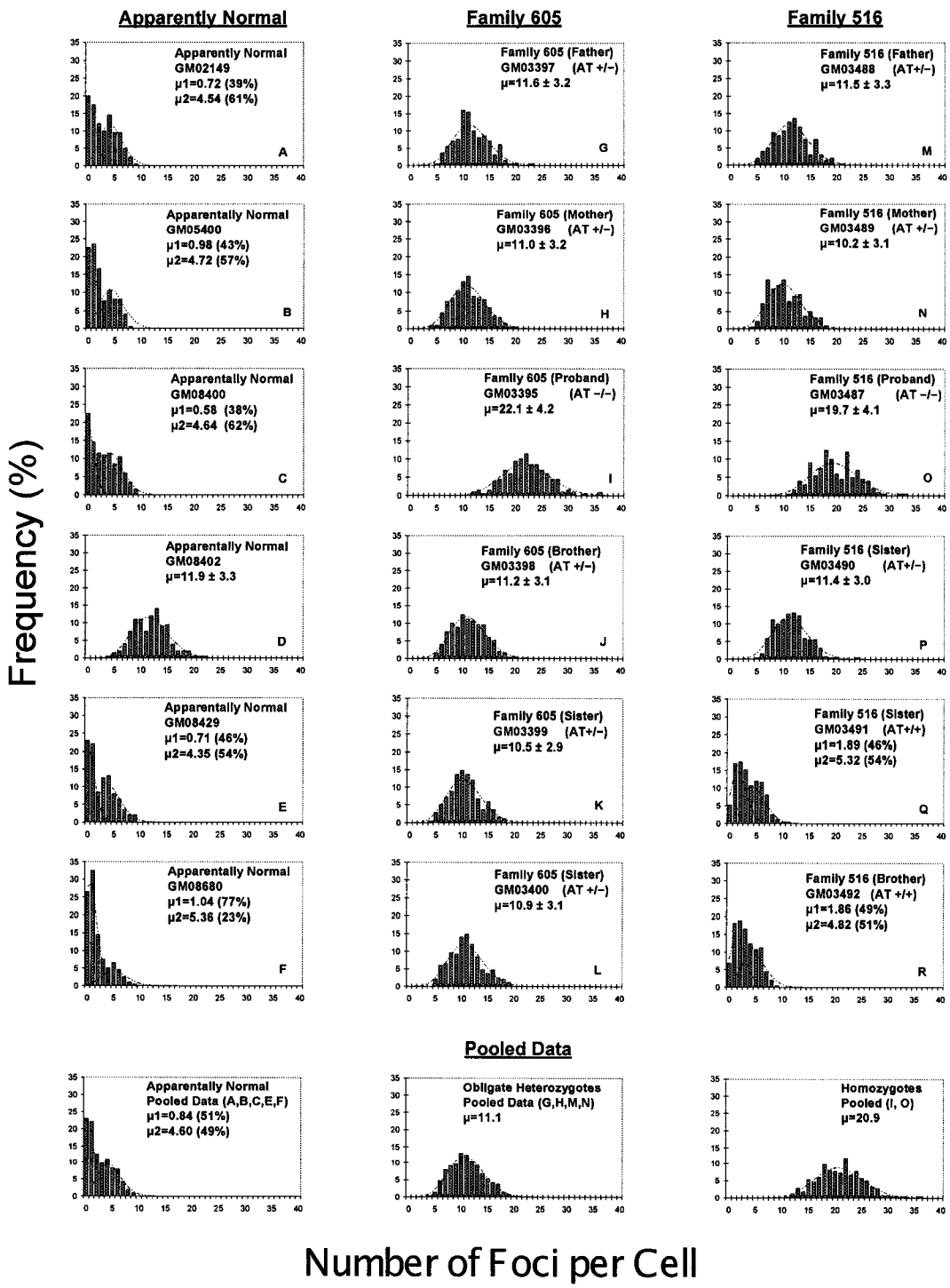

Table 3-1

Cell Source	Cell Strain	*ATM* status	*ATM* Genotype from PCR and Sequencing[1]	Mean foci per Cell (± SD)
Apparently Normal	GM02149	Unknown	(N.D.)	4.5 (± 2.2)
	GM05400			4.7 (± 2.2)
	GM08400			4.6 (± 2.2)
	GM08402			11.9 (± 3.2)
	GM08429			4.3 (± 2.0)
	GM08680			5.4 (± 2.4)
Family 605	GM03395	A-T Proband	−/−	22.1 (± 4.3)
	GM03396	Oblig.Het.(Mother)	+/−	11.0 (± 3.2)
	GM03397	Oblig.Het.(Father)	+/−	11.6 (± 3.2)
	GM03398	Unaffected Siblings	+/−	11.2 (± 3.1)
	GM03399		+/−	10.5 (± 2.9)
	GM03400		+/−	10.9 (± 3.1)
Family 516	GM03487	A-T Proband	−/−	19.7 (± 4.1)
	GM03488	Oblig.Het. (Father)	+/−	11.5 (± 3.2)
	GM03489	Oblig.Het. (Mother)	+/−	10.2 (± 3.1)
	GM03490	Unaffected siblings	+/−	11.4 (± 3.1)
	GM03491		+/+	6.3 (± 2.6)
	GM03492		+/+	4.8 (± 2.2)

Pooled Phenotypes	Mean of Means (± SEM)
Normal	4.6 (± 0.13)
Heterozygotes	11.0 (± 0.20)
A-T Probands	20.9 (± 0.27)

Footnote: [1]The same mutant *ATM* allele in family 605, a G>A substitution at nucleotide residue 7913, was present in both obligate heterozygous parents. In family 516, the mutant *ATM* allele of the father was a 4-base insertion at nucleotide residue 1141, and this was inherited by the only sibling (cell strain GM03490) shown to be heterozygous. The *ATM* mutant allele of the mother was an A>T substitution at residue 8266.

distributions were fitted only when single distributions resulted in an unacceptably high chi-square value for the fit. Thus, the means and error estimates quoted below for the samples falling in the range of foci per cell for normal-derived cells, all refer to these μ_2 estimates.

From figure 3-2, it is immediately apparent that the distributions show a much lower range of foci per cell for 5 of the 6 apparently normal samples compared to the one outlier. The results for the cells designated GM08402, showed a distribution that was well fit by a Poisson with a mean of 11.9 ± 3.3, while the higher mean values (μ_2) for the samples from the other 5 apparently normal individuals ranged from around 3.5 to 5.5. GM 08402 fibroblasts originated from an apparently healthy 32 year old male donor. While it cannot be ruled out, the likelihood of an individual being an *ATM* heterozygote as a random sampling from the general population would be expected to be of the order of 1%, so the probability that one cell strain of six obtained from randomly selected apparently normal individuals would be from an *ATM* heterozygote would be of the order of 5 to 6%.

For the samples from individuals from the two A-T families, the *ATM* −/− probands clearly showed hypersensitivity in the low dose-rate γ-H2AX assay with mean foci per cell values of 22.1 ± 4.2 for GM03395 family 605 proband cells and 19.7 ± 4.1 for GM03487 family 516 proband cells. The mean foci per cell estimates for obligate heterozygous parents in family 605 were 11.0 ± 3.2, and 11.6 ± 3.2, respectively, and in family 516, the mean foci number for heterozygous strains GM03488 and GM03489 were 11.5 ± 3.3, and 10.2 ± 3.1.

This assay shows a clear difference between the *ATM* +/– obligate heterozygous parents relative to the *ATM* –/– probands within families. Further, across the different families with their inherent genetic background heterogeneities, the results of the mean foci per cell in the assay are very similar among all the heterozygotes and similar to the mean for the sample from one of the apparently normal individuals (GM08402), though as I have already pointed out it seems unlikely that individual is an ATM heterozygote.

What is also clear is the appreciable and consistent difference in foci per cell for normal compared to the samples from *ATM* heterozygotes. Mean foci per cell values (μ_2) for samples from 5 of the 6 apparently normal individuals ranged from 4.5 to 5.4, and the mean and standard error of these means was 4.6 ± 0.2. For the obligate *ATM* heterozygotes the mean foci per cell ranged from 10.2 to 11.6, with a mean and standard error for the pooled data of 11.1 ± 0.2.

The results from the assay for unaffected siblings in the two A-T families were also interesting. As summarized in Table 3-1, in family 605, there was no significant difference in the mean numbers of foci per cell in pair-wise comparisons between any of the three siblings in this assay. For GM03398 the mean was 11.2 ± 3.1, for GM03399 the mean was 10.5 ± 2.9, and for GM03490, the mean was 10.9 ± 3.1. Neither were these values significantly different from those for samples from their obligate *ATM* heterozygous parents. In family 516 only one of the three unaffected siblings had a mean foci per cell value (11.4 ± 3.0 for GM03490) similar to that for the heterozygous parents, while the mean foci per cell for the other unaffected siblings were 5.3 ± 2.3 for GM03491 and 4.8 ± 2.2 for GM03492. These values were not significantly different from each other or from the any of the mean values from 5 of the 6 apparently normal controls.

From this assay alone, one would strongly suspect that, given the family histories, all three of the unaffected siblings in family 605 were *ATM* heterozygotes and in family 516, only one of three was an *ATM* heterozygote.

To determine whether the individual siblings suspected of being *ATM* heterozygotes by the low dose-rate γ-H2AX assay were, in fact, heterozygotes I carried out an ATM genotyping with respect to the known mutations in these families, from coded samples from the cell strains derived from individuals from these families by PCR amplification of the genomic regions of interest and sequencing of the products. The PCR/sequencing assay confirmed the known ATM mutations in the parents and probands, and showed that in family 605, all three siblings were heterozygotes. Because both heterozygous parents had the identical mutant allele, it was not surprising that all had the same G>A substitution at nucleotide residue 7913. In family 516, only one of the siblings (GM03490) was heterozygous, with the mutant allele being the 4-base insertion at nucleotide residue 1141, also present in the heterozygous father. This mutant allele was also present in the proband (GM03487) in family 516, as was the allele bearing the A>T substitution inherited from the heterozygous mother (GM03489).

Lymphoblastoid cells:

The results of the more limited set of experiments involving the cells of lymphoblast origin, designed to investigate the possibility of using the assay in further studies using more accessible peripheral blood lymphoblasts, are summarized in Table 3-2. In this case only two separate experiments were carried out for each cell strain, and only 50 cells were scored for each sample in each experiment. Further, cells from only

one normal control (*ATM* +/+), two obligate heterozygotes (*ATM* +/−), and two affected probands (*ATM* −/−) were included. From this summary in Table 3-2 it is also clear that the low dose-rate assay clearly separates and distinguishes three distinct phenotypes associated with normal, ATM+/−, and ATM −/− cells. The mean γ-H2AX foci per cell for the *ATM* +/+ normal cells was 2.7 (± 2.0). For the obligate heterozygous parents from family 516 (also used in the fibroblast study) the mean values were 6.2 (± 2.3) and 6.7 (± 2.5). For the *ATM* −/− probands, the numbers of foci per cell for the family 516 proband was 14.2 (± 4.1) and for the L3 proband cells the mean was 14.6 (± 5.1). Although the different phenotypic groups were statistically distinct, all the values appeared to be uniformly lower for the lymphoblast cells. Since the conditions of the assay and cell fixations were somewhat different for the experiments using lymphoblast vs. fibroblast derived cells, attributing the difference to cell types from our data is not warranted. For example, I used prolonged isoleucine deprivation for G_1 phase synchronization and cytocentrifuge cell preparations for the lymphoblastoid cultures, but used contact inhibited G_0 monolayers with *in situ* monolayer fixation and immunocytochemistry for fibroblasts. In spite of the limitations, however, the experiments demonstrate that that there are no fundamental problems in terms of general cell types that would preclude the use of peripheral blood lymphocytes for the assay. In fact the latter cell type should be superior to the cultured lymphoblastoid cultures, since cell cycle synchronization would not a problem.

Cell Source	Cell Strain	*ATM* status	Mean Foci per Cell (± S.D.)
Queensland Institute for Medical Research (Dr. M.F. Lavin)	C3	Normal (WT) (*ATM* +/+)	2.7 (±2.1)
	L3	A-T Affected (*ATM* −/−)	14.6 (±5.1)
Coriell Institute A-T Family 516	GM03187	Oblig. Het. (*ATM* +/−)	6.2 (±2.3)
	GM03188	Oblig. Het. (*ATM* +/−)	6.7 (±2.5)
	GM03189	Proband (*ATM* −/−)	14.2 (±4.1)

DISCUSSION

By way of connecting hyper-radiosensitivity phenotypes to cancer susceptibility, several studies have identified individuals who may be cancer prone through expression of hypersensitivity to G_2 chromosomal aberration induction following exposure to ionizing radiation or other treatments that directly or indirectly produce DNA DSBs. Particularly pertinent examples are approaches to the measurement of hypersensitivity of A-T heterozygotes who are known to be cancer prone (1). Among these, several have utilized the G_2 chromosomal radiosensitivity assay mentioned above (eg.,(2-8)). While there are numerous factors involving experimental protocols that influence the outcome of the G_2 assay itself (6), and some have reported it to be less than robust (eg, (10)), with appropriate matched controls the assay has been recognized as very useful (6). This assay has also been used to show an elevated G_2 chromosomal radiosensitivity in lymphocytes of breast cancer patients compared to cells from control individuals, and the proportion with elevated sensitivity was some 40%; far greater than the expected frequency of *ATM, BRCA1, BRCA2, and TP53* heterozygotes combined (~6%) (8,9). Another potentially useful assay involving chromosomal aberrations measured by chromosome painting was shown to distinguish differences, on average, between cells from normal individuals and from both *ATM* and Nijmegen Breakage Syndrome (*NBS*) heterozygotes, some 15 to 20% of the mean values for heterozygotes fell in the range of means for the normal controls (48) .

A different G_2 chromosomal aberration assay was reported recently by Johnson and colleagues based on their observation that Camptothecin (CPT) causes DNA DSBs

by promoting the collapse of replication forks during S phase, and that A-T fibroblasts are defective in the repair of these kinds of DSBs (12,13). Cells derived from *ATM* −/− homozygotes were by far the most sensitive in this assay, but cells from obligate *ATM* +/− heterozygotes from the two families studied were also significantly more sensitive than those from normal individuals, principally due to the appreciable hypersensitivity for induction of chromatid exchange-type aberrations in G_2 prematurely condensed chromosomes (13).

In another kind of assay measuring differences in radiation-induced G_1 blocks and delayed entry into S phase, Nagasawa and Little and their colleagues in the mid-1980's demonstrated significant differences in cells from *ATM* heterozygotes relative to cells from both normal individuals and affected probands (14,16).

The measurement of γ-H2AX foci in cells as a sensitive assay reflecting breakage and rejoining of DNA DSBs has greatly facilitated studies that may help to elucidate the possible role of variations in DNA DSBs processing pathways in the known variations in susceptibilities among individuals to cancer (15,17,18). While the chromosomal or cell cycle checkpoint radiosensitivity assays may be linked to DNA DSB processing, the link is more indirect than appears to be the case for the γ-H2AX assay, though in contrast to the chromosomal aberration assays, the γ-H2AX assay does not appear to reveal processes leading to mis-repair or mis-rejoining.

In the present study, the γ-H2AX assay using the continuous low dose-rate irradiation protocol clearly enables a distinction between cell samples derived from normal *ATM* +/+ individuals relative to *ATM* +/− obligate heterozygotes and, of course, affected *ATM* −/− probands. While it might prove very useful for distinguishing *ATM*

heterozygotes among unaffected siblings in A-T families in which the mutations were unknown, the assay, of course, is indicative only of hypersensitivity to radiation in respect to levels of these foci, which may have resulted from any of a number of other possible genetic factors.

As mentioned earlier, the hypersensitivity response in this assay for one of the cell strains from the group of six apparently normal individuals seems unlikely to have been the result of *ATM* heterozygosity in this individual, though it cannot be ruled out. However, several previous studies on radiation sensitivity of cells from apparently normal individuals, have suggested that a surprising proportion if the population, perhaps a high as 20 to 25%, show a mild hypersensitivity similar to that reported for *ATM* heterozygotes (16,36,49,49-54). We have also seen a high proportion of mildly hypersensitive cell strains derived from apparently normal individuals using a low dose-rate colony formation assay. (P. Wilson, PhD Dissertation, CSU, 2006). Further, we have reported a similar hypersensitivity for cells from the apparently normal parents of 5 Retinoblastoma (RB*) patients where the sensitivity is unlikely to be directly related to the *RB* gene (50). Additional studies using the present low dose-rate γ-H2AX assay on cells from individuals in the RB families will be reported elsewhere.

It is interesting that not only was one of six samples from the apparently normal individuals hypersensitive in the γ-H2AX assay, but the level of hypersensitivity was very similar to that for cells from *ATM* heterozygotes, and further that the levels of hypersensitivity for *ATM* heterozygotes was the same within the same family as well as between the two families. Although the numbers of individuals involved is relatively small for the *ATM* families, the similarity of radiosensitivity phenotypes that appears to

be independent of the presumably diverse genetic backgrounds represented by the parents in these families, might argue that a fairly limited number of genes affect this low dose-rate γ-H2AX radiosensitivity phenotype. This is further suggested by the similar level of hypersensitivity for the cells from one of the apparently normal individuals. Also suggesting a limited number of genes affecting radiosensitivity for the G_2 chromosomal radiosensitivity phenotype, Scott and his co-workers reported radiosensitivities by this assay in 37 first-degree relatives of 16 hypersensitive breast cancer patients (7). Some 62% (23 of these 37) were also hypersensitive, whereas only 7% or 1 of 15 first-degree relatives of 4 patients with normal G_2 sensitivity. The distribution of sensitivities was trimodal, suggesting the involvement of a limited number of genes.

Different measurements of radiation damage, ranging from molecular and cellular endpoints such as DNA DSBs, chromosomal aberrations, mutations, or cell killing, to tissue effects or late effects in animals, such as carcinogenesis, would be expected to involve contributions from a wider and wider spectrum of genetic determinants involved in the expression of biological effects. Still, genetic factors affecting responses at the cellular and molecular level are likely to exert a substantial influence on variations in the effects of radiations of concern for humans, and in this sense studies and assays such as the one described here may be helpful to better recognize the sources and explain such variations among individuals.

REFERENCES

1. D. F. Easton, Cancer risks in A-T heterozygotes, *Int.J.Radiat.Biol.* **66 (suppl)**, S177-S182 (1994).

2. R. Parshad, K. K. Sanford and G. M. Jones, Chromatid damage after G2 phase x-irradiation of cells from cancer-prone individuals implicates deficiency in DNA repair, *Proc.Natl.Acad.Sci.USA* **80**, 5612-5616 (1983).

3. K. K. Sanford, R. Parshad, R. R. Gantt and R. E. Tarone, A deficiency in chromatin repair, genetic instability, and predisposition to cancer, *CRC Critical Reviews in Oncogenesis* **1**, 323-341 (1989).

4. K. K. Sanford and R. Parshad, Detection of cancer-prone individuals using cytogenetic response to X-rays, *in* "Chromosome Aberrations, Basic and Applied Aspects" (G. Obe and A. T. Natarajan, Eds.), Springer-Verlag, Berlin (1990).

5. D. Scott, L. A. Jones, S. A. G. Elyan, A. Spreadborough, R. Cowan and G. Ribiero, Identification of A-T heterozygotes, *in* "Atataxia-telangiectasia" (R. A. Gatti and R. B. Painter, Eds.), Springer-Verlag, Berlin (1992).

6. D. Scott, A. R. Spreadborough, L. A. Jones, S. A. Roberts and C. J. Moore, Chromosomal radiosensitivity in G_2-phase lymphocytes as an indicator of cancer predisposition, *Radiat.Res.* **145**, 3-16 (1996).

7. S. A. Roberts, A. R. Spreadborough, B. Bulman, J. B. Barber, D. G. R. Evans and D. Scott, Heritability of cellular radiosensitivity: a marker of low-penetrance predisposition genes in breast cancer?, *American Journal of Human Genetics* **65**, 784-794 (1999).

8. D. Scott, J. B. Barber, A. R. Spreadborough, W. Burrill and S. A. Roberts, Increased chromosomal radiosensitivity in breast cancer patients: a comparison of two assays, *Int.J.Radiat.Biol.* **75**, 1-10 (1999).

9. J. M. Varley, D. G. Evans and J. M. Birch, Li-Fraumeni syndrome--a molecular and clinical review, *Br.J Cancer* **76**, 1-14 (1997).

10. A. Vral, H. Thierens, A. Baeyens and L. De Ridder, The micronucleus and G2-phase assays for human blood lymphocytes as biomarkers of individual sensitivity to ionizing radiation: limitations imposed by intraindividual variability, *Radiat.Res.* **157**, 472-477 (2002).

11. S. Neubauer, R. Arutyunyan, M. Stumm, T. Dork, R. Bendix, M. Bremer, R. Varon, R. Sauer and E. Gebhart, Radiosensitivity of ataxia telangiectasia and Nijmegen breakage syndrome homozygotes and heterozygotes as determined by three-color FISH chromosome painting, *Radiat.Res.* **157**, 312-321 (2002).

12. R. T. Johnson, E. Gotoh, A. M. Mullinger, A. J. Ryan, Y. Shiloh, Y. Ziv and S. Squires, Targeting double-strand breaks to replicating DNA identifies a subpathway of DSB repair that is defective in ataxia-telangiectasia cells., *Biochem Biophys Res Commun* **261**, 317-325 (1999).

13. J. C. Leonard, A. M. Mullinger, J. Schmidt, H. J. Cordell and R. T. Johnson, Genome instability in ataxia telangiectasia (A-T) families: camptothecin-induced damage to replicating DNA discriminates between obligate A-T heterozygotes, A-T homozygotes and controls, *Biosci.Rep.* **24**, 617-629 (2004).

14. H. Nagasawa, S. A. Latt, M. E. Lalande and J. B. Little, Effects of X-irradiation on cell cycle progression, induction of chromosomal aberrations and cell killing in ataxia telangiectasia, *Mutation Res.* **148**, 71-82 (1985).

15. K. Rothkamm and M. Lobrich, Evidence for a lack of DNA double-strand break repair in human cells exposed to very low x-ray doses, *Proc.Natl.Acad.Sci.U.S.A* **100**, 5057-5062 (2003).

16. H. Nagasawa, K. H. Kraemer, Y. Shiloh and J. B. Little, Detection of ataxia telangiectasia heterozygous cell lines by postirradiation cumulative labeling index: measurements with coded samples, *Cancer Res.* **47**, 398-402 (1987).

17. S. H. MacPhail, J. P. Banath, T. Y. Yu, E. H. Chu, H. Lambur and P. L. Olive, Expression of phosphorylated histone H2AX in cultured cell lines following exposure to X-rays, *Int.J Radiat.Biol.* **79**, 351-358 (2003).

18. E. P. Rogakou, D. R. Pilch, A. H. Orr, V. S. Ivanova and W. M. Bonner, DNA double-stranded breaks induce histone H2AX phosphorylation on serine 139, *J Biol.Chem.* **273**, 5858-5868 (1998).

19. K. Sax, The time factor in x-ray production of chromosomal aberrations, *Proc.Natl.Acad.Sci.USA* **25**, 225-233 (1939).

20. D. E. Lea, Actions of Radiations on Living Cells, Cambridge Univ. Press, London (1955).

21. W. L. Russell, L. B. Russell and Kelly.E.M., Radiation dose rate and mutation frequency, *Science* **128**, 1546-1550 (1958).

22. M. M. Elkind and H. Sutton, X-ray damage and recovery in mammalian cells in culture, *Nature* **184**, 1293-1295 (1959).

23. J. S. Bedford and E. J. Hall, Survival of Hela cells cultured *in vitro* and exposed to protracted gamma radiation, *Int.J.Radiat.Biol.* **7**, 377-383 (1963).

24. R. L. Ullrich, M. C. Jernigan, G. E. Cosgrove, L. C. Satterfield, N. D. Bowles and J. B. Storer, The influence of dose and dose rate on the incidence of neoplastic disease in RFM mice after neutron irradiation, *Radiat.Res.* **68**, 115-131 (1976).

25. R. L. Wells and J. S. Bedford, Dose-rate effects in mammalian cells. IV. Repairable and nonrepairable damage in noncycling C3H 10T 1/2 cells, *Radiat.Res.* **94**, 105-134 (1983).

26. R. L. Ullrich and J. B. Storer, Influence of gamma irradiation on the development of neoplastic disease in mice. III. Dose-rate effects, *Radiat.Res.* **80**, 325-342 (1979).

27. R. L. Ullrich, M. C. Jernigan, L. C. Satterfield and N. D. Bowles, Radiation carcinogenesis: time-dose relationships, *Radiat.Res.* **111**, 179-184 (1987).

28. M. A. Stackhouse and J. S. Bedford, An ionizing radiation-sensitive mutant of CHO cells: irs-20 Dose-rate effects and cellular recovery processes, *Radiat.Res.* **136**, 250-254 (1993).

29. A. Priestley, H. J. Beamish, D. Gell, A. G. Amatucci, M. C. Muhlmann-Diaz, B. K. Singleton, Smith G.C., T. Blunt, L. C. Schalkwyk, J. S. Bedford, Jackson S.P., P. A. Jeggo and G. E. Taccioli, Molecular and biochemical characterization of DNA-dependent protein kinase-defective rodent mutant irs-20, *Nucl.Acids Res.* **26**, 1965-1973 (1998).

30. M. A. Stackhouse and J. S. Bedford, An ionizing radition-sensitive mutant of CHO cells: irs-20 Isolation and initial characterization, *Radiat.Res.* **136**, 241-249 (1993).

31. M. A. Stackhouse and J. S. Bedford, An ionizing radiation-sensitive mutant of CHO cells: irs-20. III. Chromosome aberrations, DNA breaks and mitotic delay, *Int.J.Radiat.Biol.* **65**, 571-582 (1994).

32. D. Scott, Q. Hu and S. A. Roberts, Dose-rate sparing for micronucleus induction in lymphocytes of controls and ataxia-telangiectasia heterozygotes exposed to 60Co gamma-irradiation in vitro, *Int.J.Radiat.Biol.* **70**, 521-527 (1996).

33. Kato, T. A. The use of a Gamma-H2AX foci assay for measurement of radiosensitivity phenotypes and DNA DSB induction and processing. 2006. Colorado State University.

34. S. Kozlov, N. Gueven, K. Keating, J. Ramsay and M. F. Lavin, ATP activates ataxia-telangiectasia mutated (ATM) in vitro. Importance of autophosphorylation, *J Biol.Chem.* **278**, 9309-9317 (2003).

35. Y. Peng, R. G. Woods, H. Beamish, R. Ye, S. P. Lees-Miller, M. F. Lavin and J. S. Bedford, Deficiency in the catalytic subunit of DNA-dependent protein kinase causes down-regulation of ATM, *Cancer Res.* **65**, 1670-1677 (2005).

36. J. B. Little and H. Nagasawa, Effect of confluent holding on potentially lethal damage repair, cell cycle progression, and chromosomal aberrations in human normal and ataxia-telangiectasia fibroblasts, *Radiat.Res.* **101**, 81-93 (1985).

37. M. N. Cornforth and J. S. Bedford, X-ray induced breakage and rejoining of human interphase chromosomes., *Science* **222**, 1141-1143 (1983).

38. M. C. Mühlmann-Díaz and J. S. Bedford, Brakage of human chromosomes 4,19, and Y in G_0 cells immediately after exposure to gamma-rays., *Int.J.Radiat.Biol.* **65**, 165-173 (1994).

39. M. N. Cornforth and J. S. Bedford, On the nature of a defect in cells from individuals with ataxia telangiectasia., *Science* **227**, 1589-1591 (1985).

40. Hwang, Jeng-Jong. Use of DNA polymerase alpha antibodies in studies of radiation effects on cell proliferation. 1990. Colorado State University.

41. R. A. Tobey and K. D. Ley, Isoleucine-mediated regulation of genome replication in various mamalian cell lines, *Cancer Res.* **31**, 46-51 (1971).

42. R. J. Amdur and J. S. Bedford, Dose-rate effects between 0.3 and 30 Gy/h in a normal and a malignant human cell line, *Int.J.Radiat.Oncol.Biol.Phys.* **30**, 83-90 (1994).

43. L. Metzger and G. Iliakis, Kinetics of DNA double-strand break repair throughout the cell cycle as assayed by pulsed field gel electrophoresis in CHO cells, *Int.J.Radiat.Biol.* **59**, 1325-1339 (1991).

44. C. Badie, G. Iliakis, N. Foray, G. Alsbeih, B. Cedervall, N. Chavaudra, G. Pantelias, C. Arlett and E. P. Malaise, Induction and rejoining of DNA double-strand breaks and interphase chromosome breaks after exposure to X rays in one normal and two hypersensitive human fibroblast cell lines, *Radiat.Res.* **144**, 26-35 (1995).

45. G. Iliakis, H. Wang, A. R. Perrault, W. Boecker, B. Rosidi, F. Windhofer, W. Wu, J. Guan, G. Terzoudi and G. Pantelias, Mechanisms of DNA double strand break repair and chromosome aberration formation, *Cytogenet.Genome Res.* **104**, 14-20 (2004).

46. M. Lobrich and P. A. Jeggo, The two edges of the ATM sword: co-operation between repair and checkpoint functions, *Radiother.Oncol.* **76**, 112-118 (2005).

47. P. L. Olive, Detection of DNA damage in individual cells by analysis of histone H2AX phosphorylation, *Methods Cell Biol.* **75**, 355-373 (2004).

48. S. Neubauer, R. Arutyunyan, M. Stumm, T. Dork, R. Bendix, M. Bremer, R. Varon, R. Sauer and E. Gebhart, Radiosensitivity of ataxia telangiectasia and Nijmegen breakage syndrome homozygotes and heterozygotes as determined by three-color FISH chromosome painting, *Radiat.Res.* **157**, 312-321 (2002).

49. J. B. Little, W. W. Nichols, P. Troilo, H. Nagasawa and L. C. Strong, Radiation sensitivity of cell strains from families with genetic disorders predisposing to radiation-induced cancer, *Cancer Res.* **49**, 4705-4714 (1989).

50. M. M. Fitzek, W. K. Dahlberg, H. Nagasawa, S. Mukai, J. E. Munzenrider and J. B. Little, Unexpected sensitivity to radiation of fibroblasts from unaffected parents of children with hereditary retinoblastoma, *Int.J.Cancer* **99**, 764-768 (2002).

51. H. Nagasawa and J. B. Little, Radiosensitivities of ten apparently normal human diploid fibroblast strains to cell killing, G2-phase chromosomal aberrations, and cell cycle delay, *Cancer Res.* **48**, 4535-4538 (1988).

52. P. J. Deschavanne, D. Debieu, D. Fertil and E. P. Malaise, Re-evaluation of *in vitro* radiosensitivity of human fibroblasts of different genetic origins, *Internation Journal of Radiation Biology* **50**, 279-293 (1986).

53. J. B. Little, H. Nagasawa, W. K. Dahlberg, M. Z. Zdzienicka, S. Burma and D. J. Chen, Differing responses of Nijmegen breakage syndrome and ataxia telangiectasia cells to ionizing radiation, *Radiat.Res.* **158**, 319-326 (2002).

54. P. J. Deschavanne and B. Fertil, A review of human cell radiosensitivity in vitro, *Int.J Radiat.Oncol.Biol.Phys.* **34**, 251-266 (1996).

Chapter 4

Evidence for A Defect in DNA Double Strand Break Processing in Cells from Unaffected Parents of Retinoblastoma Patients and Other Apparently Normal Humans: Application of Two γ-H2AX Focus Assays

ABSTRACT

In recent previous reports we have shown that 1) a γ-H2AX focus assay applied after protracted low dose-rate irradiation allowed a clear distinction to be made between cells from *ATM* heterozygotes and other mildly hypersensitive but apparently normal individuals, relative to cells from the majority of clinically normal individuals, 2) cells from unaffected parents of Retinoblastoma (RB) patients in all 5 families tested show a mild hypersensitivity to radiation induced G_1 arrest and cell killing, and the latter is enhanced for low dose-rate irradiation, and 3) the parents in these RB families display a distinctive gene expression profile. These observations suggest the possibility of an enhanced germline mutation rate, perhaps resulting from some mild defect in genome maintenance. I therefore examined the levels of γ-H2AX foci reflecting the presence of DNA double strand breaks (DSBs) in a G_2/M assay and in non-cycling G_0 cells after low dose rate irradiation; a condition that enhances differences in processing breaks for normal vs. hypersensitive cells. The latter assay reflects the capacity of cells to process DNA DSBs by non homologous end joining (NHEJ) and the former, any additional contribution resulting from homology directed repair (HDR). I found that cells from all

parents tested in the 5 RB families were clearly hypersensitive in the low dose rate assay. In addition, low passage cultured fibroblasts from 7 of 19 apparently normal individuals that appeared to be mildly hypersensitive in cell survival assays were also hypersensitive in the low dose-rate γ-H2AX assay. The relative hypersensitivities of the cell strains seen in the low dose-rate G_0 assay were similar in the G_2/M γ-H2AX focus assay, although the statistical resolution of differences was lower.

INTRODUCTION

Previous studies have shown a mild hypersensitivity to radiation in cells derived from a surprisingly high proportion of apparently normal individuals (1) and of particular interest, a consistent mild hypersensitivity to radiation in cells derived from the parents of five unselected hereditary retinoblastoma patients (2). Further, cells from the parents in the RB families display a pattern of gene expression that is distinctly different from cells derived from age and sex matched normal individuals, when as few as 9 genes were analyzed (3). The expression array used was enriched for about 19,000 known genes, and while none of the above 9 were known DNA repair genes, this does not rule out the possibility that DNA damage processing may still be involved in the radiation hypersensitivity. For example, one or more of the 9 genes referred to above (NM23A, MCM5, HOXB2, HOXD10, HOXC10, polo-like kinase I and E2F1, (3)) might indirectly interfere with damage processing. Another possibility is that a change in expression of one or more of the other 10,000 genes not present in the expression arrays used previously might actually involve as yet unknown DNA repair related genes as a unique feature of the cells from the RB parents, or the mildly hypersensitive cells from other clinically normal individuals, or that the deficient is not manifest at the level of gene expression.

A more direct test of DNA damage processing capacity related to ionizing radiation sensitivity should involve measurement of the production and rejoining of DNA DSB in an assay where differences in repair function are enhanced. I have employed such an assay that allows a clear difference in DNA DSBs to be measured after low dose-

rate irradiation of cells from normal vs. ATM +/− individuals. This assay, involving the scoring of γ-H2AX foci in non cycling contact inhibited cells, takes advantage of the fact that for repair deficient cells dose-rate effects are generally reduced relative to their wild-type counterpart, and the damage measured is directly related to the presence of DNA DSBs.

The low dose-rate γ-H2AX assay, for reasons mentioned above, requires the use of non-cycling G_1 or G_0 cells, and reflects only the contribution to DSB rejoining from the NHEJ system. Such cells do not contain certain components required for homology directed repair (eg., *RAD51*) let alone sufficient levels of nearby homologous substrate to repair a significant fraction by a process involving homologous recombination. For this reason, I have also examined and applied another assay in which cells irradiated in G_2 are scored for the levels of γ-H2AX foci present a short time later on the chromosomes of mitotic cells. In S- and G_2 phases, cells do have the capacity and availability of homologous substrate to carry out a homology directed repair (HDR) of DSBs, in addition to the very active NHEJ system that also operates. Thus, cells defective in NHEJ would be expected to register as hypersensitive in both the low dose-rate G_0 assay and the G_2/M assay, while deficiencies in an HDR system would register as sensitive in the G_2/M, but not the low dose-rate G_0 assay.

The present study examines the radiosensitivity of cells from 8 parents of RB patients from 5 families, and from 21 apparently normal individuals, with respect to the levels of γ-H2AX foci per cell after 24 hours of continuous low dose-rate irradiation (10 cGy/h) of contact inhibited cultures, as well as in the G_2/M focus assay described above. In the low dose-rate study the cells from 7 of the 8 parents of RB patients and 6 of 18

from apparently normal individuals revealed a radiation hypersensitivity comparable to that seen previously for cells from 8 different *ATM* (+/−) heterozygotes. In the G_2/M assay cells from 7 of 8 parents of RB patients and 6 of 14 from apparently normal individuals tested were hypersensitive.

MATERIALS AND METHODS

Cells and Cell Culture

The clinical source and characteristics of the skin fibroblast cell strains from the parents and probands derived from the five retinoblastoma families was reported previously (2). The cell strains from the RB families were established at the Harvard School of Public Health, and are designated by the families of origin as MF-4F, MF-2M and MF-3R for family I; MF-6F, MF-7R from family II; MF-11F, MF-12M, and MF-10R, for family III; MF-15F, MF-13M, and MF-14R from family IV, and MF-18F, MF-16M, and MF-14R from family V. In each family the code letter F, M, and R, refers to the father, mother, and proband, respectively (2). The low passage human fibroblast cultures from individuals who were clinically apparently normal, were from the Coriell Institute for Medical Research (CIMR) in Camden, NJ. These strains are designated GM04505, GM08402, GM03440, GM05757, GM08333, GM00038, GM00500, GM08447, GM05756, GM00969, GM08429, GM08399, GM01652, and AG1522. One other cell strain, designated RMP4 from an apparently normal individual was obtained from the Harvard School of Public Health at the same time as the RB family cell strains.

Stock cultures were grown in Eagle's Minimal Essential Medium (GIBCO, Grand Island, NY) supplemented with 15% heat inactivated fetal bovine serum, penicillin (50 units/ml) and streptomycin (50 μg/ml), and were maintained at 37°C in a humidified atmosphere of 5% CO_2 in air. For experiments where γ-H2AX foci were measured, cells were grown on chamber slides or flaskettes to form confluent contact inhibited monolayers for the low dose-rate irradiation experiments, or in T75 flasks to yield

exponentially growing partly confluent monolayers for the G_2/M experiments. After preparation, the cultures were placed in the appropriate irradiation facility. For the case of low dose-rate exposures, requiring 24 hours irradiation, the flaskettes were first sealed and then placed in position in the low dose-rate irradiation facility where they were kept at 37°C throughout the 24 hour period. The cells were kept in the non-cycling contact inhibited state because there is a high background of γ-H2AX foci in S phase cells, and virtually all the cells in the contact inhibited cultures are in a G_0 state with a G_1 DNA content. Further, for the low dose-rate irradiation it was undesirable to allow cells to continue to progress through the cell cycle and proliferate during the 24 hour exposure periods. For the G_2/M experiments, the log phase cultures were irradiated and then incubated for 0.5 hours before Colcemid was added for a 1 hour period to allow accumulation of mitotic cells that had been irradiated in G_2.

Before any of the experiments were carried out, the cell cultures were coded so the person performing the experiments and scoring the slides would not know the origin of the cells. After the samples were scored, and the data compiled and summarized, the origin of the cultures was decoded. Three independent experiments were carried out for each cell strain for the different irradiation protocols involving G_0 cells, and the numbers of γ-H2AX foci were scored in each of 100 cells for each sample in each experiment. For the G_2/M γ-H2AX assay, two experiments were carried out, and 30 cells were scored in each experiment.

Irradiations

High dose rate irradiations were carried out using a J.L. Shepherd Model Mark I-68 6000 Ci ^{137}Cs irradiator. Low dose-rate irradiations were carried out in a 37°C low dose rate irradiation facility where samples can be placed on shelves parallel to, and at various distances above, a plane of from one to twelve 4 Ci ^{137}Cs sources, depending on the dose-rate desired. The sources can be remotely placed under the cultures or retracted to a shielded safe position to avoid exposure of personnel involved. The radiation facilities have been described previously (4). Dose-rates and field uniformities over the positions of samples were measured using an ionization chamber (Radcal 2025AC Radiation monitor with a 20x5-180 Electrometer/Ion chamber). For the acute high dose rate exposures the dose-rate was 250cGy/minute and for the 24 hour chronic exposures the dose-rate was 9.9 to 10.2 cGy /hour.

γ-H2AX Immunocytochemistry

Immunocytochemistry for detection and the scoring of γ-H2AX foci in this laboratory has been described in detail in previous reports. Briefly, the procedures were as follows. Immediately after irradiation, cells in the culture vessels were washed with ice cold PBS and then fixed in PBS containing 4% paraformaldehyde for 15 minutes. After three further washes with PBS for 10 minutes each, cells were treated with 0.2% Triton X-100 solution in PBS for 5 minutes. Before immunocytochemical detection of γ-H2AX, cells were blocked with a solution of 10% goat serum in PBS for 1 hour at room temperature to reduce subsequent non-specific anti- γ-H2AX antibody binding. Mouse monoclonal anti-γ-H2AX antibody from Upstate, was diluted 1:500, in PBS, and the flaskettes with the cell monolayers were incubated in the diluted antibody for 1 hour at

37°C. Cells were then washed three times with PBS for 10 minutes each time, and then secondary antibody (Alexa fluor 488 conjugated goat anti-mouse, from Molecular Probes) that had been diluted 1:500 was added and the slides were incubated for another 1 hour at 37°C. After four washes with PBS for 10 minutes each, slides were then mounted in a solution of 1.5μg/ml DAPI containing slow-fade (Molecular Probes).

The preparation of samples for scoring of γ-H2AX foci on mitotic cells after G_2 irradiation was accomplished by harvesting the cultures after the 1 hour incubation in Colcemid, and preparing slides using a cytocentrifuge. Briefly, mitotic cells were harvested by shaking them off the culture surface, then after centrifugation, cells were resuspended in swelling buffer (50mM KCl, 50mM $MgSO_4$ 5mM HEPES) for 20 minutes and centrifuged onto slide with the cytocentrifuge (Cytospin, Shandon). Cells on the slides were then fixed in 4% paraformaldehyde, washed with PBS, and permeabilized for 5 min in KCM buffer containing Triton X-100 (120mM KCl, 20mM NaCl, Tris-HCl 10mM, EDTA 0.5mM, Triton X-100 0.1%, pH 7.5). Further immunocytochemistry was similar to that used for the G_0 monolayers.

Scoring γ-H2AX Foci

Images of cells were captured using an Olympus AX-70 fluorescence microscope equipped with a PSI image analysis system utilizing the MAC-Probe package. The thickness of the cell nuclei for these cell strains when they are attached and flattened to the surface of the culture vessel was approximately 2 micrometers and the foci were sufficiently intense that focusing the microscope midway through the nuclei allowed virtually all the foci to be visualized. There was usually a low level background signal

that appeared over and between cells. This background was generally somewhat smaller and less intensely fluorescent than the γ-H2AX foci, so before scoring the numbers of foci over the nuclei a background subtraction was applied uniformly across the microscope field images captured. The images were then stored and cells from these were later scored. As previously reported, in a few cases where very low numbers of foci per nucleus were seen this subtraction can result in a spurious increase in the numbers of cells with 0 or 1 focus per cell, leading to a poor fit to the expected Poisson distribution of the frequency of cells with various numbers of foci per cell for a population of cells of uniform sensitivity. In the few instances where this occurs, I routinely fit bimodal (mixed) Poisson distributions to the observed distributions of numbers of cells with various numbers of foci per cell, and use the higher mean value for the bimodal distribution. In this way comparisons of slightly less with slightly more sensitive cells would not bias the conclusion that one cell strain was less sensitive than another, when in fact it was not. Scoring γ-H2AX foci on metaphase cells was also carried out by the same image analysis procedure.

RESULTS

The summary mean values for the complete data set for γ-H2AX foci per cell for all the irradiation conditions and the estimated standard errors of these means are summarized in Table 4-1, but the results focusing on the various different irradiation and sampling conditions are presented in Figures 4-1 to 4-3.

Figure 1 summarizes the histograms recording the percentage of cells with various numbers of γ-H2AX foci per G_0 cell in the 24 hour low dose-rate irradiation protocol. In each panel the mean value for the distribution is shown along with the standard deviation to indicate variation in focus counts among cells for that sample. The top two rows of panels (A-H) show the results for cells derived from 8 parents of RB patients and the bottom four rows of panels (I-V) from 15 clinically normal individuals. The data summarized in Figure 1 are for total spontaneous and radiation induced foci per cell, but as shown in Table 4-1, where the mean foci number from all the irradiation protocols and controls are shown, the numbers of foci in unirradiated G_0 cells is fairly low compared to the total. Also shown for each histogram are Poisson distributions derived using the observed mean values. The observed distributions, by and large, were reasonably close to the Poisson expectations. Among the samples from apparently normal individuals the majority of about 9 of the 15 are similar in sensitivity and more resistant (less sensitive) with respect to the levels of foci per cell than the other 6. Also relative to the majority of cells from apparently normal individuals, all 8 of the samples from the parents of RB patients showed an increased sensitivity similar to that for the 6 more sensitive normal samples. T- tests verified that differences in mean values for any of the

samples from the more sensitive apparently normal or RB parents groups compared to any from the more resistant normal group were all highly significant.

The spectrum of radiosensitivities obtained using this low dose-rate G_0 γ-H2AX assay is illustrated in Figure 2, where the frequencies among the sensitivity categories (induced foci per cell from Table 4-1) are shown for the different human cell strains. Also shown are the relative positions in this sensitivity spectrum of cell strains derived from the parents, probands and three siblings from each of two Ataxia-Telangiectasia families along with cells from other apparently normal individuals in another recent report from this laboratory. At one end of the spectrum there are 14 samples from apparently normal individuals with average numbers of induced foci per cell ranging from 2 to 6, and at the other end there are 2 samples from individuals with Ataxia-Telangiectasia with 18 to 21 induced foci per cell. In between, with mean numbers of induced foci per cell ranging from 6 to11, are all 8 of the samples from parents of RB patients, together with 6 samples from apparently normal individuals, and all 8 of the *ATM* heterozygotes.

Also, data reported in Table 1 include results from a series of experiments for acute high dose-rate exposures with G_0 cells where γ-H2AX foci were measured 1 and 24 hours after an exposure of 1 Gy. These two sample times correspond to post-irradiation times when the numbers of foci are near the maximum and the residual minimum after repair, respectively. Previous reports from this laboratory comparing sensitivities to the induction of γ-H2AX foci for acute high dose-rate and chronic low dose-rate exposures showed no significant differences for normal ATM +/+ vs. ATM+/− heterozygotes with the acute high dose-rate, but an appreciable difference for the low dose-rate protocol.

Likewise, no differences in sensitivities were resolved in the present study for any of the cell strains using the high dose-rate G_0 protocol.

In contrast, the G_2 assay, which did involve acute high dose-rate irradiation exposures, did reveal a significantly elevated level of γ-H2AX foci on mitotic chromosomes for samples from 7 of 8 parents of RB patients and 5 to 6 from apparently normal individuals following a dose of 0.5 Gy given to late G_2 cells. In this assay, randomly dividing log phase cultures of cells were irradiated, and after 0.5 hours incubation to allow cells in mitosis at the time of irradiation to complete mitosis, Colcemid was added and mitotic cells were harvested for scoring 1 hour later. The spectrum of relative sensitivities for induced foci in this assay is shown in Figure 3. Since earlier studies in this laboratory comparing sensitivities of cells from normal and A-T families had not included this G_2/M assay, only results from the present study were summarized in this figure. It is potentially of interest that cell strains shown as 8447 and 2M in this figure appeared in the sensitive group in this assay but in the resistant (normal) category or on the resistant side of the sensitive category in the G_0 low dose rate assay (Figure 2). Conversely strains shown as 8399 and 15F were more resistant in this G_2/M assay, but were in the sensitive category in the G_0 low dose rate assay. While these observations may tentatively suggest some underlying differences in NHEJ and HDR processes, the very high zero dose background levels, and the significantly over-dispersed distributions of frequencies of cells with various numbers of foci per cell for many of the samples warrant some reservations about such conclusions, at present. These distribution histograms are shown in Figure 4-4.

Another point worth noting regarding the G_2/M assay is that if the number of γ-H2AX foci reflect the number of DNA DSBs present then, all else being equal, cells with twice the DNA content would be expected to have twice the initial number of γ-H2AX foci. The number of induced foci in G_0 RB parent cells after 1 Gy was about 9 so I would expect about 4.5 induced foci for half that dose (0.5 Gy). Doubling this for a G_2 DNA content would return the expectation to 9 foci per cell. In fact, the net number for 0.5 Gy given to G_2 cells was around 25; nearly 3-fold higher that this simple expectation. Since the initial DNA breakage per Mb of DNA is the same for G_1 and G_2 cells (5-8), the observed difference for γ-H2AX foci would suggest a difference in initial chromatin organization, or the additional factor of chromatin condensation between irradiation in G_2 and foci observation in mitosis.

	Cell Strain	Mean Number of γ-H2AX Foci per Cell (±S.E.M.)							
		G0 Irradiation → G0 Foci					G2 Irradiaiton →M Foci		
		G0-phase 0Gy	Low dose rate 10cGy/h 24 hours		Acute High Dose Rate 1Gy		0 Gy G2 + 1 hour M	0.5Gy G2 + 1 hour M	
					+ 1 hour	+ 24 hours			
		Control	Total	Net (Induced)	Total	Total	Control	Total	Net (Induced)
Parents of Retinoblastoma	MF-2M	1.89 (±0.08)	9.68 (±0.18)	7.79 (±0.2)	13.06 (±0.21)	1.99 (±0.08)	9.07 (±0.18)	48.75 (±0.41)	39.68 (±0.48)
	MF-4F	0.62 (±0.05)	7.6 (±0.16)	6.98 (±0.17)	14.95 (±0.23)	1.4 (±0.07)	9.88 (±0.18)	36.95 (±0.36)	27.07 (±0.40)
	MF-6F	2.74 (±0.10)	12.55 (±0.21)	9.82 (±0.36)	18.3 (±0.25)	5.56 (±0.14)	8.93 (±0.18)	41.25 (±0.38)	32.32 (±0.42)
	MF-12M	0.94 (±0.06)	9.11 (±0.18)	8.17 (±0.19)	14.2 (±0.22)	1.64 (±0.08)	10.73 (±0.19)	38.76 (±0.37)	28.03 (±0.41)
	MF-13M	0.81 (±0.05)	10.97 (±0.20)	10.16 (±0.20)	16.31 (±0.24)	1.73 (±0.08)	11.28 (±0.20)	38.36 (±0.36)	27.09 (±0.41)
	MF-15F	1.02 (±0.06)	9.21 (±0.18)	8.2 (±0.19)	15.88 (±0.23)	1.32 (±0.07)	12.16 (±0.21)	32.02 (±0.33)	19.86 (±0.39)
	MF-16M	1.12 (±0.06)	9.42 (±0.18)	8.3 (±0.19)	15.59 (±0.23)	1.46 (±0.07)	7.89 (±0.17)	37.11 (±0.36)	29.22 (±0.39)
	MF-18F	0.81 (±0.05)	9.71 (±0.18)	8.9 (±0.19)	13.82 (±0.22)	1.03 (±0.06)	7.79 (±0.16)	36.87 (±0.36)	29.07 (±0.39)
Apparrently Normal	AG1522	0.84 (±0.05)	4.5 (±0.12)	3.67 (±0.14)	11.38 (±0.20)	1.65 (±0.08)	6.38 (±0.15)	21.98 (±0.28)	15.61 (±0.31)
	GM00038	0.39 (±0.04)	8.28 (±0.17)	7.89 (±0.17)	13.5 (±0.22)	1.28 (±0.07)	4.00 (±0.12)	21.72 (±0.27)	17.72 (±0.30)
	GM00500	0.82 (±0.05)	11.28 (±0.20)	10.46 (±0.20)	15.48 (±0.23)	2.92 (±.010)	6.81 (±0.15)	35.58 (±0.35)	28.77 (±0.38)
	GM00969	1.57 (±0.07)	10.62 (±0.20)	9.05 (±0.21)	17.83 (±0.25)	2.13 (±0.09)	11.88 (±0.20)	40.74 (±0.38)	28.86 (±0.43)
	GM01652	0.14 (±0.02)	4.46 (±0.12)	4.32 (±0.13)	14.28 (±0.22)	0.82 (±0.05)	4.30 (±0.12)	20.68 (±0.27)	16.38 (±0.29)
	GM03440	1.17 (±0.06)	6.27 (±0.15)	5.10 (±0.16)	16.74 (±0.24)	2.42 (±0.09)	6.89 (±0.15)	26.5 (±0.30)	19.61 (±0.34)
	GM04505	0.91 (±0.06)	9.99 (±0.19)	9.07 (±0.19)	19.89 (±0.26)	2.33 (±0.09)	10.74 (±0.19)	41.32 (±0.38)	30.57 (±0.42)
	GM05756	0.39 (±0.04)	4.84 (±0.13)	4.46 (±0.13)	12.71 (±0.21)	1.04 (±0.06)	4.77 (±0.13)	27.45 (±0.31)	22.68 (±0.33)
	GM05757	0.18 (±0.02)	4.87 (±0.13)	4.69 (±0.13)	12.00 (±0.20)	0.51 (±0.04)	3.33 (±0.11)	21.81 (±0.27)	18.48 (±0.29)
	GM08402	1.66 (±0.08)	9.66 (±0.18)	8.00 (±0.20)	13.05 (±0.21)	2.22 (±0.09)	7.07 (±0.16)	34.11 (±0.34)	27.04 (±0.38)
	GM08333	0.82 (±0.05)	5.14 (±0.13)	4.32 (±0.14)	11.62 (±0.20)	1.44 (±0.07)	5.94 (±0.14)	24.82 (±0.29)	18.88 (±0.33)
	GM08399	0.39 (±0.04)	8.50 (±0.17)	8.11 (±0.18)	14.09 (±0.22)	1.27 (±0.07)	9.21 (±0.18)	23.32 (±0.28)	14.12 (±0.34)
	GM08429	0.70 (±0.05)	5.24 (±0.13)	4.54 (±0.14)	11.86 (±0.20)	1.41 (±0.07)	5.63 (±0.14)	31.55 (±0.33)	25.92 (±0.36)
	GM08447	0.72 (±0.05)	6.27 (±0.15)	5.56 (±0.16)	12.78 (±0.21)	1.10 (±0.06)	13.53 (±0.22)	44.70 (±0.39)	31.18 (±0.45)
	RMP-4	0.05 (±0.01)	5.89 (±0.14)	5.84 (±0.14)	12.50 (±0.21)	0.82 (±0.05)	5.06 (±0.13)	27.24 (±0.31)	22.18 (±0.33)

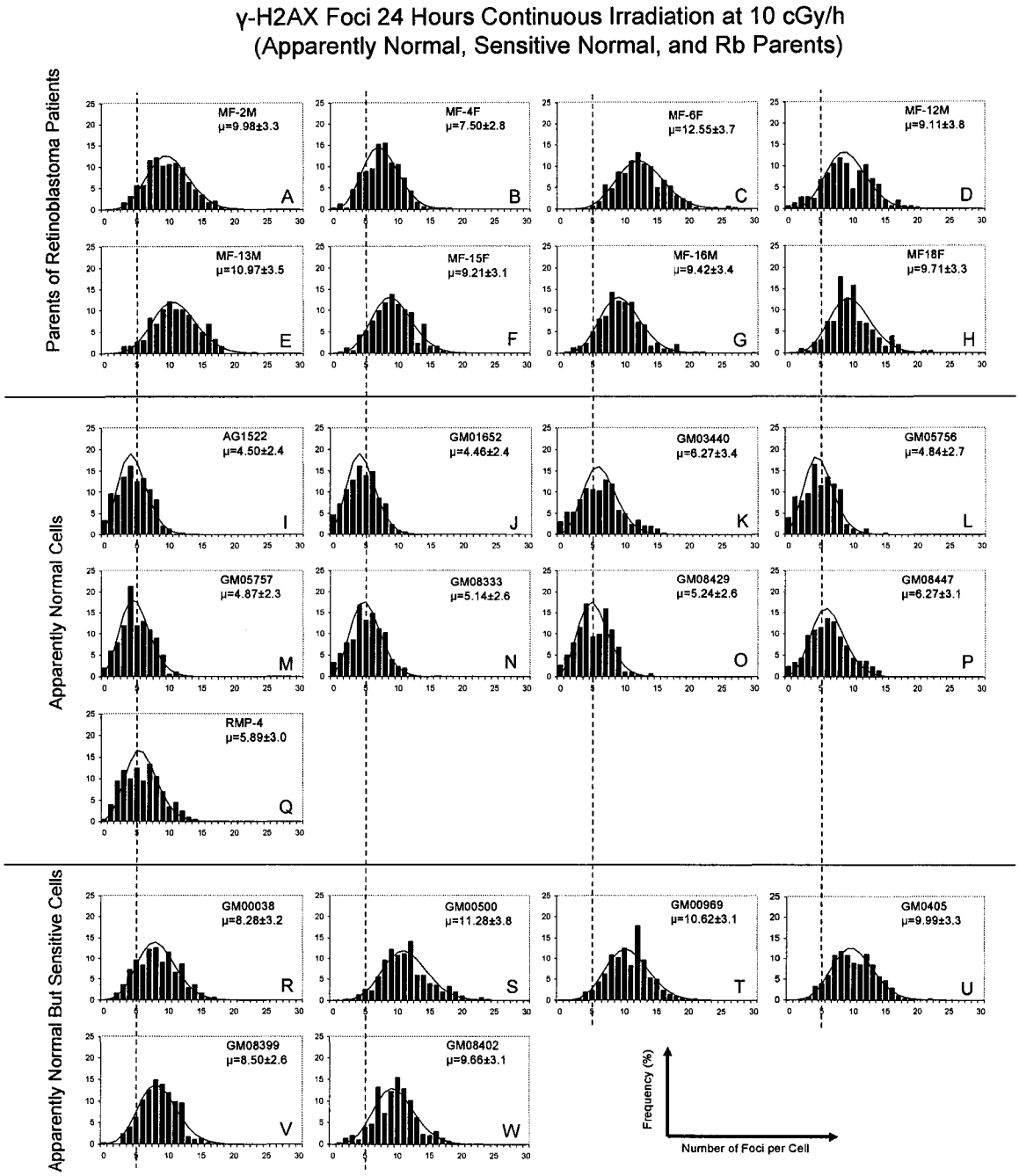

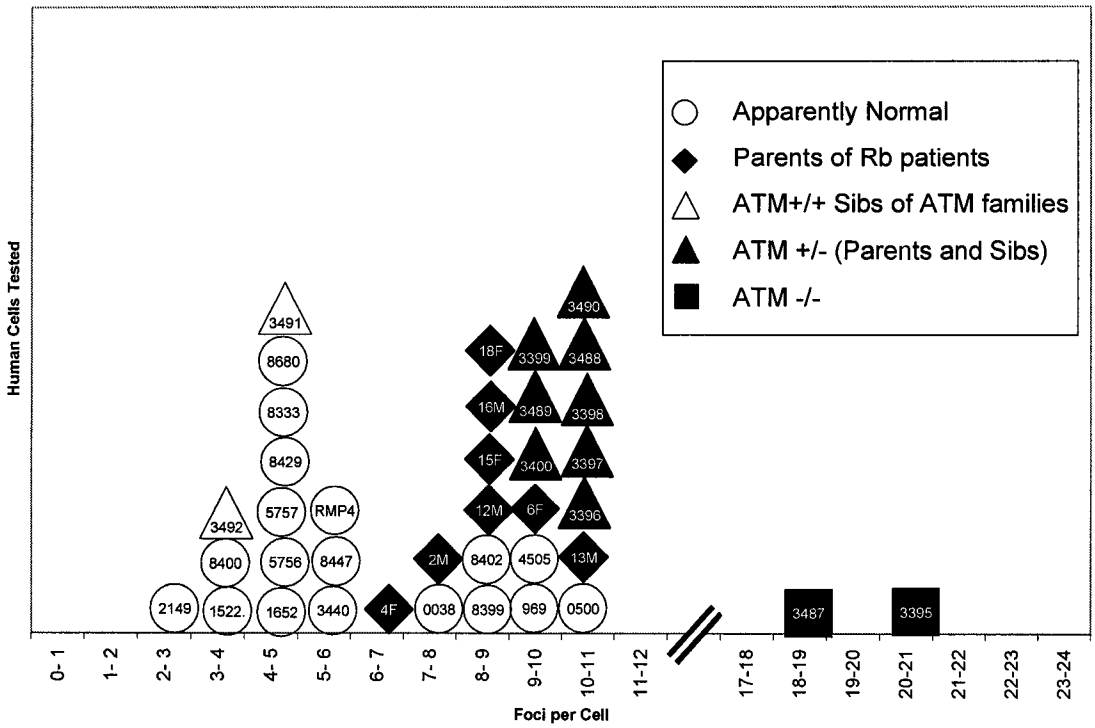

Figure 4-2

From the low dose-rate G_0 assay, the symbols designating each of the cell strains used in this study as well as several from a previous study are plotted at the position on the abscissa corresponding to the mean values for numbers of γ-H2AX foci per cell obtained for that cell strain. The open circles represent samples from apparently normal individuals, with those designated 8680, 8400, and 2149 being from a previous study. The open triangles from another study represent values for siblings with normal *ATM* genotypes from two AT families. The closed triangles were values from *ATM* +/− heterozygotes from the previous study, and the closed diamonds are the values for the RB parents from this study. The closed squares are from *ATM* −/− probands from the previous study. The overall plot represents the spectrum of radiosensitivities for γ-H2AX foci in the low dose-rate assay.

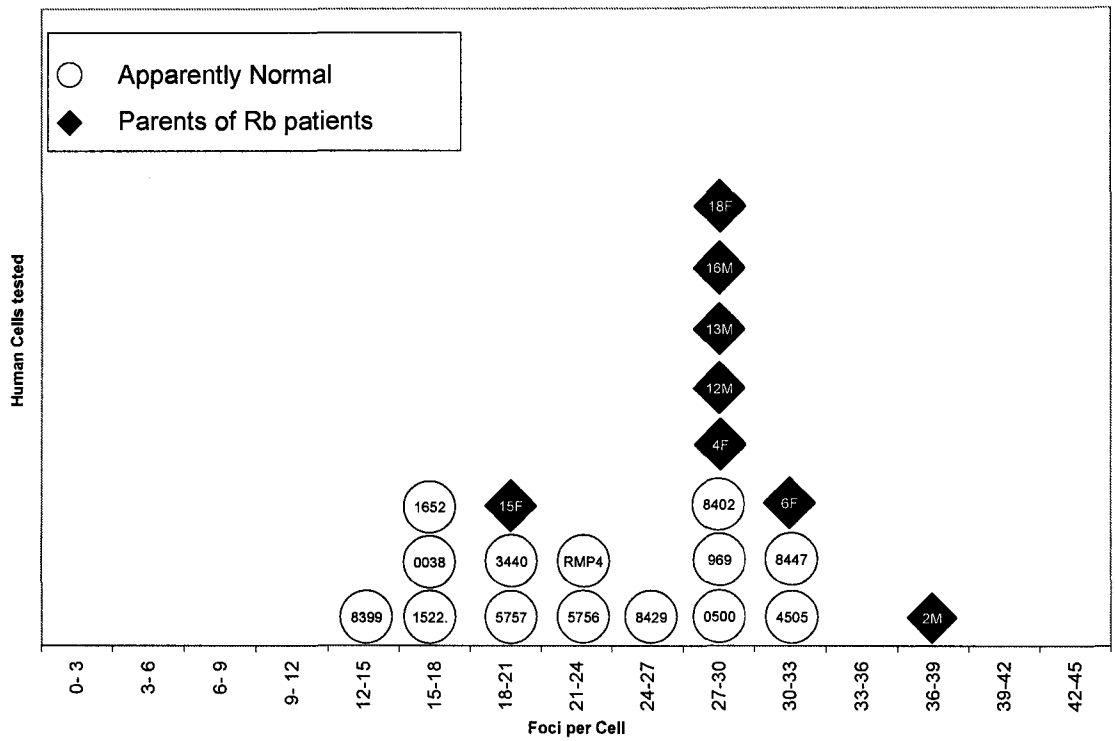

Figure 4-3

From the G_2/M assay, the symbols designating each of the cell strains in this study are plotted at the position on the abscissa corresponding to the mean values for the numbers of γ-H2AX foci per cell obtained for that cell strain. The open symbols represent samples from apparently normal individuals and the closed diamonds were from the RB parents. A similar sensitivity spectrum was observed though there were two or three cases where a strain that was sensitive in this assay was resistant in the low dose rate G_0 assay and *vice versa.*

G2/M γ-H2AX foci Assay for Unirradiated and 0.5Gy Irradiated cells
(Apparently Normal, Sensitive Normal, and Rb Parents/ Categorized from LDR G0 Assay)

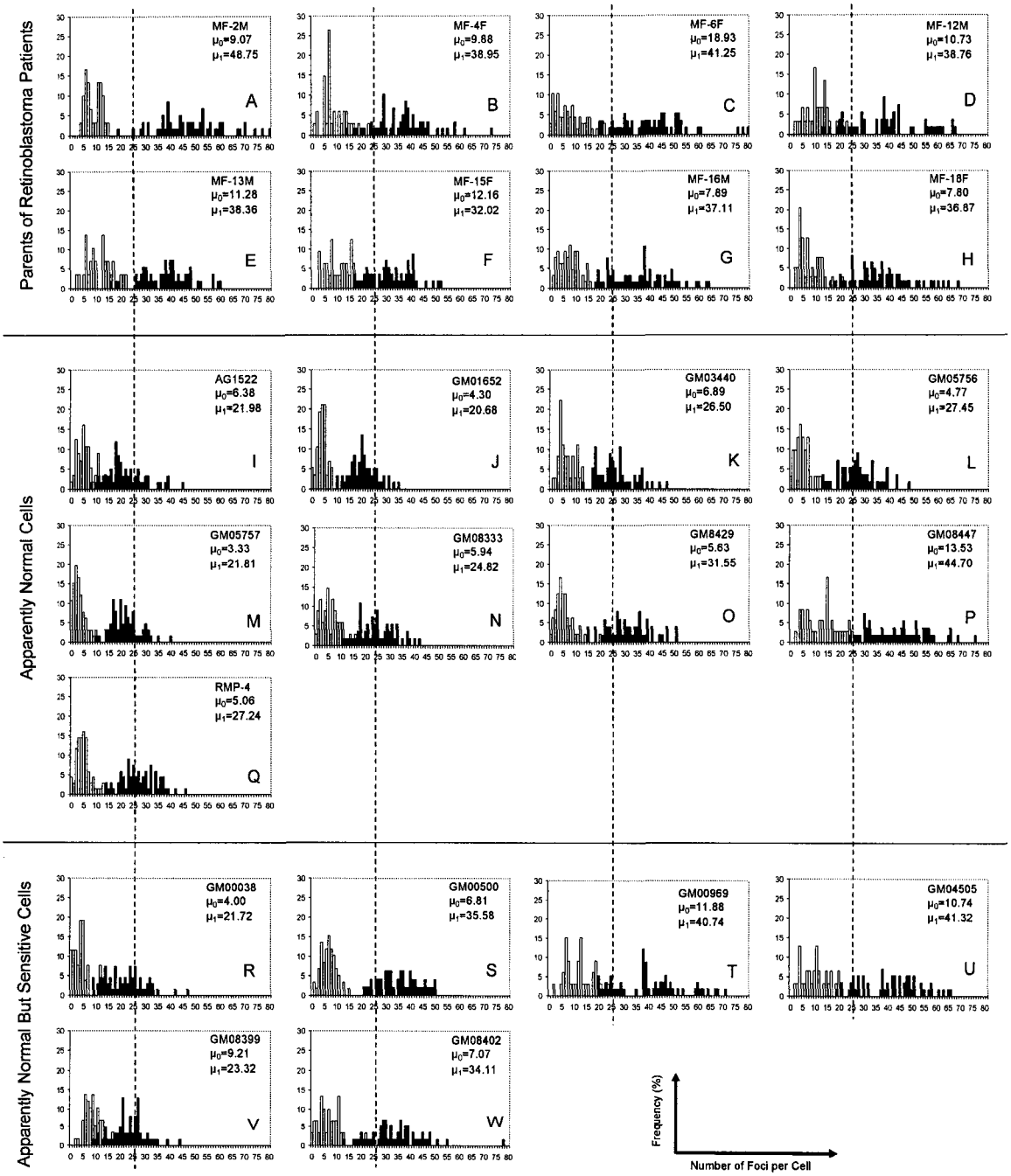

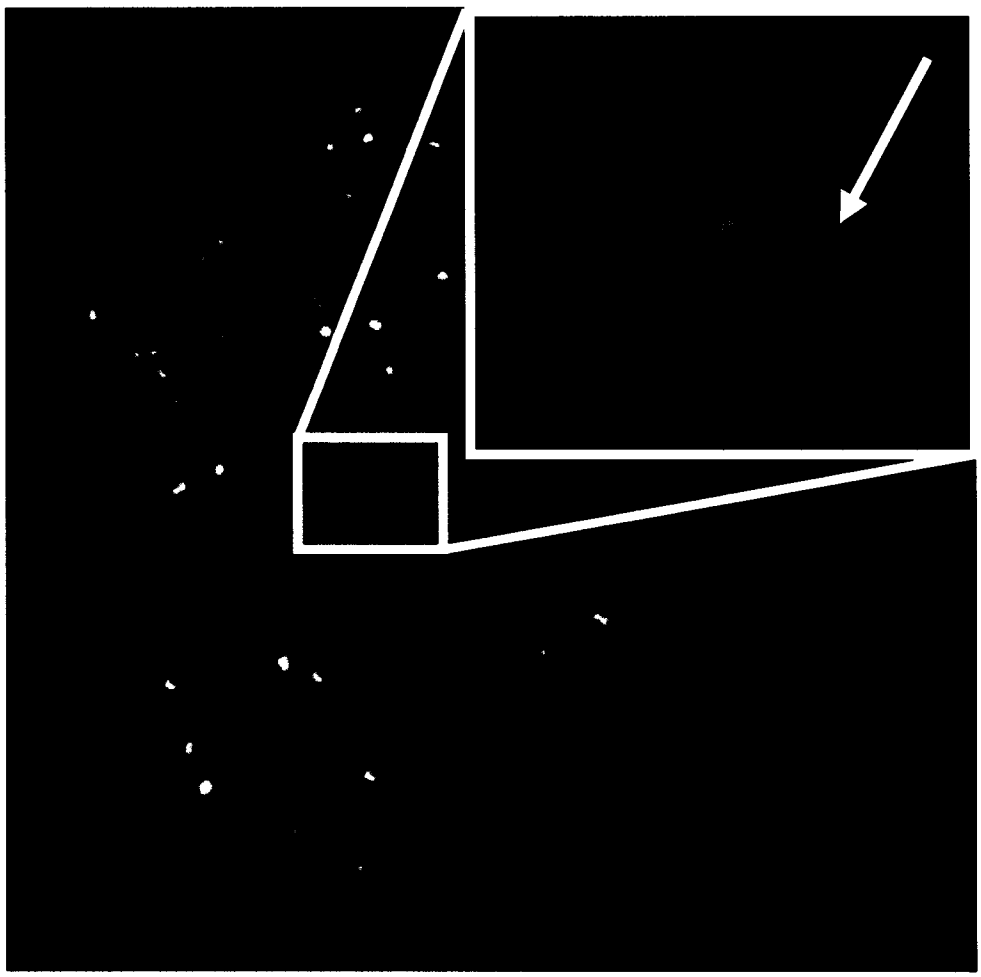

Figure 4-5

γ-H2AX assayed in metaphase after G_2 irradiation. GM8402 were irradiated 0.5Gy. Colmiced was added 0.5 hour after irradiation. Mitotic cells were harvested 1 hour after colcemid treatment.
Green indicates γ-H2AX and red, centromere region stained by CREST serum.
Arrow shows γ-H2AX foci are present on chromatid break.

DISCUSSION

It has been recognized for some time that plateau phase or contact inhibited G_1 or G_0 cultures offer distinct advantages for studying radiation damage repair processes (9-12), and are especially useful where the focus of studies is on the contribution of such repair processes to dose-rate effects (12,13). The fact that there is an appreciable difference in radiosensitivities with respect to cell killing for cells derived from numerous apparently normal individuals has been reported previously (1), and the subject, including radiosensitivities for cells derived from patients with a range of genetic disorders has been reviewed by others (eg, (14)). The present study has focused on cells from parents of patients with the hereditary form of retinoblastoma which we have used for other studies (2,3,15). The fact that cells from the parents are hypersensitive to radiation is of particular interest because clinically, they, too, are apparently normal. This has led to the suggestion that perhaps these parents harbor some genetic abnormality related to maintenance of genome stability, and one possibility is that some DNA repair function may be involved. The present study utilized a marker that reflects as closely as possible the levels of DNA DSBs in cells at levels pertinent to biological radiation responses of interest (γ-H2AX foci), and by using the low dose-rate G_0 assay to amplify differences among cells in their capacity to rejoin DNA DSBs, I was able to reveal elevated levels in cells from RB parents. The elevated sensitivity for this molecular damage end point was comparable to the level seen previously for cells from individuals heterozygous for the *ATM* gene. For the G_2/M assay, the cells from 7 of 8 RB parents were also hypersensitive for levels of γ-H2AX, indicating some defect in processing DNA DSBs,

although the statistical uncertainties in this assay. The G_2/M γ-H2AX focus assay is reminiscent of the G_2 chromosomal radiosensitivity assay studied by numerous investigators (16-19) and which has been suggested to reflect differences in DNA repair among individuals with increased cancer risk (16). Certainly, *ATM* heterozygotes and individuals in breast cancer families show elevated sensitivities in the G_2 chromosomal radiosensitivity assay, although, as suggested in the current study, these other reports indicate that the frequency of individuals whose cells show with elevated sensitivities in that assay are far greater that can be attributed to the expected frequencies of individuals who might be heterozygous even for any of a number of known genes that could affect radiosensitivity, such as *ATM, BRCA1, BRCA2 and TP53* (19).

It is interesting to note that a predisposition to the development of second cancers is also characteristic of RB patients, and second cancers often occur in the field treated by radiation (20). If the elevated sensitivities I have observed with respect to cell killing and DNA DSB processing reflected by the γ-H2AX focus assay for cells from RB parents and for cells from nearly one-third of other apparently normal individuals is indicative of some as yet unknown defect in genome maintenance that resulted in increased germ line mutation rates, this could lead to increased frequencies of heterozygosity in the offspring for any of a number of genes that could predispose an individual to cancer. Identification of such genes could provide new insights into mechanisms leading to retinoblastoma as well as cancer predisposition in general.

REFERENCES

1. H. Nagasawa and J. B. Little, Radiosensitivities of ten apparently normal human diploid fibroblast strains to cell killing, G2-phase chromosomal aberrations, and cell cycle delay, *Cancer Res.* **48**, 4535-4538 (1988).

2. M. M. Fitzek, W. K. Dahlberg, H. Nagasawa, S. Mukai, J. E. Munzenrider and J. B. Little, Unexpected sensitivity to radiation of fibroblasts from unaffected parents of children with hereditary retinoblastoma, *Int.J.Cancer* **99**, 764-768 (2002).

3. E. Y. Chuang, X. Chen, M.-H. Tsai, H. yan, C.-Y. Li, J. B. Mitchell, H. Nagasawa, P. F. Wilson, Y. Peng, M. M. Fitzek, J. S. Bedford and J. B. Little, Abnormal gene expression profiles in unaffected parents of patients with hereditary type retinoblastoma., *Cancer Reasearch* **66**, 1-7 (2006).

4. M. A. Stackhouse and J. S. Bedford, An ionizing radition-sensitive mutant of CHO cells: irs-20 Isolation and initial characterization, *Radiat.Res.* **136**, 241-249 (1993).

5. D. Blocher and W. Pohlit, DNA double strand breaks in Ehrlich ascites tumour cells at low doses of x-rays. II. Can cell death be attributed to double strand breaks?, *Int.J.Radiat.Biol.* **42**, 329-338 (1982).

6. D. Blocher, M. Einspenner and J. Zajaclowski, CHEF electrophoresis, a sensitive technique for the determination of DNA double-strand breaks, *Int.J.Radiat.Biol.* **56**, 437-448 (1989).

7. G. E. Iliakis and R. Okayasu, Radiosensitivity Throughout the Cell-Cycle and Repair of Potentially Lethal Damage and Dna Double-Strand Breaks in An X-Ray-Sensitive Cho Mutant, *Int.J.Radiat.Biol.* **57**, 1195-1211 (1990).

8. L. Metzger and G. Iliakis, Kinetics of DNA double-strand break repair throughout the cell cycle as assayed by pulsed field gel electrophoresis in CHO cells, *Int.J.Radiat.Biol.* **59**, 1325-1339 (1991).

9. J. B. Little, Repair of sub-lethal and potentially lethal radiation damage in plateau phase cultures of human cells, *Nature* **224**, 804-806 (1969).

10. J. B. Little and H. Nagasawa, Effect of confluent holding on potentially lethal damage repair, cell cycle progression, and chromosomal aberrations in human normal and ataxia-telangiectasia fibroblasts, *Radiat.Res.* **101**, 81-93 (1985).

11. B. Fertil, I. Reydellet and P. J. Deschavanne, A benchmark of cell survival models using survival curves for human cells after completion of repair of potentially lethal damage, *Radiat.Res.* **138**, 61-69 (1994).

12. R. L. Wells and J. S. Bedford, Dose-rate effects in mammalian cells. IV. Repairable and nonrepairable damage in noncycling C3H 10T 1/2 cells, *Radiat.Res.* **94**, 105-134 (1983).

13. Cox, R. A cellular description of the repair defect in ataxia-telangiectasia. Bridges, B. A. and Harnden, D. G. 141-153. 1982. Chichester, New York, Brisbane, Toronto, Singapore, John Wiley & Sons. Ataxia-Telangiectasia: A Cellular and Molecular Link Between Cancer, Neuropathology, and Immune Defeciency.

14. P. J. Deschavanne and B. Fertil, A review of human cell radiosensitivity in vitro, *Int.J Radiat.Oncol.Biol.Phys.* **34**, 251-266 (1996).

15. Kato, T. A. The use of a Gamma-H2AX foci assay for measurement of radiosensitivity phenotypes and DNA DSB induction and processing. 2006. Colorado State University.

16. R. Parshad, K. K. Sanford and G. M. Jones, Chromatid damage after G2 phase x-irradiation of cells from cancer-prone individuals implicates deficiency in DNA repair, *Proc.Natl.Acad.Sci.USA* **80**, 5612-5616 (1983).

17. R. Parshad, K. K. Sanford and G. M. Jones, Chromosmal radiosensitivity during the G2 cell-cycle period of skin fibroblasts from individuals with familal cancer, *Proc.Natl.Acad.Sci.USA* **82**, 5400-5403 (1983).

18. D. Scott, L. A. Jones, S. A. G. Elyan, A. Spreadborough, R. Cowan and G. Ribiero, Identification of A-T heterozygotes, *in* "Atataxia-telangiectasia" (R. A. Gatti and R. B. Painter, Eds.), Springer-Verlag, Berlin (1992).

19. S. A. Roberts, A. R. Spreadborough, B. Bulman, J. B. Barber, D. G. R. Evans and D. Scott, Heritability of cellular radiosensitivity: a marker of low-penetrance predisposition genes in breast cancer?, *American Journal of Human Genetics* **65**, 784-794 (1999).

20. F. L. Wong, J. D. Boice, Jr., D. H. Abramson, R. E. Tarone, R. A. Kleinerman, M. Stovall, M. B. Goldman, J. M. Seddon, N. Tarbell, J. F. Fraumeni, Jr. and F. P. Li, Cancer incidence after retinoblastoma. Radiation dose and sarcoma risk, *JAMA* **278**, 1262-1267 (1997).

Chapter 5

Comparison of the Induction and Disappearance of DNA Double Strand Breaks and γ-H2AX Foci After Irradiation of Chromosomes in G_1-phase or in Condensed Metaphase Chromosome.

ABSTRACT

The induction and disappearance of DNA double strand breaks after irradiation of G_1 and mitotic cells was compared with the γ-H2AX foci assay and a gel electrophoresis assay to determine whether cell cycle related changes in chromatin structure might influence the γ-H2AX assay which depends on extensive phosphorylation and dephosphorylation of the H2AX histone variant surrounding DSBs. The appearance and disappearance of γ-H2AX foci after irradiation were much slower for mitotic than for G_1 cells. No differences were seen for the gel electrophoresis assay.

INTRODUCTION

DNA Double Strand Breaks (DSBs) produced by ionizing radiation are believed to be the most important molecular lesion respectable for induction of cell killing, mutation and chromosome aberrations for the cells. A relationship between the rate of DNA DSB rejoining and radiosensitivity was reported in various DNA DSB repair deficient cells (1-3). A slower rate of rejoining has been linked to a higher rate of chromosome damage and radiosensitivity in cell death (4). It is also known that the sensitivities of mammalian cells to radiation vary throughout the cell cycle. Cells are typically radiation-resistant in the late S-phase. The most sensitive cells are those in M- and G_2-phase. Cells in the G_1- and early S-phase are intermediate in sensitivity (5,6).

Establishing a connection between DNA DSB rejoining efficiencies and cellular radiosensitivity depends largely on the ability to assay for the presence of DNA DSBs immediately and at various times after irradiation in a dose range that is relevant to the cellular damage endpoint of concern. While it is certainly possible to measure the initial induction of DNA DSBs by radiation after doses of a few Gy by gel electrophoresis methods, the measurement becomes very difficult after 90 to 99% of breaks have been rejoined (7,8).

Recently there has been an increased use of the very sensitive γ-H2AX focus assay as a means for measuring of the induction and rejoining of DNA DSBs (9,10). While there is considerable evidence to support the connection between DNA DSBs and γ-H2AX foci, the appearance of these foci requires the phosphorylation of thousands of H2AX molecules and their disappearance requires a corresponding dephosphorylation.

Since the condensation status of chromatin changes dramatically during cell cycle (11), it seems possible that it might also alter the rates of phosphorylation and dephosphorylation. As a test of this possibility I compared the appearance and disappearance of γ-H2AX foci in mitotic and G_1 cells after irradiation with the induction and disappearance of DNA DSBs measured by gel electrophoresis. No differences were seen for mitotic vs. G_1 cells for the gel electrophoresis assay of DNA DSBs, but the appearance and disappearance of γ-H2AX foci were much slower in mitotic than in G_1 cells

MATERIALS AND METHODS

Cell culture

CHO (CHO10B2) cells were grown in Eagle's minimal essential medium (MEM) supplemented with 10 % heat-inactivated (56°C for 30 min) fetal bovine serum, penicillin (100 units/ml), and streptomycin (100 μg/ml) in a humidified 5 % CO_2 atmosphere at 37°C.

Cell synchronization and γ -irradiation

Synchronization of cell populations in the G_1 phase of the cell cycle was accomplished by the isoleucine depletion method by Tobey and Ley (12). Synchronization of cell population in metaphase was obtained by treatment with Colcemid (0.1μg/ml) for 2 hours in 37°C incubator, and then harvesting the loosely attached mitotic cells by mechanical shaking. Synchronized cell populations were irradiated using a J.L. Shepherd Model Mark I-68 6000 Ci ^{137}Cs irradiator. The dose-rate was 2.5Gy per minute.

Gel Electrophoresis DNA DSB Assay.

DNA DSBs were measured by constant field gel electrophoresis (13). Cells were incubated with 0.01 μCi/ml [^{14}C] thymidine and 5 μM cold thymidine for at least 2 days before each experiment. Then, cells were synchronized in the G_1 phase of the cell cycle by the isoleucine depletion method. Cells were embedded in 0.5% agarose (Insert agarose (FMC)) and irradiated in ice-cold medium. This was followed by an immediate

lysis by lysis solution containing 0.5 M EDTA, 0.01 M Tris, 2% Sarcosyl, and 0.2 mg/ml proteinase K (pH 8.0) at 0°C for 1 hour and 50°C overnight. After the overnight lysis, samples were washed for 1 hour in 0.1 M EDTA, 0.01 M Tris at pH 8.0 and treated with 0.1 mg/ml RNase A for 1 hour at 37°C. Electrophoresis was carried out in 0.5×TBE buffer (45 mM Tris, 45 mM boric acid, and 1.5 mM EDTA, pH 8.2) in a normal gel box (Bio-Rad) in 0.6% agarose gel (Bio-Rad) at 14°C. The applied voltage was 0.6 V/cm for 40 hours. After electrophoresis, gels were stained and cut to separate the plug from the lane for each sample. The ^{14}C activity of each piece was measured in a scintillation counter, and the FAR (Fraction Activity Released) was calculated as the dpm of a lane divided by the total dpm (lane + plug) per sample.

γ-H2AX foci formation

The fixation procedure prior scoring γ-H2AX was based on the method described by Rothkamm and Lobrich (14) with slight modifications. For G_1-phase, cells were grown, synchronized, and irradiated on a chamberslide. At various times after irradiation, cells were fixed in 4 % paraformaldehyde for 15 minutes, washed three times in PBS for 10 minutes each, permeabilized for 5 minutes on ice in 0.2 % Triton X-100, and blocked in PBS with 10 % Goat serum for 60 minutes at room temperature. For preparation of metaphase sample, cells were swelled by treated with a hypotonic swelling buffer (50mM KCl, 50mM $MgSO_4$ 5mM HEPES) for 20 minutes and centrifuged onto slides using a cytocentrifuge (Cytospin, Shandon). Cells were then fixed on the slides by paraformaldehyde, washed with PBS, and permeabilized for 5 minutes in KCM solution (120mM KCl, 20mM NaCl, Tris-HCl 10mM, EDTA 0.5mM, Triton X-100 0.1%, pH 7.5).

Immunocytochemistory

The slides were incubated with anti-γ-H2AX antibody (Upstate) for 1 hour, washed three times in PBS for 10 minutes each, and incubated with Alexa fluor-conjugated goat anti-rabbit secondary antibody (Molecular Probe) for 1 hour at room temperature. Cells were washed four times in PBS for 10 minutes each and mounted by using Slow Fade (Molecular Probes). Fluorescence images of cells were obtained using an Olympus AX-70 fluorescence microscope equipped with a PSI image analysis system utilizing the MAC-Probe package. Foci were then scored by recalling these images.

RESULTS

Figure 5-1 summarizes results for the measurement by gel electrophoresis of DNA DSBs initially produced in the G_1-phase and metaphase cells showed no difference in the increased fraction of activity released with increased dose. These results suggested no difference in the production of DSB per Gy per Dalton of DNA. The initial induction of DSB per DNA for both G_1-phase and metaphase was the same. It is worth to note FAR (Fraction Activity Released) measures relative amount of DNA DSBs compared to total DNA. It means that metaphase cells have twice more DNA than G_1 phase cells because the metaphase cells have 4n DNA; G_1-phase cells, 2n.

Results on the rejoining of DSB in G_1-phase and metaphase CHO cells are summarized in Figure 5-2. Plotted in the figure is the fraction of activity released as a function of the post-irradiation incubation time at 37°C after exposure to 40 Gy γ-rays. It is evident that there was no difference in repair kinetics between G_1-phase and metaphase CHO cells with this assay. In both the G_1-phase and metaphase cells, 50% DNA DSBs were rejoined within about less than 25 minutes. Most of the repair was completed within two to three hours after irradiation although the sensitivity of the assay to detect differences in the FAR is very low.

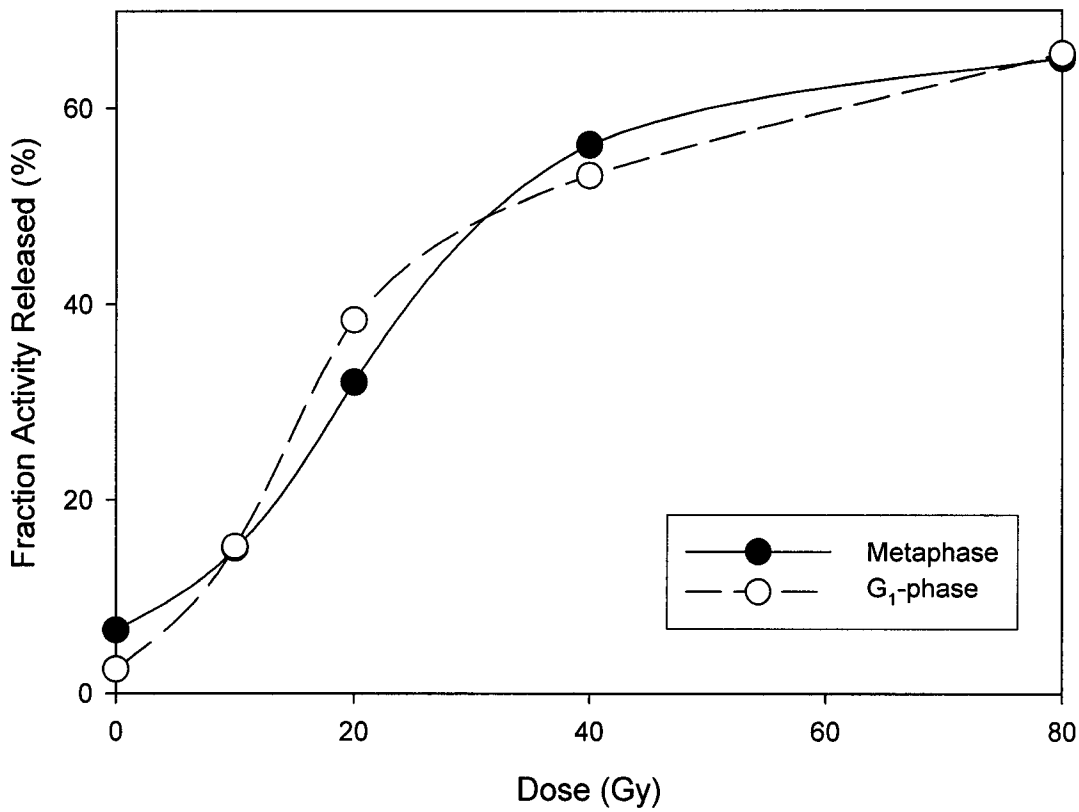

Figure 5-1.

A measurement of DNA DSBs in synchronized CHO cells exposed to high doses of γ-rays, as measured by Constant field gel electrophoresis. The results were obtained from three independent experiments. Filled circle presents metaphase CHO cells and open circle presents G_1-phase CHO cells.

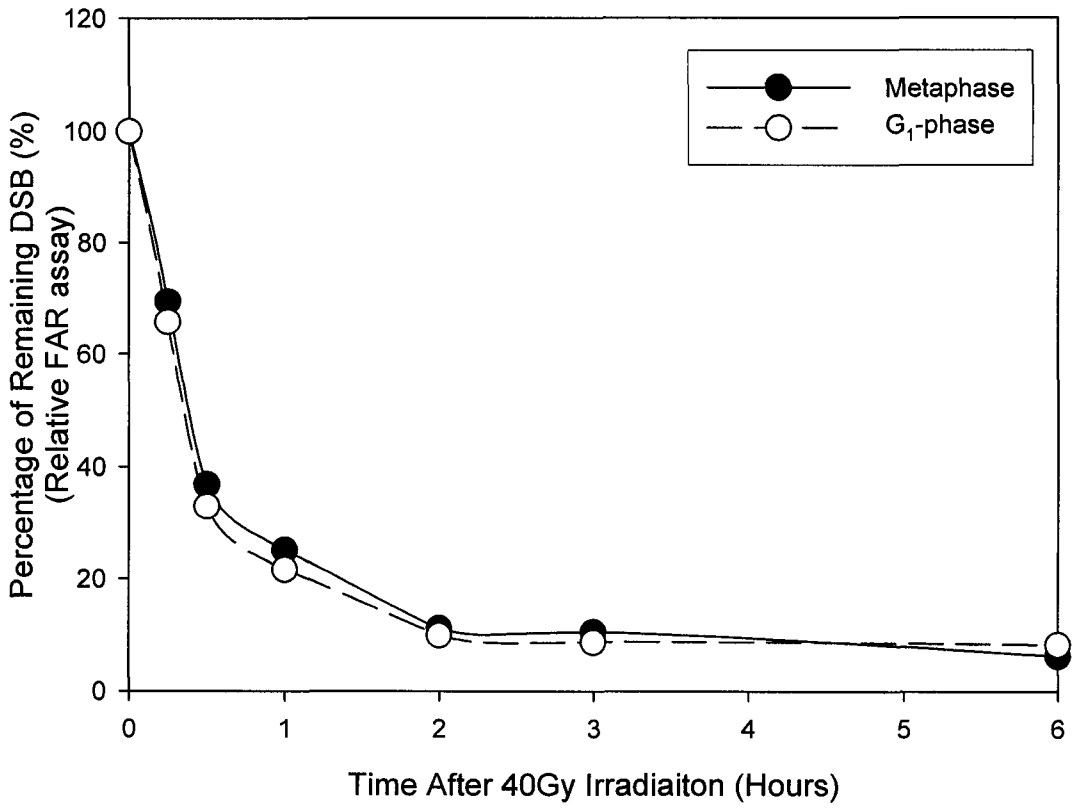

Figure 5-2

Kinetics of DSB repair in synchronized CHO cells measured with a FAR assay using constant field gel electrophoresis. Cells were irradiated with 40 Gy on ice followed by incubation at 37°C. Filled circles present results obtained with metaphase CHO cells and open circles for G_1-phase CHO cells.

Using the more sensitive γ-H2AX focus assay, dose response curves for the induction of foci were obtained for G_1-phase and metaphase CHO cells, and the results are summarized in Figure 5-3. The foci numbers presented were the maximum seen in experiments measuring their change with and after irradiation. Twice as many γ-H2AX foci were observed in metaphase cells for a given dose relative to G_1 cells. This observation might be expected based on the two fold increase in DNA content for mitotic vs. G_1 cells. The increase for the metaphase cells showed a linear dose response up to 100cGy.

Summarized in Figure 5-4 are results in which the increase and disappearance of γ-H2AX foci were measured in G_1-phase and metaphase CHO cells after a 1Gy dose of γ-rays. There were obvious differences in kinetics of foci disappearance for G_1-phase vs. metaphase CHO cells. As expected from the difference in DNA content, the maximum number of foci after irradiation in metaphase cells was almost twice the amount in G_1-phase cells. However, the disappearance of foci in metaphase cells is much slower. Figure 5-5A-C show the examples of mitotic irradiated chromosomes with γ-H2AX foci.

For the purpose of comparison the percentages of the remaining DNA DSBs and γ-H2AX foci for the G_1 and mitotic cells were plotted on the same graph (Figure 5-6). The fast component of DNA DSB rejoining kinetics and γ-H2AX foci disappearance kinetics was very similar in G_1 cells, but clearly only γ-H2AX foci disappearance was much slower for mitotic cells.

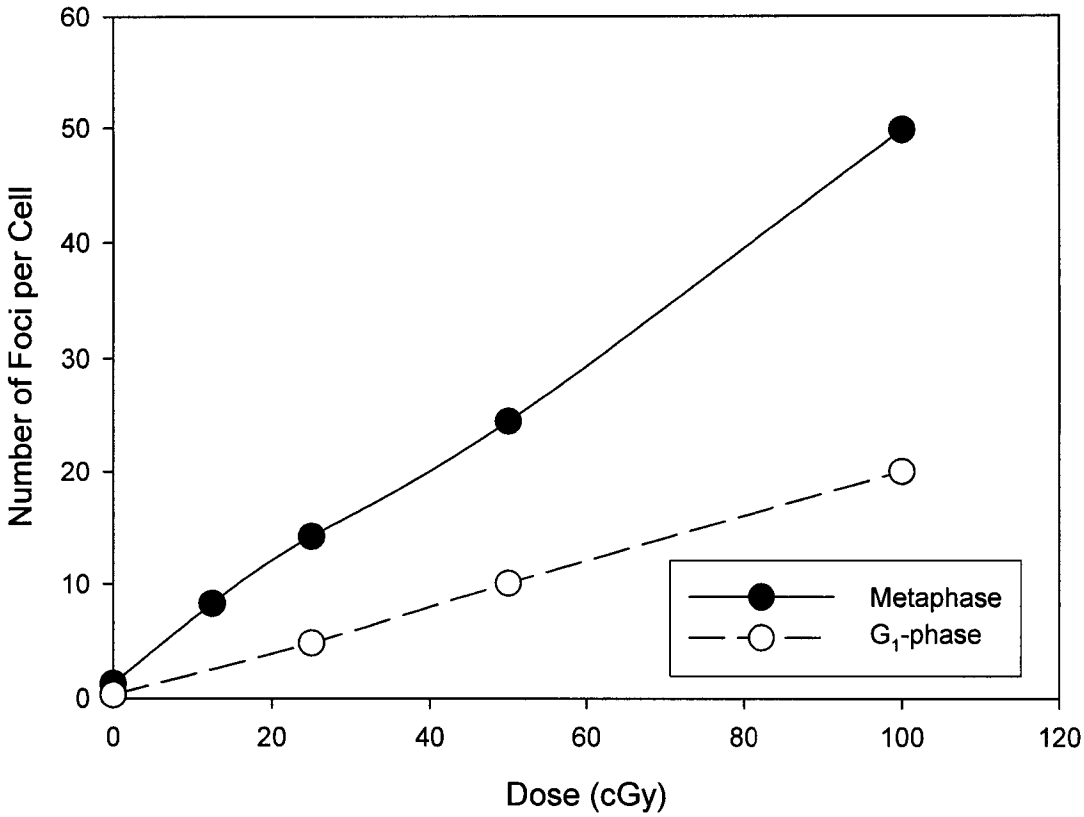

Figure 5-3

The maximum number of γ-H2AX foci in G_1-phase and metaphase CHO cells measured by immunocytochemistry. Cells were irradiated at room temperature followed by incubation at 37°C for 20 minutes. Filled circles trace the results found using metaphase CHO cells and open circles; G_1-phase CHO cells.

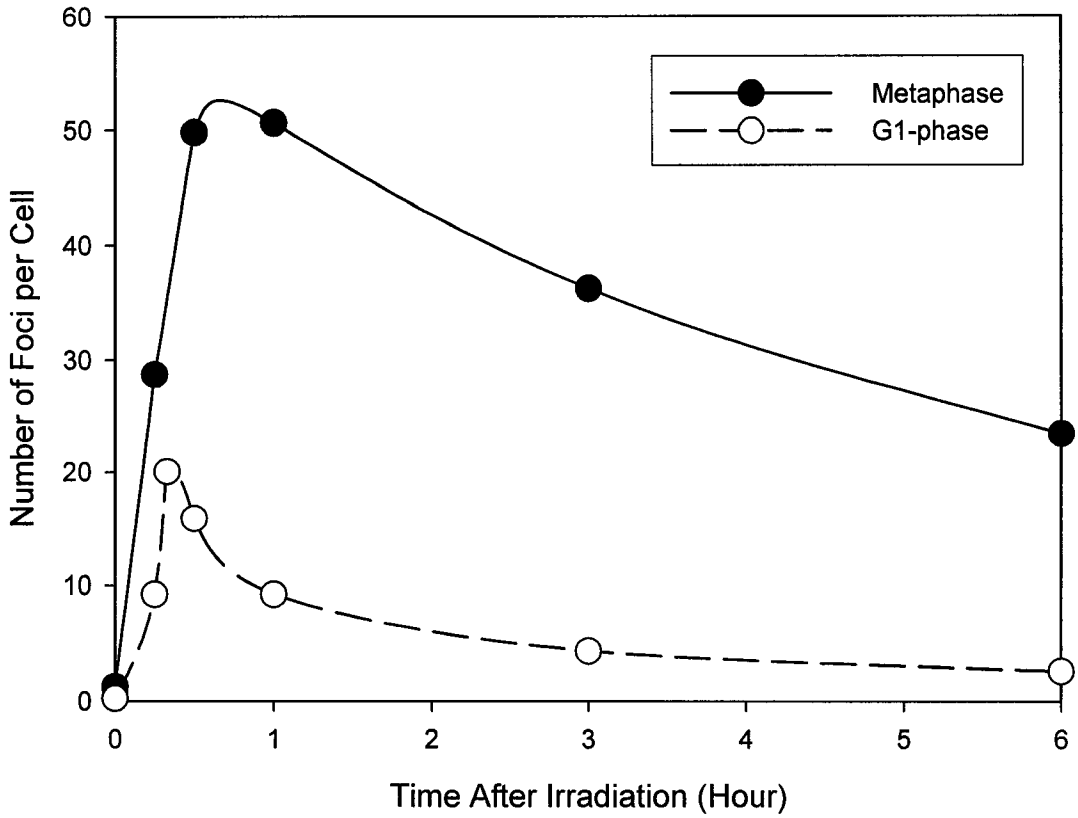

Figure 5-4

The γ-H2AX analysis after 1 Gy γ-irradiation in G_1-phase and Metaphase CHO cells was measured by immunocytochemistry. Cells were irradiated at room temperature followed by incubation at 37°C for the various times shown. Filled circles trace the results seen for metaphase CHO cells and open circles for G_1-phase CHO cells.

Figure 5-5

γ-H2AX foci with metaphase chromosomes. Green represents γ-H2AX foci. Chromosomes were counterstained by DAPI (blue). Cells were irradiated in metaphase, and then assayed in metaphase after 30 minutes.

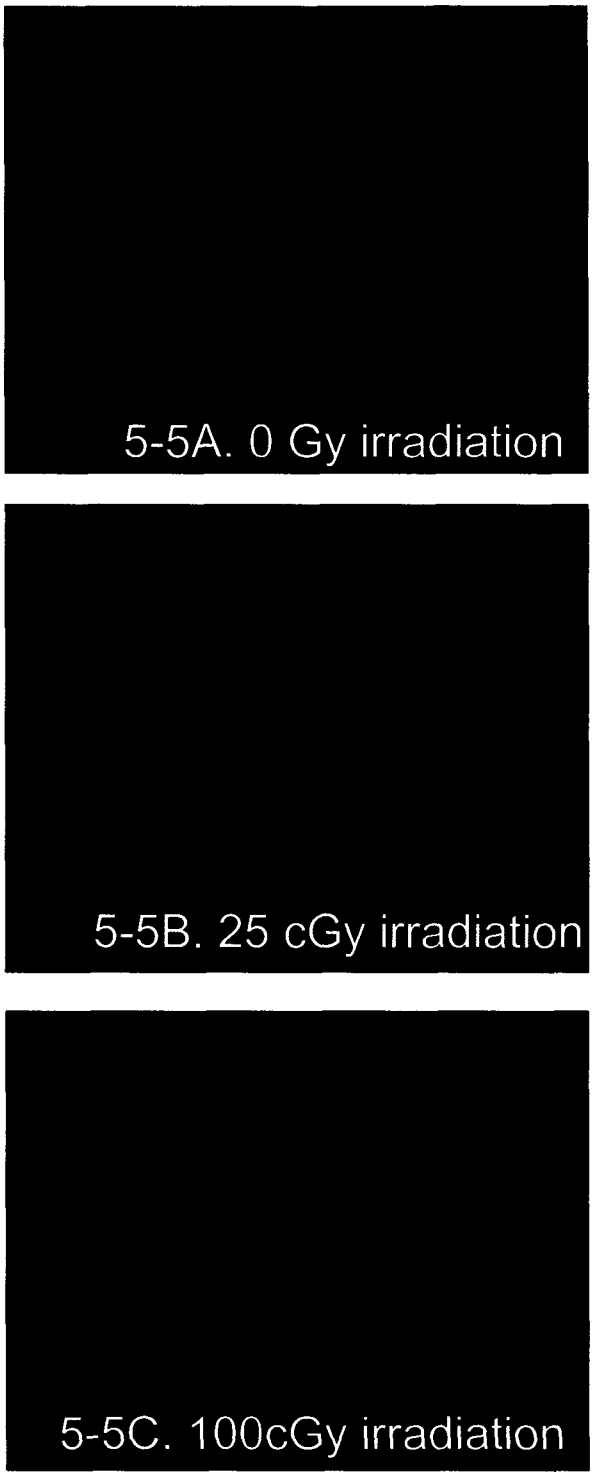

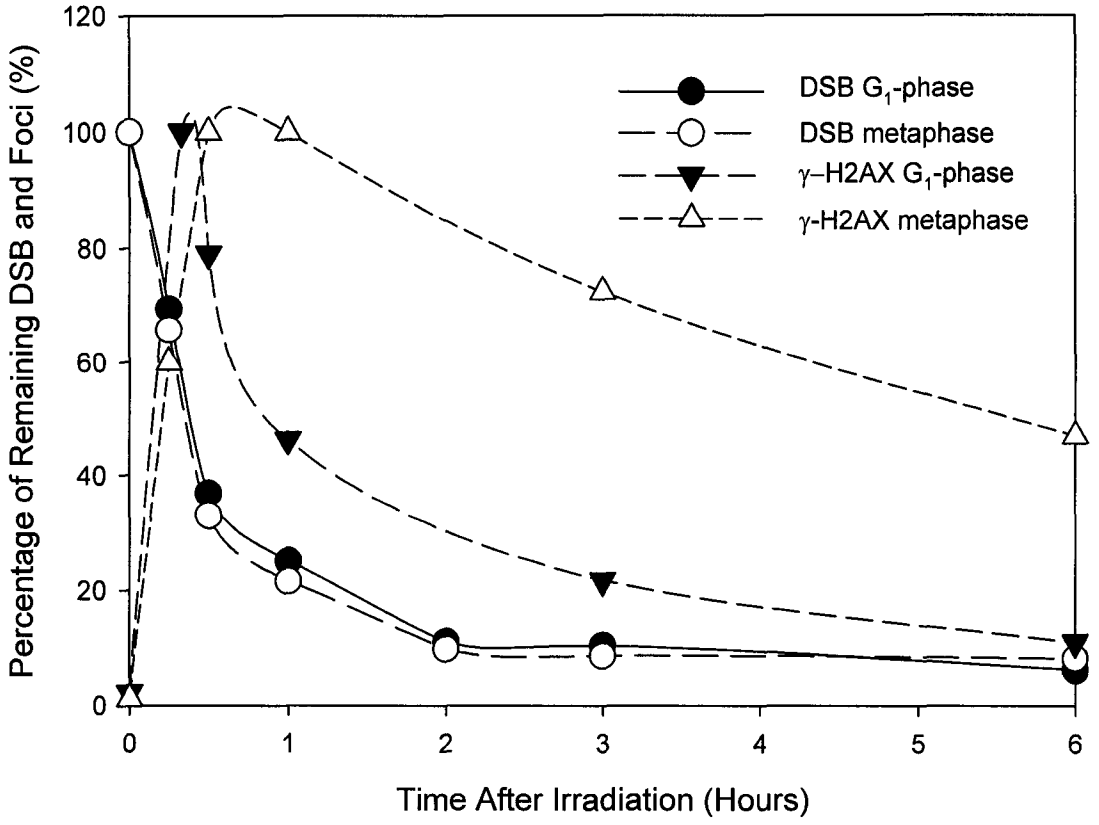

Figure 5-6

The percentage of DNA DSBs and γ-H2AX foci for the G_1 and mitotic cells is plotted on the same graph.

DISCUSSION

It is known that DNA is highly organized and packed in metaphase chromosomes. Each DNA molecule has been packaged into a mitotic chromosome that is 10,000-times shorter than its extended length. For G_1 cells the packing ratio is approximately 1:200-1000 (11). This may suggest that because the histone proteins are so tightly packed around the site of DNA DSBs, the accessibility of enzymes involved in dephosphorylating γ-H2AX molecules may be more limited in metaphase chromosomes than G_1 chromosomes even after DNA DSBs were rejoined.

It may be pertinent that Calyculin A, an inhibitor of protein phosphatase 1, enhanced cell killing from ionizing radiation (15) and inhibits the dephosphorylation of γ-H2AX in interphase cells (16). Nazarov suggested there is a relationship between protein phosphatase1 and elimination of γ-H2AX. But Calyculin A is also known as an inducer of PCC (premature chromosome condensation) (17). This may also suggest that slow γ-H2AX dephosphorylation may be correlated with not only phosphatase inhibition but also condensed chromatin structure.

Another possibility is a balance between kinase and phosphorylase in mitotic cells. There are plenty amount of MPF (Maturation Promoting Factor, Mitosis Promoting Factor) in mitotic cells. Active form of MPF is strong kinase and it may not allow unknown phosphatase to dephosphorylate γ-H2AX. Again, calyculin A, phosphatase inhibitor, inhibits the dephosphorylation of γ-H2AX. This may be another evidence to show kinase-phosphatase unbalance is important to dephosphorylation of γ-H2AX.

REFERENCES

1. R. Okayasu, K. Suetomi, Y. Yu, A. Silver, J. S. Bedford, R. Cox and R. L. Ullrich, A deficiency in DNA repair and DNA-PKcs expression in the radiosensitive BALB/c mouse, *Cancer Res.* **60**, 4342-4345 (2000).

2. B. Nevaldine, J. A. Longo and P. J. Hahn, The scid defect result in much slower repair of DNA double- strand breaks but not high levels of residual breaks, *Radiat.Res.* **147**, 535-540 (1997).

3. E. Marangoni, N. Foray, M. O'Driscoll, S. Douc-Rasy, J. Bernier, J. Bourhis and P. Jeggo, A Ku80 fragment with dominant negative activity imparts a radiosensitive phenotype to CHO-K1 cells, *Nucleic Acids Res.* **28**, 4778-4782 (2000).

4. J. L. Schwartz and A. T. Vaughan, Association among DNA/chromosome break rejoining rates, chromatin structure alterations, and radiation sensitivity in human tumor cell lines, *Cancer Res.* **49**, 5054-5057 (1989).

5. W. K. Sinclair and R. A. Morton, X-ray sensitivity during the cell generation cycle of cultured Chinese hamster cells, *Radiat.Res.* **29**, 450-474 (1966).

6. T. Terasima and L. J. Tolmach, Variations in several responses of HeLa cells to X-irradiation during the division cycle, *Biophysical Journal* **3**, 11-33 (1963).

7. D. Blocher, M. Einspenner and J. Zajaclowski, CHEF electrophoresis, a sensitive technique for the determination of DNA double-strand breaks, *Int.J.Radiat.Biol.* **56**, 437-448 (1989).

8. Waldren, C., Leser, S., Gardiner, K., Harvey, W., and Johnson, R. T. Measurement by pulsed field gel electrophoresis (PFGE) of DNA damage from low doses of ionizing radiation. Radiation Research 37th Annual Meeting, 88. 1989.

9. E. P. Rogakou, D. R. Pilch, A. H. Orr, V. S. Ivanova and W. M. Bonner, DNA double-stranded breaks induce histone H2AX phosphorylation on serine 139, *J Biol.Chem.* **273**, 5858-5868 (1998).

10. O. A. Sedelnikova, E. P. Rogakou, I. G. Panyutin and W. M. Bonner, Quantitative detection of (125) IdU-induced DNA double-strand breaks with gamma-H2AX antibody, *Radiat.Res.* **158**, 486-492 (2002).

11. J. B. Lawrence, R. H. Singer and J. A. McNeil, Interphase and metaphase resolution of different distances within the human dystrophin gene, *Science* **249**, 928-932 (1990).

12. R. A. Tobey and K. D. Ley, Regulation of initiation of DNA synthesis in Chinese hamster cells. I. Production of stable, reversible G1-arrested populations in suspension culture, *J.Cell Sci.* **46**, 151-157 (1970).

13. R. Okayasu, K. Takakura, S. Poole and J. S. Bedford, Radiosensitization of normal human cells by LY294002: Cell killing and the rejoining of DNA and interphase chromosome breaks, *Journal of Radiation Research* **44**, 329-333 (2003).

14. K. Rothkamm and M. Lobrich, Evidence for a lack of DNA double-strand break repair in human cells exposed to very low x-ray doses, *Proc.Natl.Acad.Sci.U.S.A* **100**, 5057-5062 (2003).

15. K. Nakamura and S. Antoku, Enhancement of X-ray cell killing in cultured mammalian cells by the protein phosphatase inhibitor calyculin A, *Cancer Res.* **54**, 2088-2090 (1994).

16. I. B. Nazarov, A. N. Smirnova, R. I. Krutilina, M. P. Svetlova, L. V. Solovjeva, A. A. Nikiforov, S. L. Oei, I. A. Zalenskaya, P. M. Yau, E. M. Bradbury and N. V. Tomilin, Dephosphorylation of histone gamma-H2AX during repair of DNA double-strand breaks in mammalian cells and its inhibition by calyculin A, *Radiat.Res.* **160**, 309-317 (2003).

17. E. Gotoh, Y. Asakawa and H. Kosaka, Inhibition of Protein-Serine Threonine Phosphatases Directly Induces Premature Chromosome Condensation in Mammalian Somatic-Cells, *Biomedical Research-Tokyo* **16**, 63-68 (1995).

Chapter 6

Signature of DNA DSBs Produced in Irradiated G_1 Cells Persist into Mitosis.

ABSTRACT

I have observed that some of the DNA damage resulting from irradiation of G_1 cells persists through the cell cycle and is expressed as γ-H2AX foci in mitotic chromosomes. This mitotic expression of damage after irradiation of G_1 cells was compared in DNA repair deficient XR-1 and UV-1 mutants of CHO cells and their wild-type counterparts. For the mutants I also compared the mitotic expression of γ-H2AX foci for immediate or delayed subculture of irradiated G_1 cells as well as for irradiation of cells in G_2. The latter comparison allowed deduction to be made on the contribution of S-phase related generation of DNA DSBs from damages produced in G_1 to the observed foci on mitotic chromosomes.

Most of the γ-H2AX foci appeared as single foci on one the other chromatid but in some cases foci appeared on both chromatids as isolocus paired foci. The dose response relationship for DNA DSB repair deficient mutant XR-1 indicated a 5 fold higher radiosensitivity relative to wild-type cells. With delayed subcultures there was about a 2-fold reduction in sensitivity for wild-type cells but no reduction for XR-1 cells. UV-1 cells were even more sensitive than XR-1 cells. Relative to wild type cells, UV-1 cells showed 10 times more sensitive for mitotic γ-H2AX foci with immediate subculture

but the yield of UV-1 cells was decreased like wild-type CHO cells with delayed subculturing. In contrast to the results with the different cell lines observed for G_1 cells, no significant differences were observed for cells irradiated in G_2.

The large number of foci in metaphase cells after G_1 irradiation of UV-1 cells may correlate with DSBs formation from unrepaired base damagesas a result of replication fork collapse during S-phase. Along with DSBs, these are expected to be repaired with delayed subculture after irradiation in G_1 phase.

I conclude the persistence of damage expressed as γ-H2AX foci in metaphase is dependent on the repair capacity for the different DNA damages. γ-H2AX foci can disappear with either rejoined or misrejoined DSBs.

INTRODUCTION

Misrepaired or unrepaired DSBs may contribute for the formation of chromosomal aberrations, which in turn can lead to various effects such as cell killing, mutation and oncogenic transformation (1-3). Recently, a relationship between radiosensitivity and γ-H2AX expression after irradiation is also reported (4).

The phosphorylation of the H2AX histone variant to form γ-H2AX foci in cells after irradiation is a very sensitive assay for DSB measurement, since each such break has been shown to result in the formation of a γ-H2AX focus (5,6). γ-H2AX foci disappear with time as these DSBs are rejoined. The formation of γ-H2AX foci involves phosphorylation of thousands or even tens of thousands of γ-H2AX molecules extending perhaps as far as a megabase from the DSB, and one postulated explanation for this has been that a DSB results in massive relaxation of chromatin coiling (7). According to this idea, the rejoining of the ends of DSB with themselves or with ends from other nearby DSBs these allows reestablishment of the coiling which subsequently leads to dephosphorylation of the γ-H2AX and disappearance of the foci.

If these proposed ideas of the processes of γ-H2AX formation and disappearance are true, then what would be the fate of an unrejoined break in mitotic chromosomes after G_1-irradiaiton that appears on a chromosomes terminal deletion, and do all rejoinings completely restore the coiling and dephosphorylation status of γ-H2AX?

To examine the behavior of the γ-H2AX foci after formation, I studied γ-H2AX foci in metaphase chromosomes after G_1- and G_2-phase irradiation of DNA repair deficient mutant CHO cell lines and their wild type counterparts. I found that some γ-

H2AX foci persist into metaphase and this is dependent on the repair capacity of the cells. In a base damage deficient CHO mutant cell I observed a huge contribution of S-phase dependent DSB formation, possibly due to base damage rather than DSBs initially produced in G_1 cells.

MATERIALS AND METHODS

Cell lines and culture

XR-1 cells are a DNA DSB repair deficient mutant of CHO cells and were kindly supplied by Dr. T.D. Stamato of the Lankenau Institute for Medical Research. These cells were highly radiosensitive and deficient in LIG4/XRCC4 which leads to a deficiency in NHEJ (8-10). UV-1 was kindly supplied by Dr. C.A. Waldren of the Radiation Effect Research Foundation. It is sensitive to UV, alkylating and DNA crosslinking agents (11-13).

Cells were grown in Eagle's minimal essential medium (MEM) supplemented with 10 % heat-inactivated (56°C for 30 min) fetal bovine serum, penicillin (100 units/ml), and streptomycin (100 μg/ml) in a humidified 5 % CO_2 atmosphere at 37°C. Synchronization of cell populations in the G_1 phase of the cell cycle was accomplished by the isoleucine depletion method previously described by Tobey and Ley (14).

γ-irradiation

Irradiations were carried out using either a J.L. Shepherd Model Mark I-68 6000 Ci ^{137}Cs irradiator at room temperature. The dose rate was 250 cGy/min.

Cell survival assay

Cell survival was measured by a standard clonogenic assay. Cells were seeded at a density designed to yield approximately 50 viable colony-forming cells per dish after the various treatments. Colonies were scored 7-10 days after irradiation. The dishes were

then treated with 100 % methanol to fix the colonies, and stained with 0.1 % crystal violet. A colony containing more than 50 cells was recorded as a survivor.

γ-H2AX foci formation

G_1 irradiation G_1 assay: for measurement of the appearance and disappearance of γ-H2AX foci in cells irradiated in G_1 and assayed in G_1, cells were grown, synchronized, and irradiated on a chamberslides. At the appropriate times after irradiation, cells were fixed in 4% paraformaldehyde for 15 minutes, washed three times in PBS for 10 minutes each, permeabilized for 5 minutes on ice in 0.2% Triton X-100, and blocked in PBS with 10% Goat serum for 60 minutes at room temperature.

G_1 irradiation, mitosis assay: for preparation of cells for irradiation in G_1 and sampling in mitosis, cells were grown and synchronized in T25 flasks and after irradiation the G_1 cells were subcultured either immediately or after a 12 hours delay. At 10 hours after subculture, cultures were incubated in the presence of Colcemid (0.1ug/ml) for 6 hours to collect mitotic cells. For G_2-irradiated cells, exponentially growing cells were irradiated and Colcemid was added 30 minutes later then, cells were harvested 1 hour later. Harvested metaphase samples were treated with a hypotonic swelling buffer (50mM KCl, 50mM $MgSO_4$ 5mM HEPES) for 20 minutes and centirfuged onto slide with cytocentrifuge (Shandon). Cells on these slides were then fixed with paraformaldehyde, washed with PBS, and permeabilized for 5 min in KCM solution (120mM KCl, 20mM NaCl, Tris-HCl 10mM, EDTA 0.5mM, Triton X-100 0.1%, pH 7.5).

Immunocytochemistory

The slides were incubated with anti-γ-H2AX mouse monoclonal antibody (Upstate) with human CREST serum anti-kinetochore antibody for metaphase analysis for 1 hour, washed three times in PBS for 10 minutes each, and incubated with Alexa Fluor-conjugated goat anti-mouse secondary antibody (Molecular Probe) with Alexa Fluor-conjugated anti-human secondary antibody (Molecular Probe) for metaphase analysis for 1 hour at room temperature. Cells were washed four times in PBS for 10 minutes each and mounted by using Slow Fade (Molecular Probes). Fluorescence images were captured by using an Olympus Provis fluorescent microscope. The anti-kinetochore antibody staining was carried out as it serves as an indicator that all the chromosomes are receptive to the immunocytochemical procedure.

RESULTS

Figure 6-1 shows dose survival responses for CHO, XR-1 and UV-1 cells γ-irradiated in G_1-phase and subcultured immediately or after a 12 hour delay. For immediate subculture, the survival curve for the wild type CHO cells showed a shoulder with D_0=150 cGy. The survival curve for UV-1 cells had similar shoulder and D_0 value. Delayed subculturing for CHO wild type and UV-1 cells increased their survival due to potentially lethal damage repair. XR-1 cells were much more radiosensitive than CHO wild type and UV-1 cells. No increase in survival for delayed subculture was observed in XR-1 .

Figure 6-2 shows the time course for the formation and disappearance of γ-H2AX foci for synchronized cells irradiated in G_1 and arrested later in G_1. CHO wild-type and UV-1 mutant cells showed a rapid increase in the number of foci until 30 minutes after a 1 Gy irradiation dose. The number of foci reached maximum around 20 to 30 minutes after exposure and then the number of foci per cell decreased fairly rapidly so that by 1 hour only half the maximum number of foci remained. The residual level of foci number was less than 3 for each cell line at 24 hours after exposure. The number of γ-H2AX foci increased more slowly in XR-1 cells, but reached a higher maximum of 26 foci per cell at 3 hour after irradiation. The residual level of foci after long incubation time XR-1 was more than 10; clearly higher than other two cell lines.

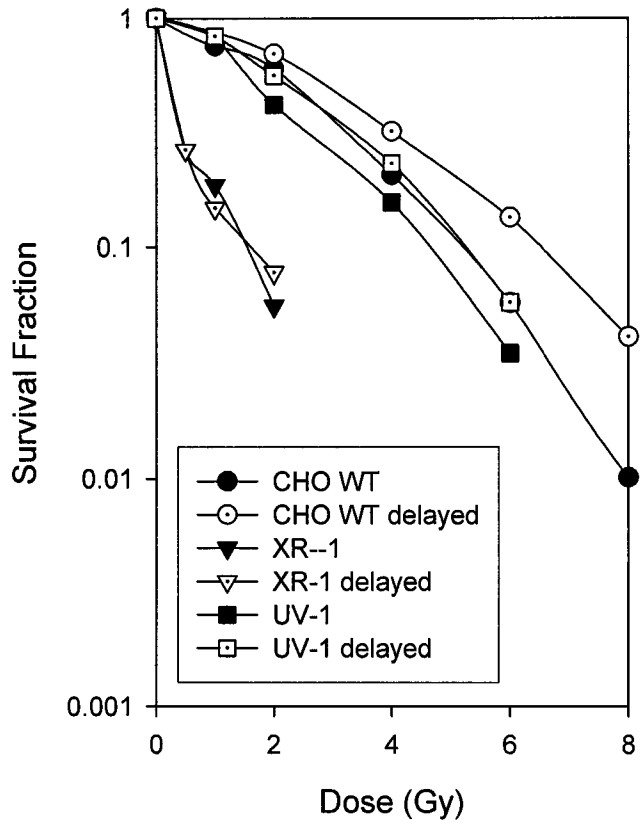

Figure 6-1

Survival curves in CHO cells and their mutants for G_1-irradiated immediate or after a 12-hour delay at 37°C. Solid lines indicate immediate subculture and dashed line for delayed subculture. Closed boxes indicate immediate subculture after irradiation and open boxes, 12 hour delayed subculture.

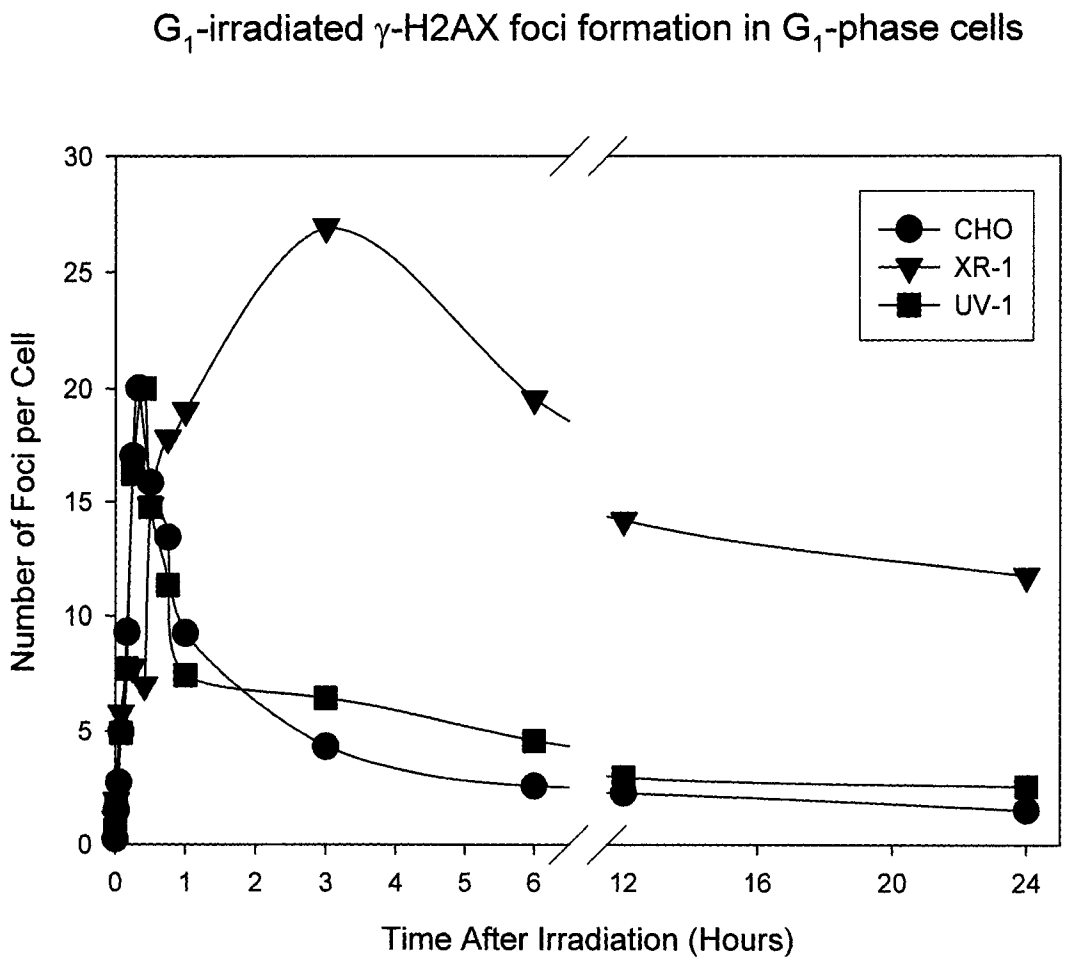

Figure 6-2

γ-H2AX scored in G_1-phase CHO, UV-1 and XR-1 cells as a function of time after irradiation of 1 Gy at G_1-phase, and then cells were arrested in G1-phase until fixation.

The appearance of these mitotic γ-H2AX foci after irradiation of G_1 CHO wild type, XR-1 and UV-1 cells is illustrated in figure 6-3. The top row refers to CHO wild-type cells, the middle to XR-1 cells and the bottom row to UV-1 cells. The zero dose background levels of foci for the three cell lines were illustrated down the left column. There were virtually no background foci on unirradiated mitotic wild-type but some background levels were seen foci the UV-1 and XR-1 mutant cells. For a dose of 0.5 Gy given to G_1 cells there were clearly many more foci not only on mitotic XR-1 cells but also on UV-1 cells.

The dose response relationships for γ-H2AX foci on metaphase chromosomes after irradiation of G_1 cells with immediate or delayed subculture are shown in Figure 6-4A, B and C. Most of the γ-H2AX foci appeared as single foci on one the other chromatid but in some cases foci appeared on both chromatids as isolocus paired foci. I categorized the localization of foci as single, paired and total. Figure 6-4A shows the frequency of single (unpaired) foci as a function of dose. Figure 6-4B shows the frequency of paired foci with increasing dose and Figure 6-4C shows the total. CHO wild type cells were least sensitive, and delayed subculturing reduced the induction of foci per unit dose to about half. XR-1 showed six to seven times more foci per unit dose than CHO wild type for both single or paired foci and delayed subculture did not reduce the number of foci in XR-1 cells. UV-1 also showed an even larger foci number for the immediate subculture group. There were about 65 total foci per cell for a dose of 0.5 Gy given to G_1 UV-1 cells. With delayed subculturing, the number of foci for these cells was decreased by about half comparing single to paired foci, about 15% of total foci were paired and 85 % were single.

Figure 6-3

γ-H2AX foci formation in metaphase chromosome. 0 Gy (A, C, E) or a 0.5 Gy (B, D, F) exposure of G_1 cells and immediately subcultured. Centromeres are stained red and γ-H2AX foci, green.

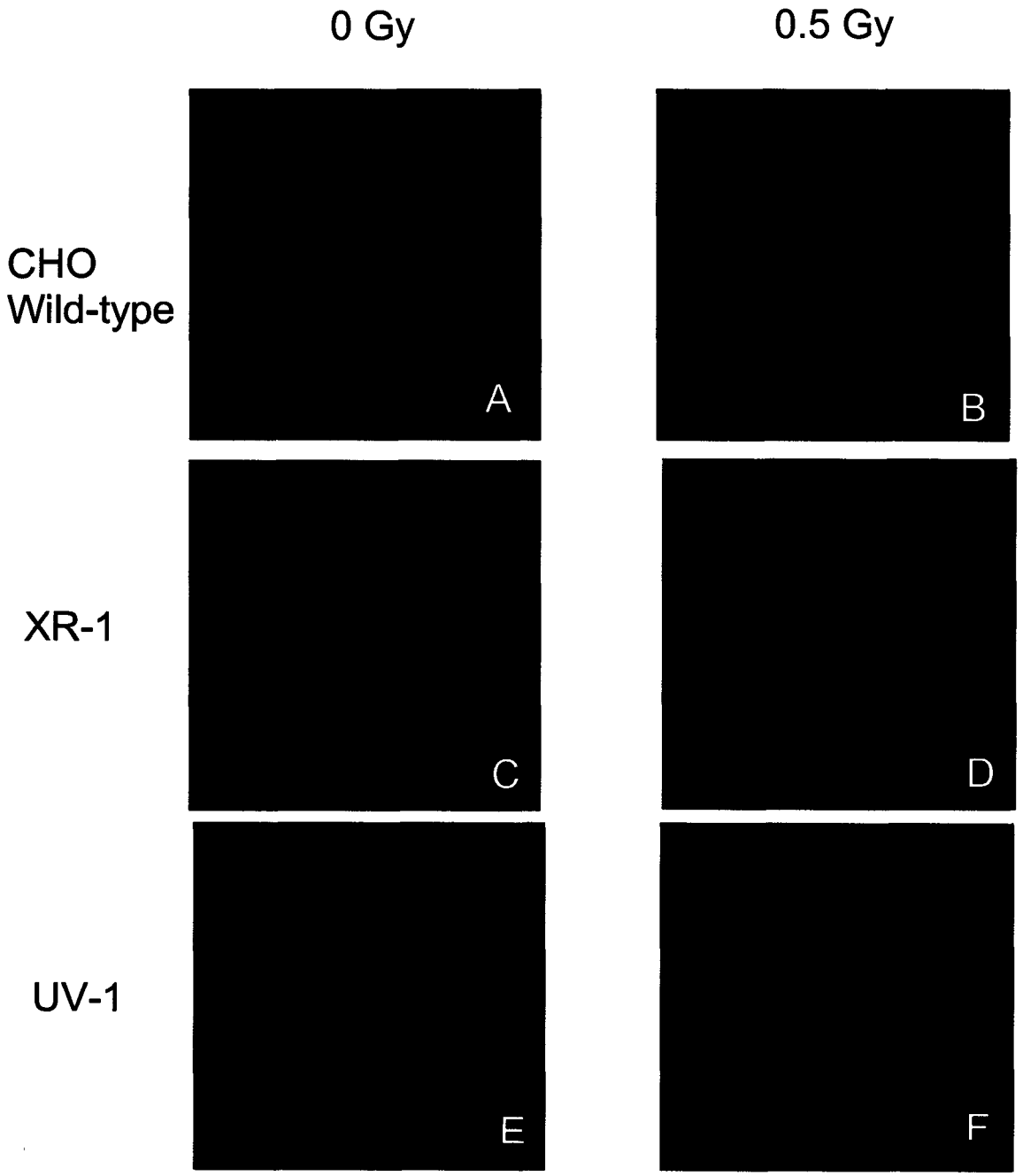

Figure 6-4

γ-H2AX foci induction in wild-type and various mutant CHO cells by γ-irradiation. Cells were irradiated in G1-phase and assayed in metaphase after immediately or delayed subculture. 6-4A shows single foci; 6-4B, paired foci, and 6-4C, total foci.

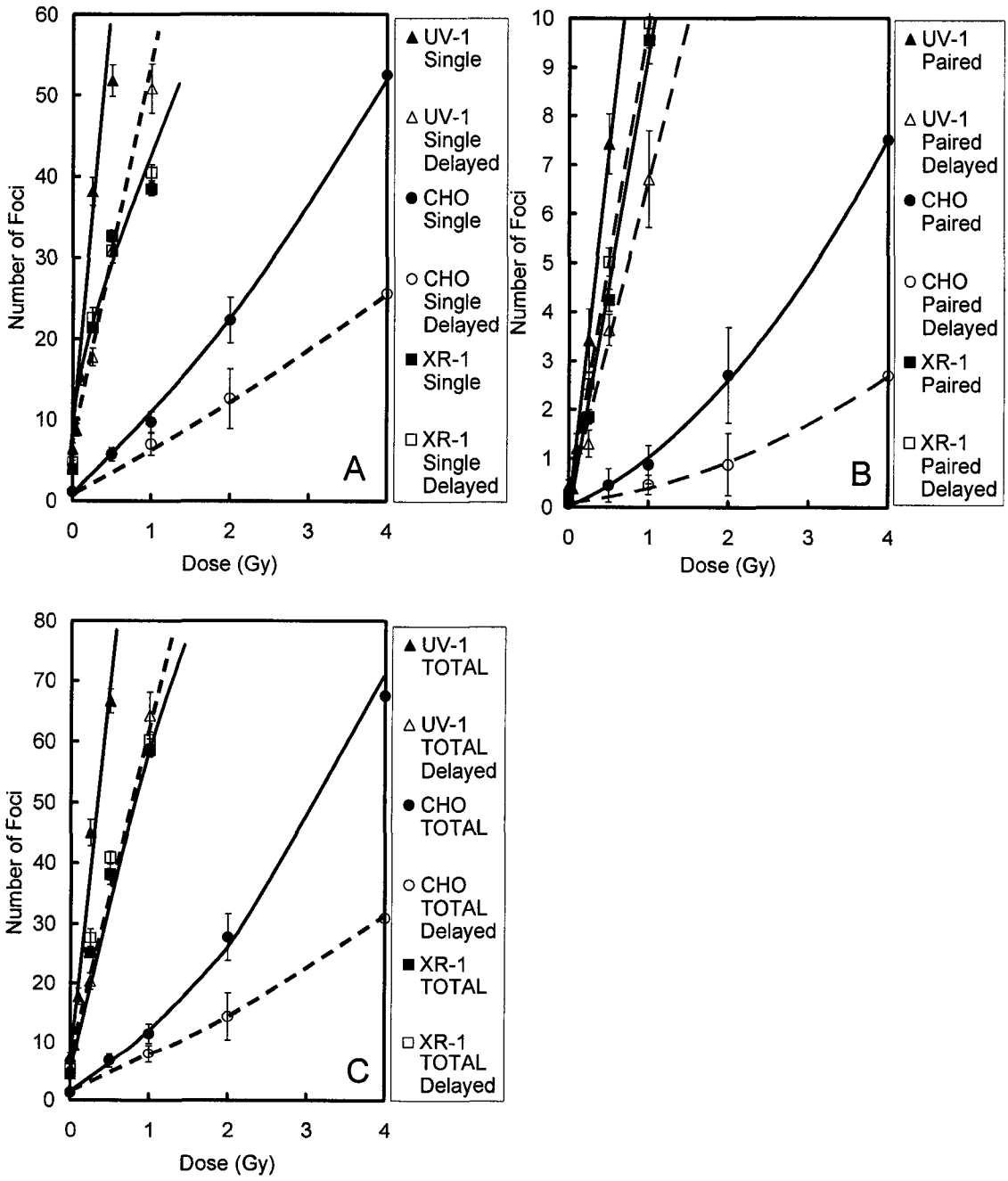

Figure 6-5

Subculture timing affects γ-H2AX persistence to metaphase. Cells were irradiated to obtain consistent amount of foci (about 40 as total; CHO 3Gy, XR-1 0.5Gy, and UV-1 0.2Gy). 6-5A shows single foci; 6-5B, paired foci, and 6-5C, total foci.

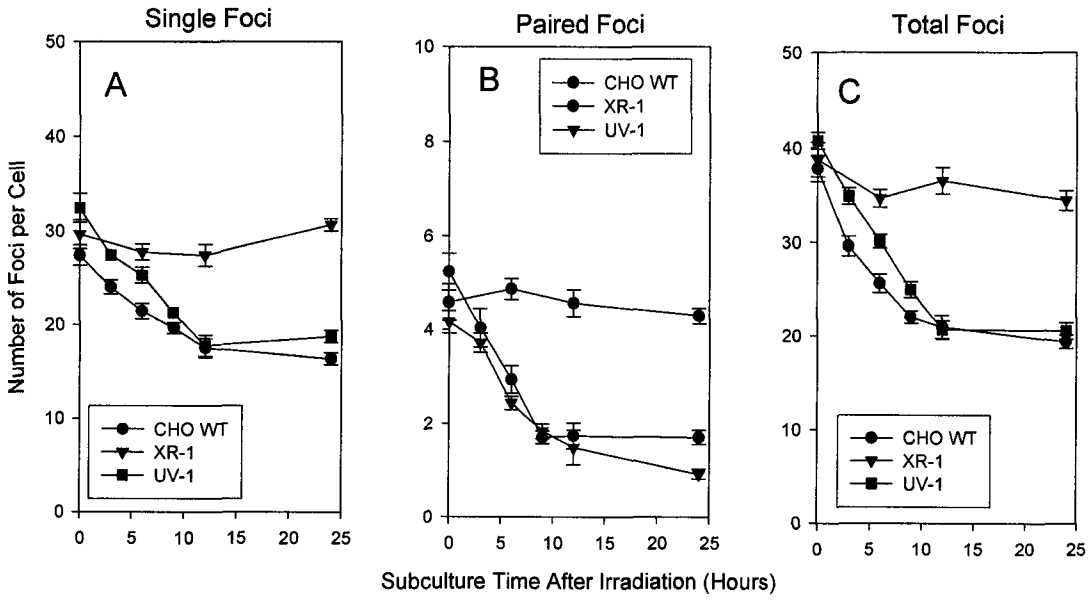

I also measured the rates of change in γ-H2AX foci seen in metaphase cells with delayed subculture of the G_1 irradiated cells as shown in figure 5. To obtain approximately the same number of foci for the 3 cell lines for the immediate subculture point; a 3 Gy dose was given wild-type cells, 0.5 Gy for XR-1 cells and 0.2 Gy for UV-1. For CHO and UV-1 cells a rapid decrease was seen in the number of foci until about the subculture was delayed for 12 hours or more. After that the residual level of foci stayed at about 20 for a 24 hour delayed subculture. In XR-1 however no appreciable reductions were observed for delayed subcultured up to 24 hours.

To determine the extent to which progression through S phase might be important, especially for the UV-1 cells. The G_2 assay was carried out. The dose response for 0.5 and 1 Gy were very similar for all three cells lines (Figure 6-6). Per unit dose, the induced number of foci in the G_2/M assay (about 36 for 0.5 Gy) was almost 3 times that seen with maximum foci number for cells irradiated and assayed both in G_1 cells (20-25 for 1Gy) (Figure 6-2 and 6-5). The fraction of paired foci per total foci in G_2-irradiated cells was very low; less than about 3 to 5 % compared to around 15 % for G_1 irradiated cells assayed in mitosis.

Finally, the localization of γ-H2AX was measured in wild-type CHO chromosome aberrations. In wild-type CHO cells dicentrics had paired foci 22.7% in immediate subculture and 0 % in 12 hours delayed subculture, and single focus 45.5% in immediate subculture and 66.7% in 12 hours delayed subculture.

Figure 6-6

G_2-irradiated foci number on metaphase cells for various cell lines. G_2-irradiated cells were scored by G_2-assay.

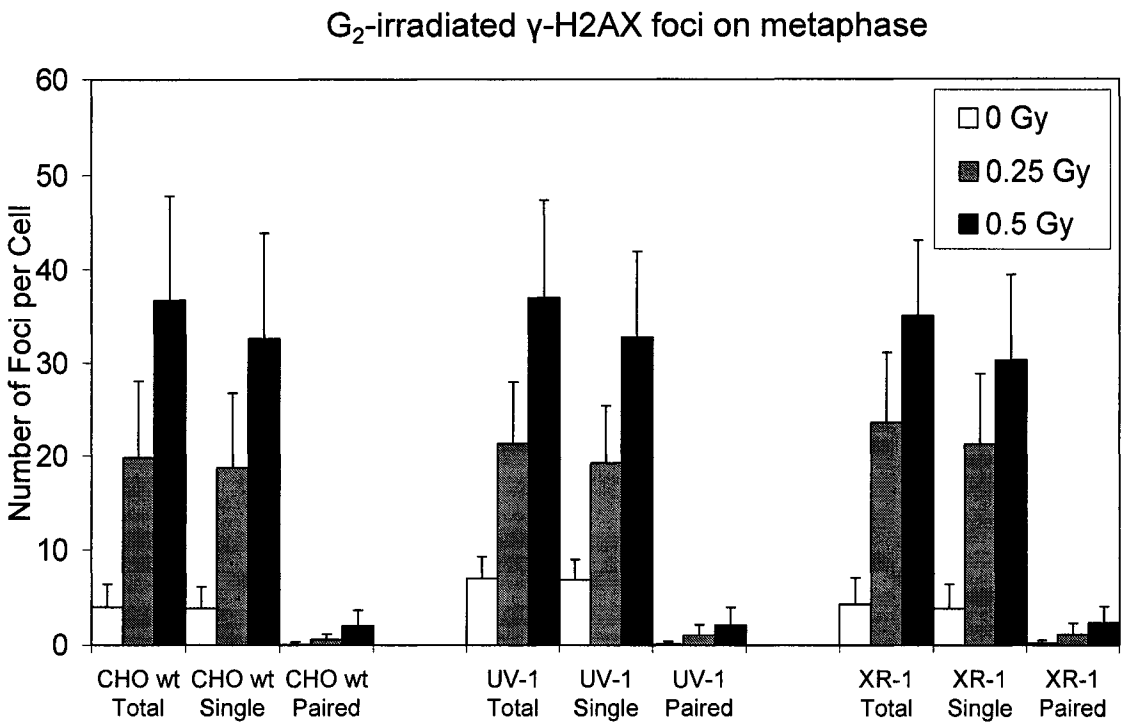

DISCUSSION

At least qualitatively residual level of γ-H2AX foci number in G_1-phase is well correlated with cellular radiosensitivity (4,16). Both CHO wild-type and UV-1 cells showed rapid γ-H2AX disappearance in G_1-phase and both have a similar sensitivity for cell killing. On the other hand, the highly radiosensitive XR-1 cells showed slower γ-H2AX foci formation and a much higher residual level of these foci.

One view concerning the appearance and disappearance of γ-H2AX foci is that these foci appear initially, one for each DNA DSB, and they disappear after the DSBs rejoin or misrepair by interaction with another DSB and the γ-H2AX histones are dephosphorylated. If this were entirely so, I might expect unrejoined breaks that lead to terminal deletions would be the only remaining broken ends at mitosis and unless ends were processed to allow dephosphorylation they might be expected to yield a γ-H2AX focus on both the centric and acentric portions of the terminal deletion. All other aberrations following G_1 irradiation are exchanges that involve rejoining. A 1Gy dose to these wild type G_1 cells would be expected to produce only about 0.1 to 0.2 aberration per cell of which only a fraction would be terminal deletion. I have observed about 10 γ-H2AX foci per mitotic cell, even for the more resistant wild type CHO cells. The residual level in G_1 after irradiation of G_1 cells for 24 hours is about 2 or 3. Thus γ-H2AX foci from some other S phase related residual damage must be responsible for the levels seen in mitosis. This is dramatically apparent in the UV-1 cells where the levels in mitosis after G_1 irradiation are some 10 fold greater.

Because XR-1 cells show a greatly reduced ability to repair DNA DSBs (17), I might expect the same number of foci on metaphase cells for either immediate or delayed subculture and this is what was observed. The UV-1 cells showed greatly reduced number of γ-H2AX foci in G_1. The reduction was similar to that seen for wild-type CHO cells so the residual levels in G_1 after 1 Gy were also only about 2 or 3 per cell. Yet the number of γ-H2AX foci was some 10 fold higher in UV-1 mitosis than wild type CHO cells. This again would indicate that some damages other than DNA DSBs in G_1 is resulted in the additional production of additional DSBs as cells progressed through S phase to mitosis. The fact that delayed subculture after irradiation in G_1 reduced the yield in mitosis I would interpret as results from some repair of the DSB's (as occurred for wild type CHO cells) but a lack of repair in UV-1 cells of some type of base damage that is fully repaired with delayed subculture in wild type but not in UV-1 cells.

There are only two ways to produce paired γ-H2AX foci on chromosomes after G_1 irradiation. One might be that a rejoined but distorted region of DNA is replicated in S-phase and remains distorted to prevent dephosphorylation in both sister chromatids. Another possibility is simply two independent single base damage in opposite chromatids are close enough to recognize them as paired foci. But latter case hardly happens if the total number of foci per cell is less than 100. A single focus on a chromatid could be generated in several ways. One of the paired foci might disappear during the G_2-phase. Another possibility might be that an S-phase dependent DSB formation might occur from primary DNA lesion such as SSB, base damage or DNA crosslink and result in single focus on metaphase.

Chromosomal aberrations such as dicentrics are produced from DNA DSBs. If the γ-H2AX foci remain even after DSB misrejoined, I should observe paired foci between two centromeres. In wild-type CHO cells dicentrics had paired foci 22.7% in immediate subculture and 0 % in 12 hours delayed subculture, and single focus 45.5% in immediate subculture and 66.7% in 12 hours delayed subculture. This indicates γ-H2AX dephosphorylation occurs in most instances after rejoining even when DNA DSBs are misrejoined. The result of decreased paired foci with increased single focus suggests some single foci result from loss of one focus of paired foci. It is interesting that both foci of a pair did not disappear at the same time. γ-H2AX foci in chromosomes may be an unrepaired DSB or a "a scar" recently form a DSBs.

In summary, γ-H2AX foci persist until metaphase after G_1-irradiation. Paired foci are generated from G_1-DSB, and single foci may be generated from loss of one of paired foci and S-phase dependent DSB formation. γ-H2AX foci can disappear after DNA is misrejoined.

REFERENCES

1. M. Frankenberg-Schwager, Induction, repair and biological relevance of radiation-induced DNA lesions in eukaryotic cells, *Radiat.Environ.Biophys.* **29**, 273-292 (1990).

2. A. J. Pierce and M. Jasin, NHEJ deficiency and disease, *Mol.Cell* **8**, 1160-1161 (2001).

3. D. Murray, R. Simpson, E. Rosenberg, A. Carraway and R. Britten, Correlation between gamma-ray-induced DNA double-strand breakage and cell killing after biologically relevant doses: analysis by pulsed-field gel electrophoresis, *Int.J.Radiat.Biol* **65**, 419-426 (1994).

4. P. L. Olive and J. P. Banath, Phosphorylation of histone H2AX as a measure of radiosensitivity, *Int.J Radiat.Oncol.Biol.Phys.* **58**, 331-335 (2004).

5. E. P. Rogakou, D. R. Pilch, A. H. Orr, V. S. Ivanova and W. M. Bonner, DNA double-stranded breaks induce histone H2AX phosphorylation on serine 139, *J Biol.Chem.* **273**, 5858-5868 (1998).

6. O. A. Sedelnikova, E. P. Rogakou, I. G. Panyutin and W. M. Bonner, Quantitative detection of (125) IdU-induced DNA double-strand breaks with gamma-H2AX antibody, *Radiat.Res.* **158**, 486-492 (2002).

7. E. P. Rogakou, C. Boon, C. Redon and W. M. Bonner, Megabase chromatin domains involved in DNA double-strand breaks in vivo, *J.Cell Biol.* **146**, 905-915 (1999).

8. A. J. Giaccia, N. Denko, R. MacLaren, D. Mirman, C. Waldren, I. Hart and T. D. Stamato, Human chromosome 5 complements the DNA double-strand break-repair deficiency and gamma-ray sensitivity of the XR-1 hamster variant, *Am.J Hum.Genet.* **47**, 459-469 (1990).

9. T. D. Stamato, A. Dipatri and A. Giaccia, Cell-Cycle-Dependent Repair of Potentially Lethal Damage in the Xr-1 Gamma-Ray-Sensitive Chinese-Hamster Ovary Cell, *Radiation Research* **115**, 325-333 (1988).

10. A. J. Giaccia, E. Richardson, N. Denko and T. D. Stamato, Genetic-Analysis of Xr-1 Mutation in Hamster and Human Hybrids, *Somatic Cell and Molecular Genetics* **15**, 71-77 (1989).

11. L. L. Hinkle, C. A. Waldren and T. D. Stamato, Tentative Identification of Cho-Uv-1 As A Uv-Sensitive Mutant Deficient in Post-Replication Repair, *Environmental Mutagenesis* **2**, 300 (1980).

12. T. D. Stamato, L. Hinkle, A. R. Collins and C. A. Waldren, Chinese hamster ovary mutant UV-1 is hypomutable and defective in a postreplication recovery process, *Somatic.Cell Genet.* **7**, 307-320 (1981).

13. C. A. Hoy, L. H. Thompson, E. P. Salazar and S. A. Stewart, Different genetic alterations underlie dual hypersensitivity of CHO mutant UV-1 to DNA methylating and cross-linking agents, *Somat.Cell Mol.Genet.* **11**, 523-532 (1985).

14. R. A. Tobey and K. D. Ley, Regulation of initiation of DNA synthesis in Chinese hamster cells. I. Production of stable, reversible G1-arrested populations in suspension culture, *J.Cell Biol.* **46**, 151-157 (1970).

15. K. Rothkamm and M. Lobrich, Evidence for a lack of DNA double-strand break repair in human cells exposed to very low x-ray doses, *Proceedings of the National Academy of Sciences of the United States of America* **100**, 5057-5062 (2003).

16. T. T. Paull, E. P. Rogakou, V. Yamazaki, C. U. Kirchgessner, M. Gellert and W. M. Bonner, A critical role for histone H2AX in recruitment of repair factors to nuclear foci after DNA damage, *Current Biol.* **10**, 886-895 (2000).

17. T. D. Stamato, R. Weinstein, A. Giaccia and L. Mackenzie, Isolation of cell cycle-dependent gamma ray-sensitive Chinese hamster ovary cell, *Somatic Cell Genet.* **9**, 165-173 (1983).

Chapter 7

Tracking Connection between the Formation and Disappearance of γ-H2AX foci in Nuclei and the Prematurely Condensed Chromosomes of G_0 Human Fibroblasts after γ-Irradiation.

ABSTRACT

The time courses of the development and disappearance of γ-H2AX foci after irradiation were measured in the nuclei of non cycling G_0 human fibroblasts and in the same cells after induction of premature chromosome condensation. The purpose was to investigate possible connections between the rejoining and mis-rejoining of DNA DSBs and the early formation of chromosome aberrations.

For γ-H2AX foci assayed in G_0 nuclei after irradiation of G_0 human fibroblasts, a maximum of about 30 foci per cell was observed after 1 Gy, in agreement with estimate of the number of DNA DSBs expected for this dose. However, about twice the numbers of foci were seen for same dose after induction of premature chromosome condensation. For both assays the number of foci then decreased at about the same rate when foci were measured at various times after irradiation. The apparent excess number of foci above expectation may be related to the unbalance of kinase-phosphatase by MPF that occurs when mitotic and interphase cells were fused.

γ-H2AX foci in the prematurely condensed chromosomes were often seen at the broken ends of PCC fragments, and instances were also seen of γ-H2AX foci at the

junction point of translocations. Lesions allowing expression γ-H2AX foci persisted even after irradiated G_0 cells were subcultured and allowed to progress to mitosis, but incubation of G_0 cells up to for 12 hours after irradiation before subculture resulted in the disappearance of these foci on mitotic chromosomes.

Numerous γ-H2AX foci were seen in the nuclei of unirradiated S phase cells, and an enormous phosphorylation of H2AX was seen in unirradiated S cells but not G_0 cells after fusion with mitotic HeLa cells. And those γ-H2AX was colocalized with BrdU.

INTRODUCTION

γ-H2AX focus is a signature of DNA DSB. Histone H2AX phosphorylation occurs within a megabase or so around the location of each DSB (1,2). The detailed of the mechanisms involved in phosphorylation and dephosphorylation of H2AX, however, is still unknown (3). To attempt to relate the development and disappearance of γ-H2AX with chromosome breaks I followed these in prematurely condensed chromosomes (PCC) (4-6).

PCC allows an analysis of the breakage and rejoining of interphase chromosome (4-6). Because γ-H2AX foci localizes on DNA DSBs, I set out to determine whether localization of γ-H2AX occurred on G_0-PCC breaks after irradiation. The hypothesis or expectation being tested was as follows (Figure 7-1).

First, since some 30 or so DNA DSBs are initially produced in G_0 cells but only 5 to 6 PCC breaks are observed after a 1 Gy radiation dose, many of the DNA breaks may be rejoined by the time the induction of PCC is completed (5). Thus, the maximum number of γ-H2AX foci expected in the G_0 PCCs might be 30 or less. Second, while many γ-H2AX foci would be expected interstitially in PCCs I might expect a focus to be present initially at the end of each unrejoined PCC break. Third, there should be at least some γ-H2AX foci present at the break points of translocation formed when PCC breaks misrejoined to form an exchange. Forth, some H2AX phosphorylated regions of chromatin may persist and may be observed in mitosis.

Each of these expectations was tested in the experiments reported below. The measurement of radiation induced γ-H2AX foci in S phase cells has been recognized as a

potential problem become of high background frequencies in S phase cells even without radiation. I therefore examined more closely the relationship between γ-H2AX foci and followed by DNA synthesis in S phase cells measurement of incorporated BrdU. Further studied the degree of γ-H2AX phosphorylation after induction of PCC in S phase cells since the PCC process involves itself inhibition of phosphatases.

Figure 7-1

Possible scheme for the phosphorylation of H2AX and the dephosphorylation of γ-H2AX. γ-H2AX foci formation occurs after DSB formation and it disappears following rejoining.

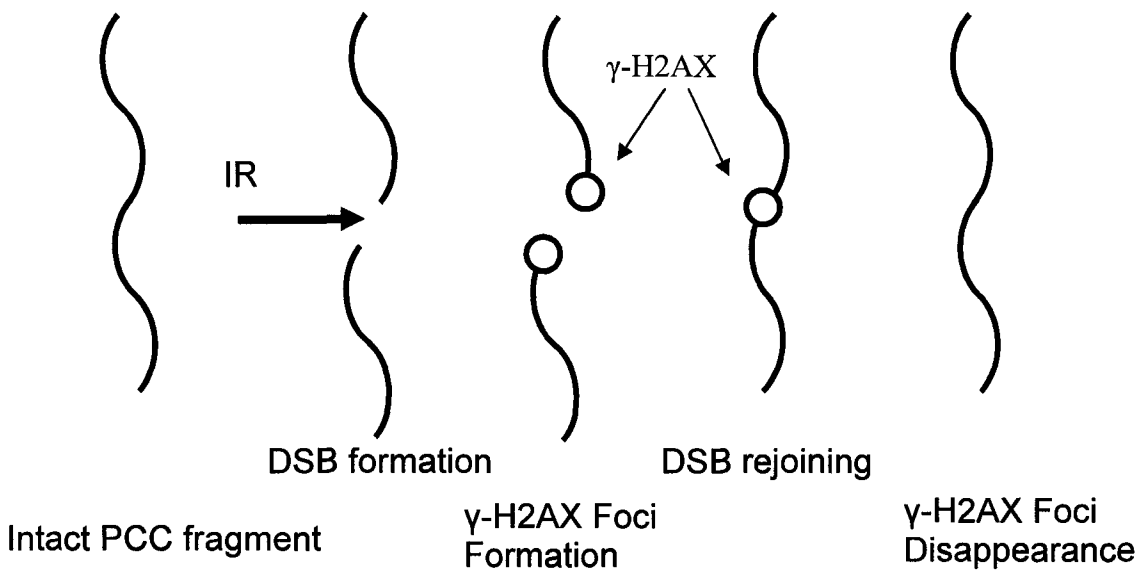

MATERIALS AND METHODS

Cell lines and culture

Normal human fibroblast cell lines (AG1522 and GM8429) were grown in Eagle's minimal essential medium (MEM) supplemented with 15 % heat-inactivated (56°C for 30 min) fetal bovine serum, penicillin (100 units/ml), and streptomycin (100 μg/ml) in a humidified 5 % CO_2 atmosphere at 37°C. To establish contact inhibited population of cells in G_0 cells were inoculated into T25 flasks or chamberslides and after the cultures reached a confluent monolayer they were kept and additional 3 days to insure they were fully contact inhibited. Cell cultures were irradiated using a J.L. Shepherd Model Mark I-68 6000 Ci ^{137}Cs irradiator. The dose-rate was 2.5Gy per minute. T25 flasks were irradiated on ice for G_0 PCC initial time point. For the time course G_0 nucleus and G_0 PCC, flasks were irradiated at room temperature.

Premature chromosome condensation (PCC)

PCC protocol was carried out as previously described (5,7). Colcemid were added to the exponentially growing HeLa cells for 3 hours. Mitotic HeLa (M-HeLa) cells were obtained by mitotic shake. For measuring initial damages after irradiation, cells were irradiated on ice after trypsinization. For time course, cells were kept 37°C for various times after irradiation, and then cells were trypsinized to get single cell suspension. The numbers of M-HeLa and sample cells were counted and same number of cells (5×10^5 each) were mixed in cold medium. Cells were span down at 1500rpm for 4 minutes, and the supernatant was discarded and 10ml of ice cold MEM with Colcemid was added.

Cells were centrifuged, medium was discarded, and 0.5 ml of ice cold serum free MEM with Colcemid was added to the cell pellet and mix well. 10μl of Sendai-virus were added the final concentration of virus was 200 HAU*/ml and the samples were mixed well. The tube was then kept on ice for 15 minutes. After slow centrifugation to form a loose pellet, the tube was incubated in 37°C for 10 minutes. 5 ml of MEM containing 15% FBS and Colcemid was then added and the tubes were incubated for an additional 35 minutes in 37°C. Cells were then centrifuge down and the supernatant was removed.

γ-H2AX assay

Cell suspensions were treated with a hypotonic swelling buffer for 20 minutes and cytocentrifuged on slides. Cells were fixed in 4% Paraformaldehyde for 15 minutes and washed with PBS for 10 minutes repeated 3 times. After treatment in KCM solution for 5 minutes, cells were blocked by 10% goat serum for 1 hour. Anti-γ-H2AX mouse monoclonal antibody (Upstate) and CREST serum was treated for 1 hour at 37°C. Primarily antibodies were washed in PBS for 10 minutes 3 times. Alexa 488 anti-mouse secondary goat antibody (Molecular Probes) and Alexa 592 anti-human secondary goat antibody (Molecular Probes) were treated for 1 hour at 37°C. Excess antibodies were washed in PBS for 10 minutes 4 times. Nucleus was counterstained by 1.5ug/ml DAPI in slowfade (Molecular Probes).

Images of cells were obtained using an Olympus AX-70 fluorescence microscope equipped with a PSI image analysis system utilizing the MAC-Probe package. The processed images were stored and cells from these were later scored.

Immuno-FISH

To detect translocations in PCCs, cells were analyzed by FISH (fluorescence *in situ* hybridization) (8,9) with γ-H2AX staining. Firstly, slides were stained for γ-H2AX by immunocytochemistry. Slides were then denatured by 70% formamide / 2x SCC at 70°C for 2 minutes to denature the chromosomes. Following denaturation, the slide was dehydrated for 2 minutes each in 70%, 90%, and 100% ethanol. Human chromosome 1 specific painting probe labeled with digoxigenin (Original probes were established by Dr. A. Christian of Lawrence Livermore National Laboratory) was mixed by hybridization mix (50% formamide, 2×SCC, 10% dextrin sulfate, 1μg probe and 1μg human Cot-1 DNA). This mixture was incubated at 84°C for 15 minutes to denature the probe, and then kept at 37°C in 45 minutes to preanneal repetitive sequences. The probe was added to the slide, and it was kept overnight in a humid 37°C chamber. Slides were washed at 45°C for 10 minutes in 50% formamide/2×SSC, and 10 minutes in 2×SSC. A solution of 10% goat serum in PN buffer (0.1M sodium phosphate, 0.1% NP-40 detergent) was added to the slide for 5 minutes at room temperature to decrease the binding of anti-digoxigenin antibody. Alexa 594-conjugated anti-digoxigenin antibody (Molecular Probes) was then added to the slide for 1 hour, and rised off in PN buffer. The slide was counterstained with DAPI/slowfade solution, and photographed using Olympus AX70 microscope with a Sensys CCD camera (Photometrics, Tucson AZ) equipped with a PSI image analysis system utilizing the MAC-Probe package.

G_0-phase Irradiation followed by Metaphase Analysis

For preparation of cells to be irradiated in G_0 and assayed in metaphase, the irradiated G_0 phase cells were either subcultured immediately or after various periods of time for the delayed subculture. Thirty hours after subculture, Colcemid was added for 6 hours before mitotic cells were harvested by mechanical shaking of the flasks. Harvested metaphase samples were treated in a swelling buffer for 20 minutes and centrifuged onto slides by a cytocentrifuge. Cells were then fixed and stained as outlined above for immunostaining.

Bromodeoxyuridine (BrdU) pulsed label

Exponentially growing cells cultured in chamberslides or T25 flasks were prepared and 30 μg/ml of BrdU in cell culture medium was then added and the cultures were incubated for 10 minutes. For interphase experiments, cells were washed with PBS and fixed by 4% Paraformaldehyde for γ-H2AX assay.

For PCC experiments, culture medium was removed and cells were washed with PBS once. Cells were harvested by trypsinization and cell fusion was carried out with M-HeLa cells.

γ-H2AX assay for interphase cells and PCC cells

For fixation of interphase cells, after fixation in 4% Paraformaldehyde, cells were washed with PBS three times for 5 minutes each, the cells were then incubated in 0.2% TritonX-100 in PBS treatment for 5 minutes to enhance permeability for antibody reaction, and 10% goat serum in PBS was added to block non specific binding of

secondary antibody and the cells were then incubated at 4°C for overnight or 37°C for 1 hour.

For fixation of PCC cells, fused cell suspensions were treated by hypotonic swelling buffer for 20 minutes and centrifuged onto slides by cytocentrifugation. Cells were then fixed stained as above.

S-phase γ-H2AX / BrdU in interphase and PCC

Exponentially growing cells were pulsed labeled by 30μg/ml of BrdU for 10 minutes. For interphase analysis, cells were washed and fixed directly on chamberslides. For PCC analysis, cells were washed followed by trypsinization to prepare suspension for cell fusion as previously described. Slides were fixed in 4% Paraformaldehyde for 15 minutes and washed three times in PBS for 10 minutes and treated in 0.2% Triton X-100 for 5 minutes. After blocking with 10% goat serum, γ-H2AX was stained as previously mentioned. Slides were treated with 70% formamide/2×SSC for 2 minutes at 70°C. Slide was rinsed twice in 2×SSC for 3 minutes at RT, and then in PBS for 5 minutes. Cells were incubated in 1:100 anti-BrdU rat antibody for 1 hour at 37°C and slides were rinsed three times in PBS for 5 minutes. Slides were then incubated with Alexa 594 conjugated anti-rat goat secondary antibody diluted in 1:100 for 1 hour at 37°C. The slides were then washed in PBS for 5 minutes 4 times. Nuclei were counterstained by 1.5ug/ml DAPI in slowfade.

RESULTS AND DISCUSSION

Preparing good "spreads" of PCCs proved to be difficult with the cytocentirfuge approach, but better preparations with drying in 3:1 (Methanol: Acetic Acid) is not compatible with immunocytochemistry. Therefore the number of good PCC spreads, sufficient for good localization of γ-H2AX foci was very limited. The results from a few of the reasonably well spread PCCs, however are shown in Figures 7-2A-D. γ-H2AX foci were stained green. To distinguish acentric PCC fragments, I used CREST serum for staining centromeres by binding red fluorescent anti-kinetochore protein antibody. So the PCC fragments without red signals (centromere) must be excess PCC fragments.

γ-H2AX foci on G_0 *PCCs and* G_0 *nuclei*

Figure 7-1A and 1B illustrate γ-H2AX foci on G_0 PCCs immediately after 1Gy. At this early time after irradiation many of the PCC breaks have not rejoined, and numerous γ-H2AX foci are present. Arrows point of several instances where γ-H2AX foci appear at the ends of acentric (centric in some cases) PCC fragments. Figure 7-2B shows that even at this early sampling time what appears to be a recently rejoined break can be seen as a double focus (paired arrows in Figure 2B). Figure 7-2C and D show G_0 PCCs at 24 hours after irradiation increasingly fewer γ-H2AX foci are present. Dicentric PCC fragment did not have γ-H2AX foci between two centromere signals in figure 7-2D. It indicates γ-H2AX foci can be dephosphorylated even after misrejoining of DSBs.

Figure 7-2.

PCC with γ-H2AX foci after 1Gy of irradiation.
Green represents γ-H2AX and Red represents centromere.
Figure 7-2A and B. PCC with γ-H2AX foci, 0 minutes after 1Gy of irradiation.

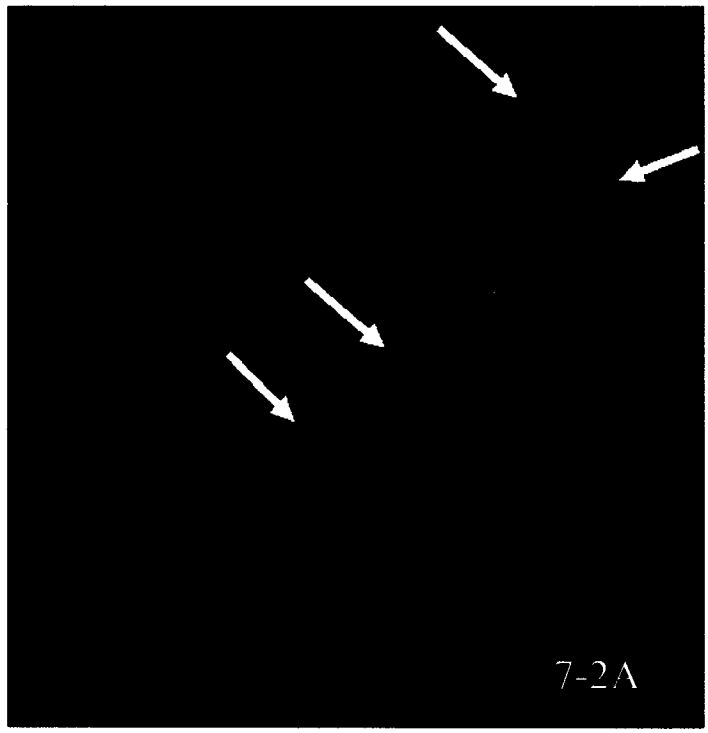

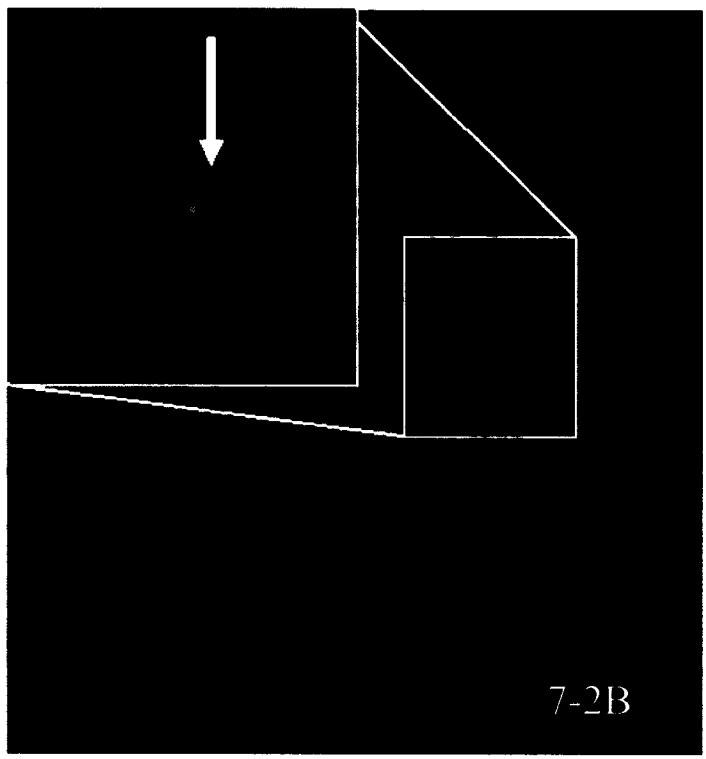

Figure 7-2C and D. PCC with γ-H2AX foci 24 hours after irradiation. Arrows indicate no γ-H2AX foci between two centrome regions.

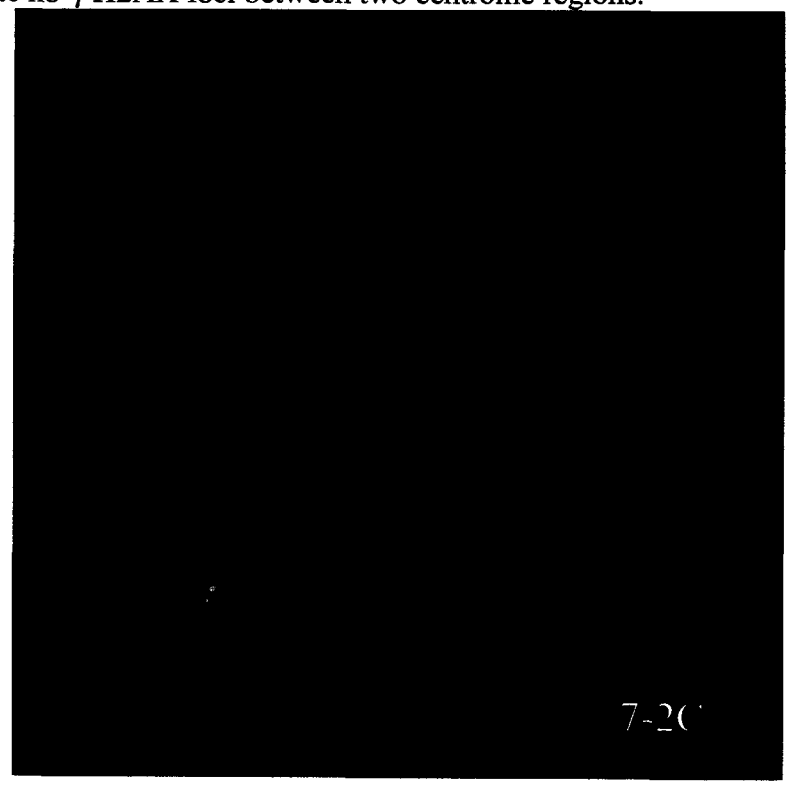

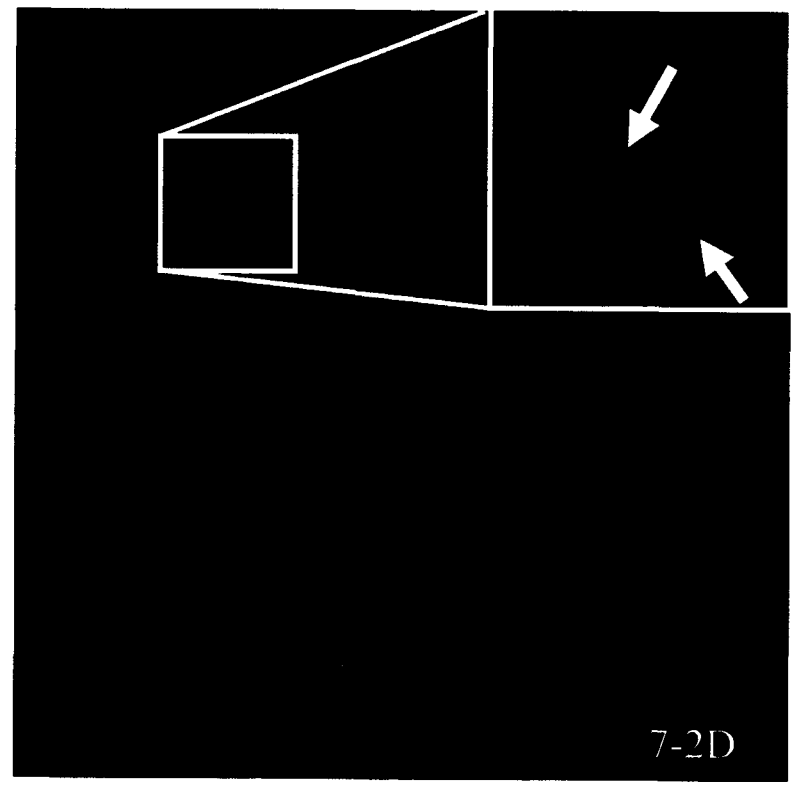

Figure 7-3 shows a PCC carried out 1 hour after irradiation and then stained with a whole chromosome 1 specific FISH paint probe as well as immunocytochemistry for γ-H2AX foci. This illustrates a γ-H2AX focus located directly at the break point of the translocation.

Because of overlapping PCC chromosome spreads were not adequate for more quantitative scoring of γ-H2AX foci and these chromosomal locations. However, the spreads were adequate for scoring total number of foci. Figure 7-4 shows the dose response for induction of γ-H2AX foci in PCCs carried out immediately after irradiation. The dose response is very steep, with a slope indicating the induction of about γ-H2AX foci per G_0 PCC per Gy.

Figure 7-5A and 5B show the number of γ-H2AX foci on G_0 PCCs for two human cell lines at various times after a 1Gy radiation dose. As seen earlier in figure 7-4, foci number per cell was much higher than expected at the earliest sample times. The so called 0 hour time, however, represents the time, where the PCC procedure was started immediately after irradiation, but actually some 20 minutes at 37°C is required for cell fusion and PCC to occur. Still, 70 foci per cell is about twice the maximum number of foci seen in G_0 interphase nuclei where PCC has not been induced by fusion with mitotic HeLa cells. After 30 minutes or so, however, the rate of decrease in foci number on PCCs is slower.

The relative rates of change in γ-H2AX foci after 1 Gy in the G_0 interphase nuclei and the G_0 PCCs are shown for comparison in figures 7-6A and 6B. Figure 7-6A show the changes in γ-H2AX foci in the G_0 nuclei out to 24 hours after 1 Gy, and the relative rates of change in both the G_0 nuclei and the G_0 PCCs are plotted together in figure 7-6B.

Figure 7-3

Figure 7-3 represents an example immuno-FISH in PCC after irradiation. Cells were irradiated and fixed after 1 hour of repair time. Green represents γ-H2AX foci (immunocytochemistry) and red shows chromosome 1 (FISH).

Figure 7-3A (merged color)

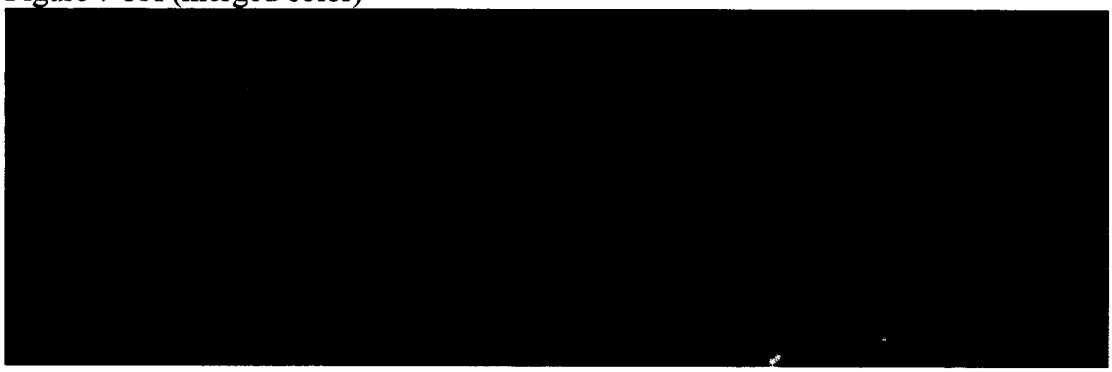

Figure 7-3B (only chromosomes)

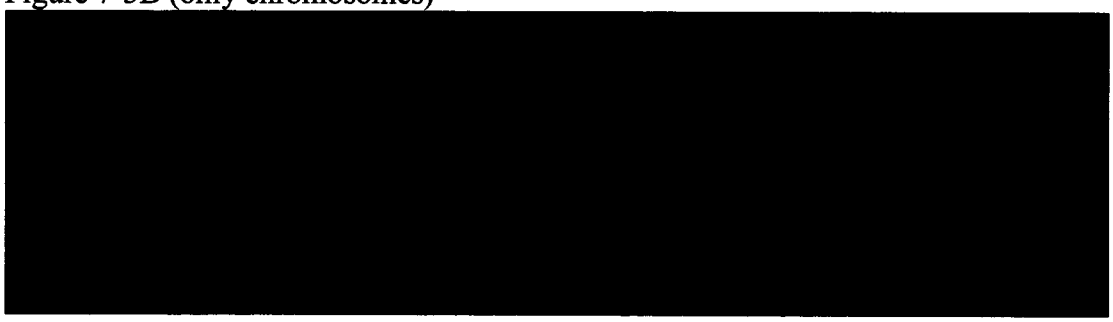

Figure 7-3C
Merged

Figure 7-3D
chromosome

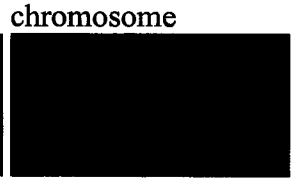

Figure 7-3F
γ-H2AX (green)

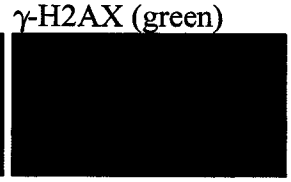

Figure 7-3E
translocation (Ch1)

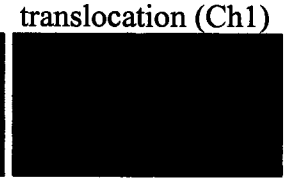

Figure 7-4

Figure 7-4 represents the dose response curve of initial γ-H2AX foci on PCC in AG1522. Cells were irradiated and processed PCC immediately after irradiation.

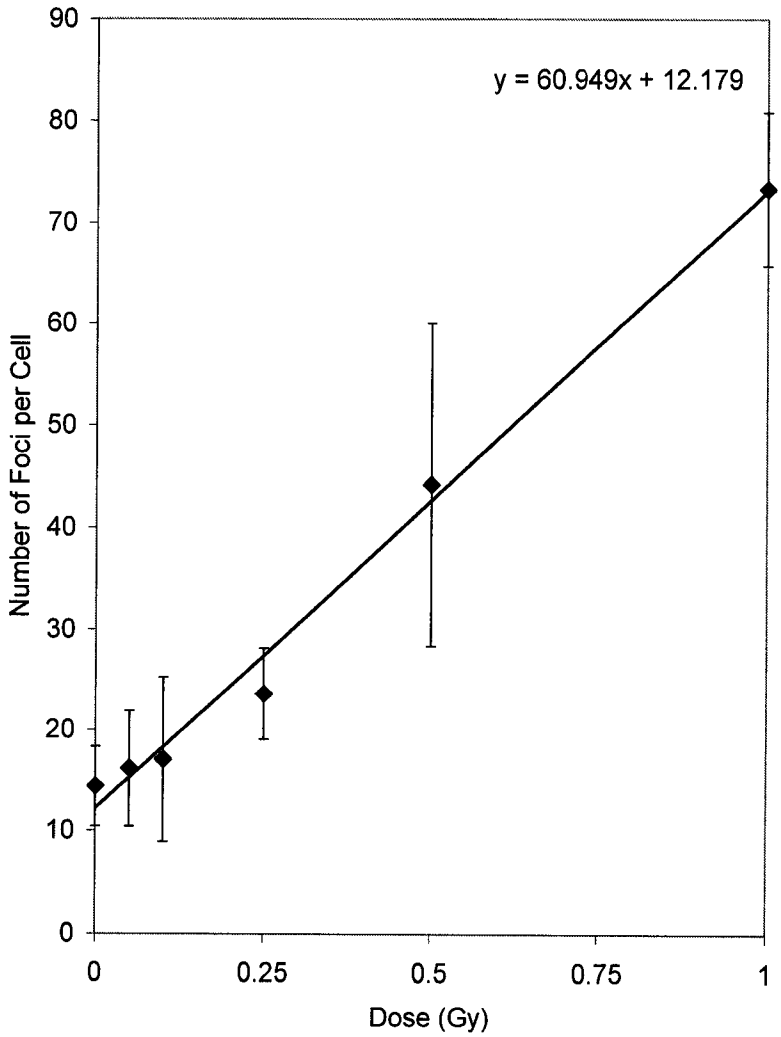

Figure 7-5.

Time course of γ-H2AX foci on PCC after 1Gy of irradiation. G_0-phase cells were irradiated and processed PCC after certain repair time.

Figure 7-5A

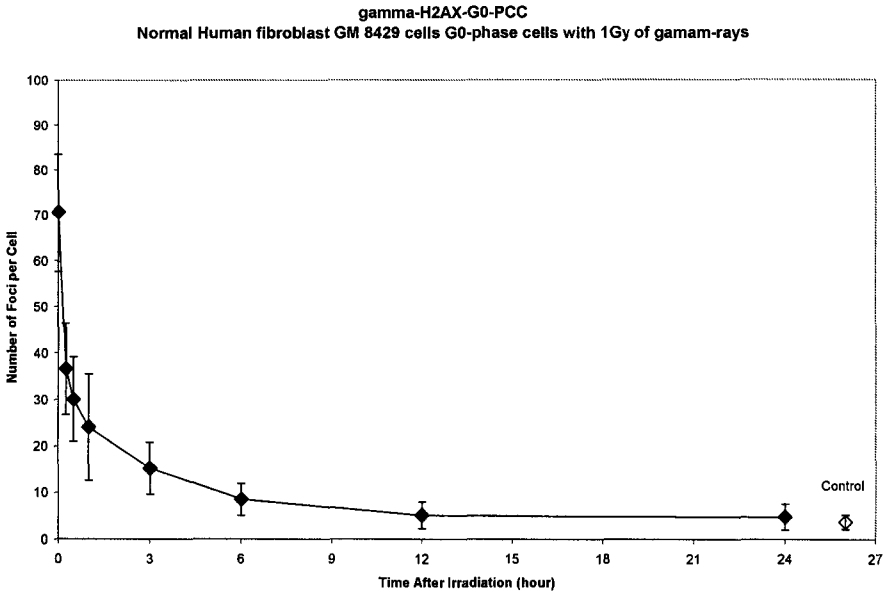

Figure 7-5B

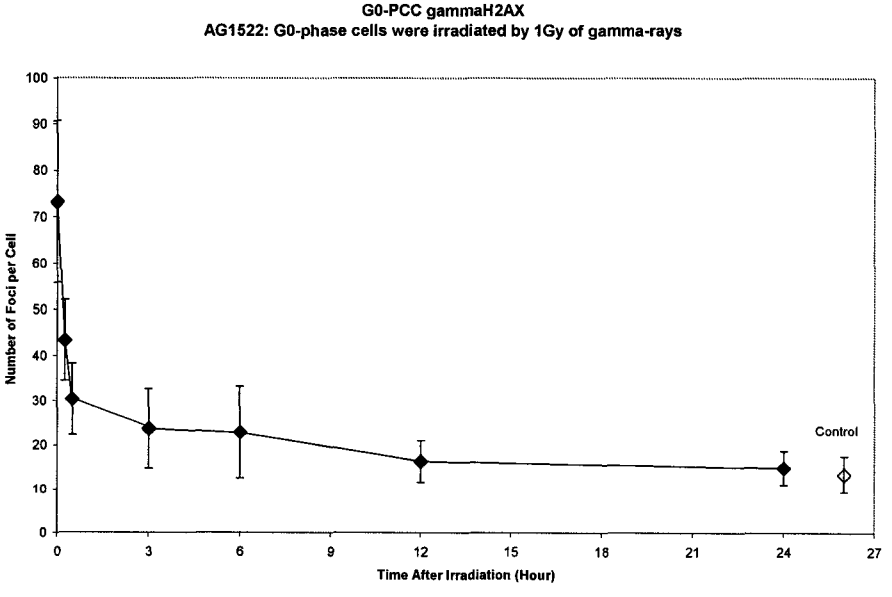

Figure 7-6.

Comparison γ-H2AX time course between G_0-interphase nucleus and G0-PCC. Figure 3A represents γ-H2AX foci formation and disappearance in G_0-phase interphase nucleus after 1 Gy of irradiation. Figure 3B shows the remained foci frequencies in G_0-phase interphase nucleus (solid line) and G_0-PCC (dashed line).

Figure 6A

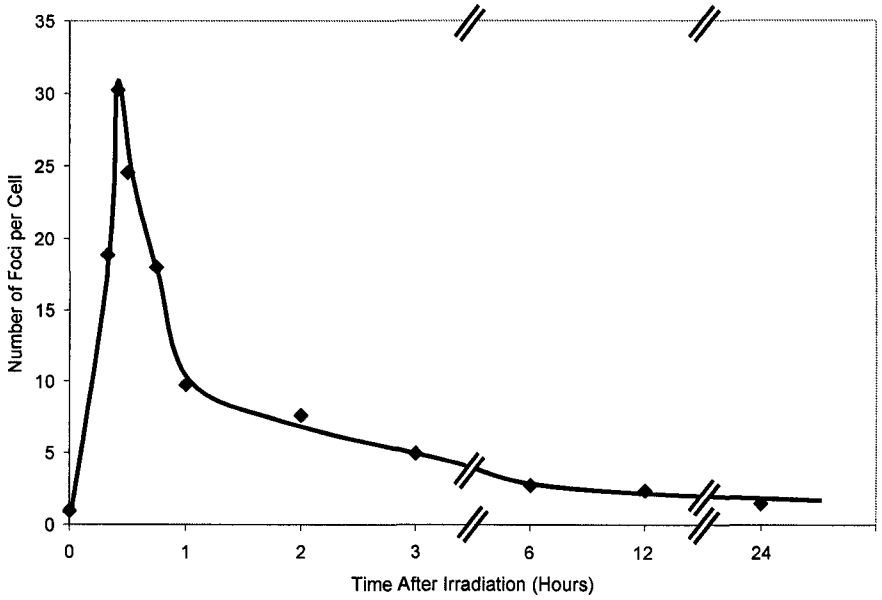

Figure 6B

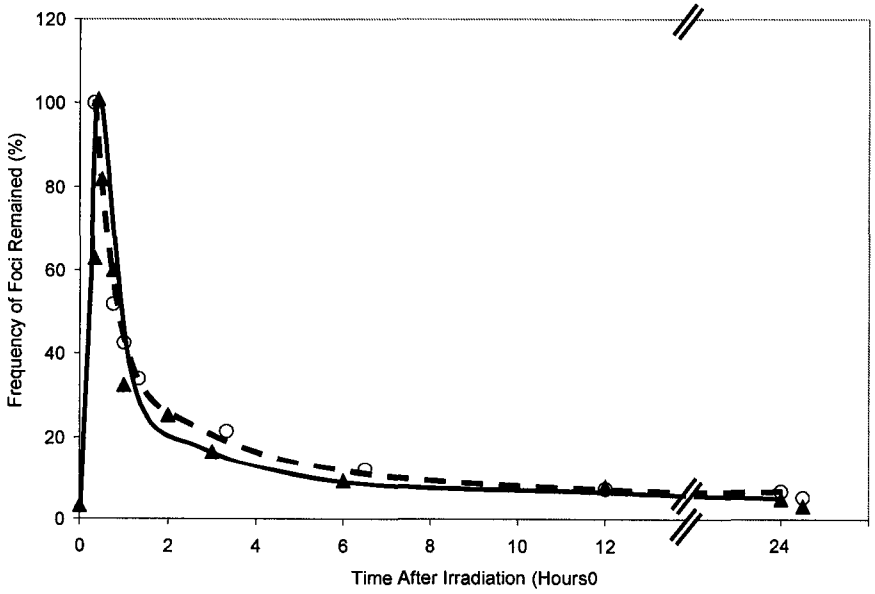

Residual lesion on Mitotic Chromosomes after G_0 Irradiation:

To determine whether residual lesions affecting long after then previous induction early in G_0 cells I examined first post-irradiation mitotic cells. For these experiments I either subcultured immediately or at various times up to 12 and 24 hours after irradiation. The results are plotted in figure 7-7A and 7B. Figure 7-7A shows the dose response for γ-H2AX foci on mitotic cells when G_0 cells were subcultured immediately or 12 hours after irradiation. A very large (10 fold) difference in sensitivity was seen for immediate vs. delayed subculture. The lesions leading to foci in mitosis disappeared after irradiation of G_0 cells with a half time of about 2 to 3 hours, and only about 5% remained after 24 hours.

As discussed previously, with immediate subculture cells may enter S phase before repair of DSBs or even SSBs and base damage is complete, so impediments to replication during S phase may well generate additional DNA DSBs not persist initially in the irradiated G_0 cells.

γ-H2AX foci in S-phase nuclei and S-phase PCCs

We and other have repeatedly observed problem issues with γ-H2AX assays involving S phase cells, with or without irradiation (10). A simple example of this is illustrated in Figure 7-8 which shows unirradiated human AG1522 cells from a log phase population (Figure 7-8A) and from a contact inhibited G_0 population of the same cells (Figure 7-8B). There are very few γ-H2AX foci on any of the cells of the contact inhibited population but some 30 to 40 % of the cells in the log phase population contain several foci each while others contain none.

Figure 7-7.

γ-H2AX foci in metaphase after irradiated G_0-phase

Figure 7-7A represents dose response curves for immediate subculture (solid line) and 12 hours delayed subculture (dashed line). Figure 7-7B represents that time course of delayed subculture after irradiation of 4Gy.

Figure 7A

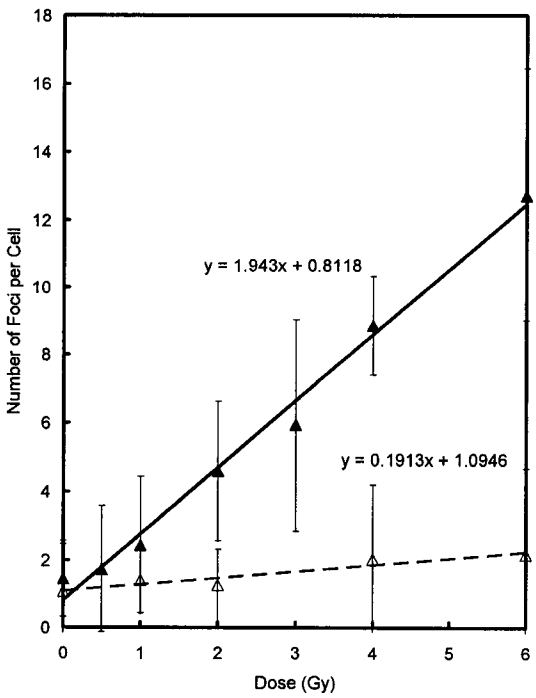

Figure 7B

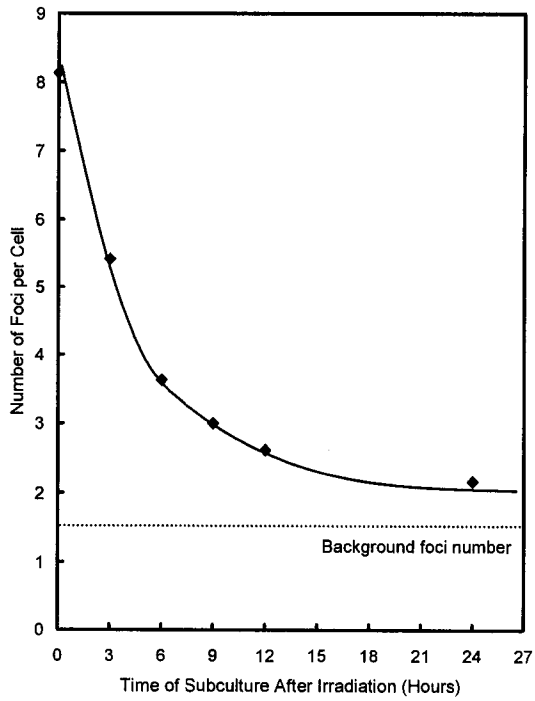

The thymidine analog BrdU is selectively incorporated into DNA and can be detected with anti-BrdU antibodies. To more closely examine the correlation between the appearance of γ-H2AX foci as related to the synthesis of DNA, I labeled cells with BrdU for 10 minutes and then several simultaneously carried out an immunocytochemical staining for γ-H2AX and BrdU. Figure 7-9 illustrates the result in nucleus did not incorporate BrdU were no γ-H2AX foci (Figure 7-9A), and in cells that did incorporate BrdU (Figure 7-9B) were also regions with γ-H2AX (Figure 7-9C and 9D).

Because I had observed high levels of radiation induced γ-H2AX foci in G_0 PCCs and high levels in nuclei of unirradiated S phase cells I decided to examine γ-H2AX foci levels in unirradiated S phase PCCs. The surprising result is illustrated in figure 7-10 and 7-11. Ordinarily, S phase PCCs are diffuse with non replicating regions of chromatin condensing interspersed with uncondensed replicating chromatin. Surprisingly, I found enormously high levels of γ-H2AX distributed throughout the unirradiated S phase PCCs. This is illustrated in Figure 7-10. Panel A shows an S phase PCC with the centromeres stained with an antikinetochore antibody (red). Panel B shows the same PCC stained of γ-H2AX (green).

Figure 7-11 shows the result of an experiment where unirradiated S phase cells were flash labeled with BrdU and PCC was induced. These were then stained with anti-BrdU antibody (red) shown in panel A or with anti-γ-H2AX antibody (green) shown in panel B. The areas stained in both cases indicating a close association between replication of DNA and the expression of γ-H2AX. However, there appeared to be lower quantities of γ-H2AX in S phase nuclei that had not been fused with mitotic HeLa cells.

Figure 7-8.

γ-H2AX foci formation in interphase cells without any irradiation.
Figure 7-8A shows asynchronous log growing cells with γ-H2AX foci (green).
Figure 7-8B shows contact inhibited G_0-phase cells with γ-H2AX foci (green)

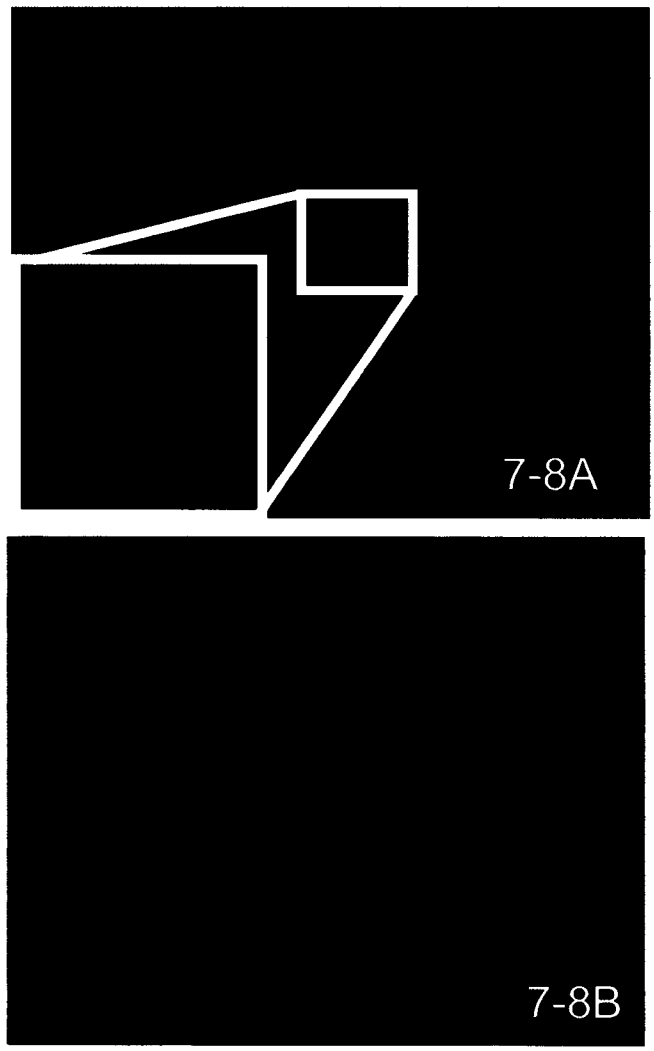

Figure 7-9.

The localization of γ-H2AX foci and DNA replication sites. Cells were pulsed label with BrdU and fixed. Red represents BrdU uptake sites, and Green represents γ-H2AX foci. Yellow color indicates colocalization between BrdU and γ-H2AX.

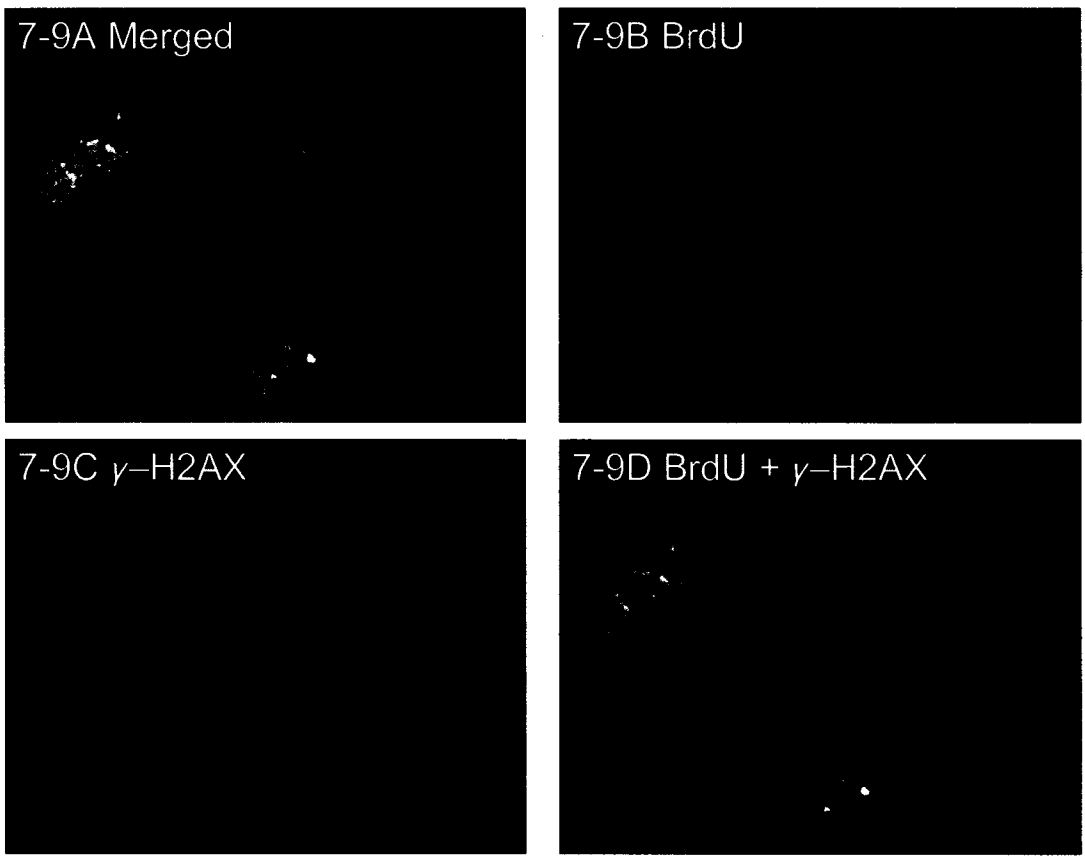

Figure 7-10.

High expression of γ-H2AX foci in S-phase PCC cells without any radiation and BrdU incorporation.
Figure 7-10A shows γ-H2AX foci (green) locates on S-phase PCC dotted fragments. Figure 7-10B is same picture with figure 7-10A but no γ-H2AX. Red represents centromeres.

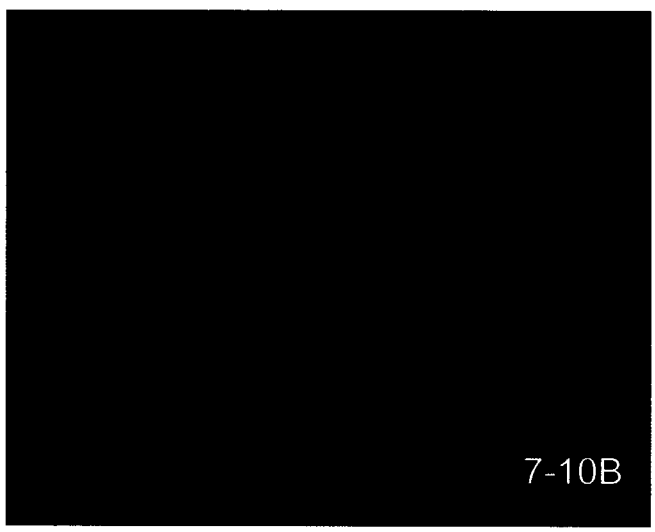

Figure 7-11.

γ-H2AX foci in S-phase PCC colocalized with BrdU uptaken sites.
Cells were pulsed labeled with BrdU and processed PCC. BrdU was stained by Red. γ-H2AX was stained by Green. Yellow represents colocalization between BrdU and γ-H2AX.

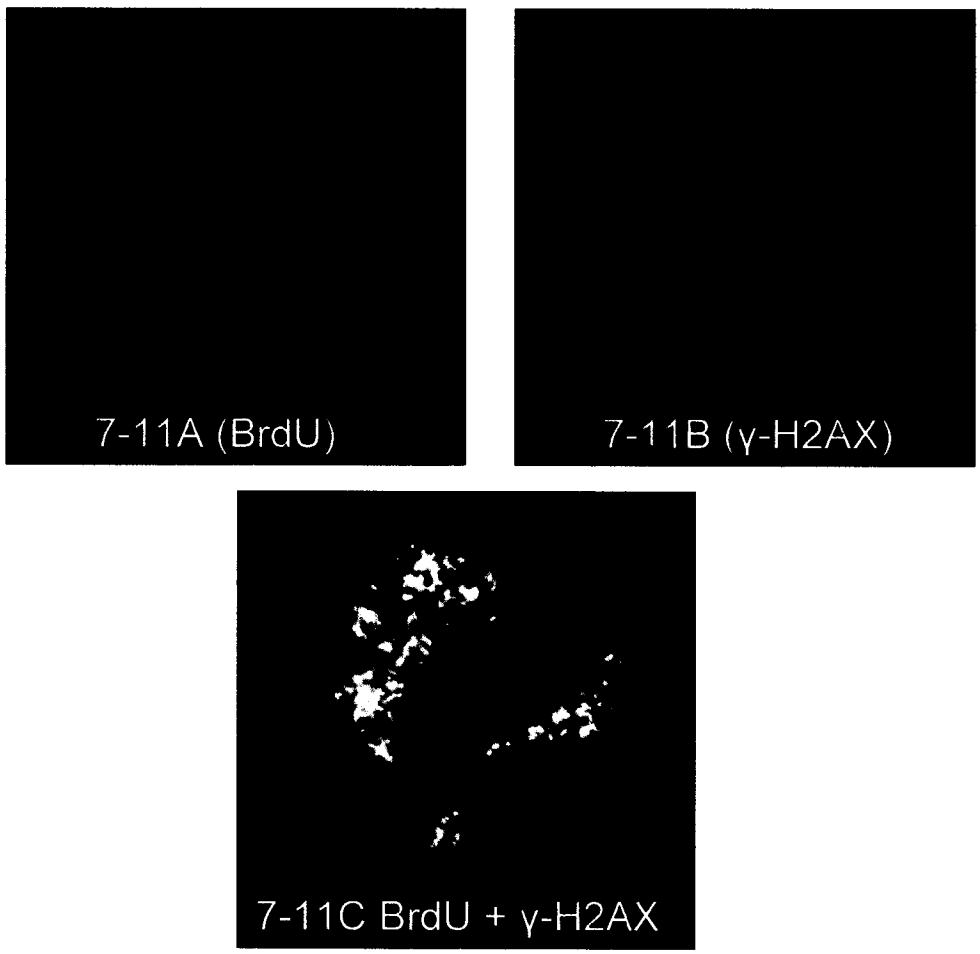

Limili and co-workers suggested that replication collapse may be the reason for S-phase dependent DSB formation in UV-exposed cells (11). Cells that have base damage or single strand breaks may produce DSBs during replication. Another possibility is that the PCC process causes DSB. In the process of condensation, chromatin fibers may be under high tension and stretch during conformation changes. But I did not see excessive γ-H2AX foci on unirradiated G_0 PCCs although there were relatively higher background γ-H2AX foci in these G_0-PCCs than G_0-nucleus..

Topoisomererases are one candidate source for the DSB production. DNA topoisomerase is an essential enzyme involved in resolving the torsional stress associated with DNA replication, transcription, and chromatin condensation (12). Topoisomerase IB and IIA associate with replication (13). Topoisomerase IB does not produce DSB but SSB during DNA replication, but the inhibitor of Topoisomerase IB like CPT is known to produce DSB in S-phase (14). Another Topoisomerase which has function during replication in mammalian cells is Topoisomerase IIA (13). Topoisimerase IIA directly produces DSBs to untight supercoiled chromatin structure. Since I did not carry out further experiments, Topoisomerases are just candidate for S-phase γ-H2AX foci expression.

It is known about 300 replication forks are actively replicating DNA at any one time in mammalian cells. If all 300 replication forks produce DSBs, upon S phase PCC it would have a huge impact on γ-H2AX foci seen in these cells (about 10Gy of γ-irradiation) and it would be detectable by other methods of DNA DSB assays. Another novel method for DNA DSB detection is Pulsed field gel electrophoresis (15-17). This

method separates Megabase size of DNA and can directly detect as fewer 150 to 300 DSBs per cell (it means 5 to 10 Gy exposure). So far, there are no reports about high background DSBs in S-phase cells (16). This indicates those DNA DSB during replication may be different from the ones produced by ionizing radiation. The possible characteristics of replication mediated DNA DSBs are 1) DSB formation occurs only very few moments and it does not affect cell function. Because DSB rejoins so quickly, gel electrophoresis can't detect it. But each DSB causes histone H2AX phosphorylation and can be observed by immunocytochemistry. 2) It is not actually DSB but histone H2AX phosphorylation occurs in the unknown process during replication.

Even topoisomerase function is the reason for producing DSB during replication, still S-phase PCC has too many foci to explain it. Further there are many more foci in the S-phase PCC than are seen in interphase cells.

I concluded S-phase cells contain more γ-H2AX foci than G_0-contact inhibited cells and it is associated with DNA double strand breaks during DNA replication process. But still the reason for the high expression of γ-H2AX especially in S-phase PCC is unclear.

REFERENCES

1. E. P. Rogakou, D. R. Pilch, A. H. Orr, V. S. Ivanova and W. M. Bonner, DNA double-stranded breaks induce histone H2AX phosphorylation on serine 139, *J Biol.Chem.* **273**, 5858-5868 (1998).

2. E. P. Rogakou, C. Boon, C. Redon and W. M. Bonner, Megabase chromatin domains involved in DNA double-strand breaks in vivo, *J.Cell Biol.* **146**, 905-915 (1999).

3. A. Takahashi and T. Ohnishi, Does gammaH2AX foci formation depend on the presence of DNA double strand breaks?, *Cancer Lett.* **229**, 171-179 (2005).

4. C. A. Waldren and R. T. Johnson, Analysis of interphase chromosome damage by means of premature chromosome condensation after X-ray and ultraviolet irradiation, *Proc.Natl.Acad.Sci.USA* **71**, 1137-1141 (1974).

5. M. N. Cornforth and J. S. Bedford, X-ray induced breakage and rejoining of human interphase chromosomes., *Science* **222**, 1141-1143 (1983).

6. M. N. Cornforth and J. S. Bedford, On the nature of a defect in cells from individuals with ataxia telangiectasia., *Science* **227**, 1589-1591 (1985).

7. M. N. Cornforth and J. S. Bedford, High-resolution measurement of breaks in prematurely condensed chromosomes by differential staining, *Chromosoma* **88**, 315-318 (1983).

8. M. C. Muhlmann-Diaz and J. S. Bedford, Breakage of human chromosomes 4, 19 and Y in G0 cells immediately after exposure to gamma-rays, *Int.J.Radiat.Biol.* **65**, 165-173 (1994).

9. A. T. Christian, E. McNiel, J. Robinson, R. Drabek, S. LaRue, C. Waldren and J. Bedford, A versatile image analysis approach for simultaneous chromosome identification and localization of FISH probes, *Cytogenet.Cell Genet.* **82**, 172-179 (1998).

10. S. H. MacPhail, J. P. Banath, Y. Yu, E. Chu and P. L. Olive, Cell cycle-dependent expression of phosphorylated histone H2AX: reduced expression in unirradiated but not X-irradiated G1-phase cells, *Radiat.Res.* **159**, 759-767 (2003).

11. C. L. Limoli, E. Giedzinski, W. M. Bonner and J. E. Cleaver, UV-induced replication arrest in the xeroderma pigmentosum variant leads to DNA double-strand breaks, gamma -H2AX formation, and Mre11 relocalization, *Proc.Natl.Acad.Sci.U.S.A* **99**, 233-238 (2002).

12. O. Espeli and K. J. Marians, Untangling intracellular DNA topology, *Mol.Microbiol.* **52**, 925-931 (2004).

13. J. B. Leppard and J. J. Champoux, Human DNA topoisomerase I: relaxation, roles, and damage control, *Chromosoma* **114**, 75-85 (2005).

14. J. C. Leonard, A. M. Mullinger, J. Schmidt, H. J. Cordell and R. T. Johnson, Genome instability in ataxia telangiectasia (A-T) families: camptothecin-induced damage to replicating DNA discriminates between obligate A-T heterozygotes, A-T homozygotes and controls, *Biosci.Rep.* **24**, 617-629 (2004).

15. K. Gardiner, W. Laas and D. Patterson, Fractionation of large mammalian CNA restriction fragments using vertial pulse-field gradient gel electrophoresis., *Somat.Cell Mol.Genet.* **12**, 185-195 (1986).

16. L. Metzger and G. Iliakis, Kinetics of DNA double-strand break repair throughout the cell cycle as assayed by pulsed field gel electrophoresis in CHO cells, *Int.J.Radiat.Biol* **59**, 1325-1339 (1991).

17. C. R. Contopoulou, V. E. Cook and R. K. Mortimer, Analysis of DNA double strand breakage and repair using orthogonal field alternation gel electrophoresis., *Yeast* **3**, 71-76 (1987).